

FACIES ANALYSIS, PALEOENVIRONMENTAL IN-
TERPRETATION, AND DIAGENETIC HISTORY
OF BRITT SANDSTONE (UPPER MISSIS-
SIPPIAN), IN PORTIONS OF CADDO
AND CANADIAN COUNTIES,
OKLAHOMA

By

JOHN PAUL HAIDUK

Bachelor of Science

Oklahoma State University

Stillwater, Oklahoma

1983

Submitted to the Faculty of the
Graduate College of the
Oklahoma State University
in partial fulfillment of
the requirements for
the Degree of
MASTER OF SCIENCE
May, 1987

Thesis
1987
H149F
cop. 2



FACIES ANALYSIS, PALEOENVIRONMENTAL IN-
TERPRETATION, AND DIAGENETIC HISTORY
OF BRITT SANDSTONE (UPPER MISSIS-
SIPPIAN), IN PORTIONS OF CADDO
AND CANADIAN COUNTIES,
OKLAHOMA

Thesis Approved:

Cary J. Stewart
Thesis Advisor

Zachariah Childs

Arthur W. Cleaver

Norman N. Durham
Dean of the Graduate College

ACKNOWLEDGEMENTS

The author wishes to express his sincerest appreciation to all who contributed to this study. Special acknowledgements are given to those most closely associated with this project: Dr. Gary F. Stewart, main thesis advisor, for his efforts in coordinating this study, his many helpful hints, and critical review of the manuscript, maps, and cross-sections; Dr. Zuhair Al-Shaieb, committee member, for his invaluable assistance in the petrologic and diagenetic aspects of this thesis; and Dr. Arthur W. Cleaves, committee member, for his critical review of the plates and discussions of depositional environments.

Special thanks is extended to Amoco Production Company for its financial support and for providing the opportunity for this author to study several cores and associated data which were essential in many of the interpretations made concerning the thesis area. Mr. Steve Crews was responsible for coordinating Amoco's portion of the thesis. The author is grateful for his suggestions and advice concerning depositional environments and diagenesis.

Advice given by the Geology and Drafting Departments of Ward Petroleum throughout the length of the study was greatly appreciated. The thesis topic was suggested by Mike O'Donnell, Ward Petroleum geologist. Mike's review of the

plates, initial review of the manuscript, and constant advice had much to do with the final interpretations presented. In addition, Mike's humor, alleviated much of the tension during crucial periods of the study.

Information and material came from numerous sources: Ward Petroleum Corporation provided access to their extensive well log library and production data; Unocal provided type logs, and the Oklahoma Geological Survey provided many of the cores used in this research. Eldon Cox of the OGS Core and Sample Library were very helpful throughout the course of this study.

Major funding for this research was provided by James Gungoll through Henry Gungoll Operating, Inc. of Enid, Oklahoma. The author is most thankful to Jim not only for his financial support but also for the opportunity to learn how honesty and integrity in business can lead to a successful financial enterprise and bolster the spirits of those persons associated with such an individual.

Finally, very special appreciation is extended to my wife Lynn. Without her love and moral support many of tense periods encountered during this research would have been difficult to overcome.

TABLE OF CONTENTS

Chapter	Page
ABSTRACT	1
I. INTRODUCTION	3
General Characteristics and Location of Thesis Area	3
Purpose of Investigation	6
Methods and Procedures	6
Previous Investigations	8
II. STRATIGRAPHIC FRAMEWORK	12
Introduction	12
Upper Mississippian-Lower Pennsylvanian Stratigraphy	14
Regional Attributes	14
Local Attributes	15
Cross-Section Network	16
Mississippian-Pennsylvanian Unconformity Regional Attributes	18
Local Attributes	19
Method for Interpreting Systemic Boundary from Well Logs	19
Depositional Hiatus Between Cunningham and Britt Members	24
III. STRUCTURAL FRAMEWORK	28
Introduction	28
Episodes of Structural Activity in the Anadarko Basin	30
Local Structural Geology	33
IV. PETROLOGY, DIAGENESIS, AND POROSITY	39
Introduction	39
Detrital Constituents in Britt Sandstones	40
Quartz	40

Chapter	Page
Detrital Clay Matrix	41
Fossils	43
Ooids and Coated Grains	44
Siliceous Detrital Matrix	46
Feldspars	46
Rock Fragments	46
Other Detrital Grains	47
Glauconite	47
Authigenic Constituents in Britt	
Sandstones	48
Authigenic Clays	49
Siliceous Cements	50
Carbonate Cements	53
Collophane	57
Pyrite	58
Organic Material	59
Origins of Authigenic Constituents	59
Authigenic Clays	62
Siliceous Cements	63
Carbonate Cements	64
Collophane	66
Pyrite	66
Organic Material	67
Deformation Fabrics	67
Porosity	70
Primary Porosity	70
Secondary Porosity	71
Microporosity	75
Relationship Between Porosity, Silica Cement, Authigenic Clay, and Depositional Environ- ments	76
Relationship Between Silica and Carbonate Cements	78
Paragenetic Sequence	81
 V. DEPOSITIONAL ENVIRONMENTS AND SEDIMENTOLOGICAL CHARACTER	 88
Introduction	88
Shelf Regimes and Sediment Movement	89
Phase I: Description of Principle Facies	94
Bar-Finger Sands	94
Delta-Destructional Sand Bars	95
Shelf Sand-Ridges	99
Storm Deposits	102
Phase II: Paleoenvironmental Interpreta- tion of Principle Facies	105
Bar-Finger Sands	105
Delta-Destructional Sand Bars	109
Shelf Sand-Ridges	112

Chapter	Page
Storm Deposits	119
Phase III: Depositional Model for Strata of the Britt	125
Summary of Britt Depositional System	131
 VI. SUMMARY AND CONCLUSIONS	 134
Conclusions	134
REFERENCES	141
APPENDIX A - METHODS USED FOR CONSTRUCTION OF GROSS- SAND ISOPACH AND STRUCTURAL MAPS	147
APPENDIX B - DESCRIPTIONS OF CORES	149
APPENDIX C - CONSTITUENT TYPES AND PERCENTAGES IN THIN SECTIONS	179

LIST OF FIGURES

Figure	Page
1. Morrow - Springer Trends	4
2. Location of Study Area	5
3. Cross-section, Core, and Drill-cutting Location Map	9
4. Stratigraphic Column	13
5. Type Log	17
6. Paleogeology of the Mid-Continent at the Close of the Mississippian	20
7. Interpretation of Mississippian-Pennsylvanian Unconformity from Well Logs	23
8. Core from the Apexco, Inc. - Buell No. 1-A demon- strating erosional contact between Lower Britt sandstone and black, laminated, sparsely fos- siliferous Cunningham shale	26
9. Principle Pennsylvanian Physiographic Features of the Southern Mid-Continent	29
10. Types of Deformation Along the Wichita Mountain Front	31
11. Stratigraphic Position of Additional Cunningham Strata on Downthrown Side of Eakly Fault	36
12. Major Structural Features of Western Oklahoma	38
13. Photomicrograph of authigenic chlorite, recryst- tallized from detrital clay matrix, supporting detrital grains	42
14. Photomicrograph of oolitic limestone unit with medium-grained detrital quartz grains and fos- sils serving as ooid nuclei	45

Figures	Page
15. SEM Photomicrograph. Platy authigenic chlorite shows edge-to-face morphology with detrital grains	49
16. Photomicrograph illustrating advanced syntaxial-quartz-overgrowth cementation	51
17. SEM Photomicrograph. Syntaxial quartz overgrowths in a quartzitic sand	52
18. Photomicrograph. Chert cement fills pores between detrital grains	52
19. Core photograph demonstrating elongated siderite nodules in a prodeltaic shale	54
20. Photomicrograph. Poikilotopic carbonate cement is an early diagenetic mineral	56
21. Photomicrograph. Saddle or "baroque" dolomite replaces both fossils and calcite cements	58
22A. Detrital Constituents in Britt Sandstones	60
22B. Authigenic Constituents in Britt Sandstones	61
23. Photomicrographs demonstrating deformation fabrics in Britt sandstones	68
24. Trends of Productive Britt Sandstone	70
25. SEM Photomicrograph. Secondary porosity resulted from the partial dissolution of detrital quartz	72
26. Photomicrograph demonstrating dissolution of detrital clay matrix	74
27. Photomicrographs for comparison of the extent of silica cementation in quartzitic sands	77
28. Relationship between authigenic chlorite and porosity	79
29. Relationship between authigenic chlorite and syntaxial quartz overgrowths	80
30. Relationship between carbonate and silica cements	82
31. Paragenetic Sequence of Britt Sandstones	83

Figure	Page
32. SEM Photomicrograph	86
33. Known Extent of Britt Sandstones in Western and Southern Oklahoma	90
34. Summary Classification of Offshore Regimes . . .	93
35. Stratigraphic Cross-section Illustrating Various Facies in the Lower Britt Submember	96
36. Lower Britt Delta-Destructional Bar Complex Gross-Sand Isopach Map	98
37. Core photograph showing wavy, lenticularly- interbedded sands, silts, and shales typ- ical of strata underlying Britt shelf sand-ridges	101
38. Petrologic nature of Britt storm deposits . . .	104
39. Significant Subfacies of the River-Dominated Delta	106
40. Idealized Vertical Sequence of Distributary- Channel/Bar-finger Sandstone	107
41. Block Diagram Illustrating Idealized Geometry and Relationships Among Shelf Sand-Ridges . .	113
42. Idealized Vertical Sequence of Britt Shelf Sand-Ridge	117
43. Origin of Graded Storm Deposits in the Shelf Regime	122
44. Photomicrograph of sediment from a storm deposit	124
45. Approximate Basinward Limit of Britt Delta-Des- tructional Sand Bars	129
46. Type Log Illustrating Stratigraphic Position of Upper Britt "A" and "B" Shelf Sand-Ridges	131

LIST OF PLATES

Plate

- I. Structural Contour Map - Britt Marker . . . in pocket
- II. Structural Contour Map - Mississippian-Pennsylvanian Unconformity in pocket
- III. Gross Sand Isopach Map - Lower Britt . . . in pocket
- IV. Gross Sand Isopach Map - Upper Britt
"A" Sand in pocket
- V. Gross Sand Isopach Map - Upper Britt
"B" Sand in pocket
- VI. Isopach Map - Springer Group in pocket
- VII. Cross-Section A - A' in pocket
- VIII. Cross-Section B - B' in pocket
- IX. Cross-Section C - C' in pocket
- X. Cross-Section D - D' in pocket
- XI. Cross-Section E - E' in pocket

ABSTRACT

This study is concerned with documenting the importance of the Upper Mississippian Britt sandstones of southwestern Canadian and northern Caddo Counties of Oklahoma. Specific objectives include: 1) characterizing Upper Mississippian and Lower Pennsylvanian stratigraphy, 2) defining the setting in which Britt strata were deposited, 3) analyzing the petrography of sandstones, 4) describing diagenetic events that affected the sandstones, and 5) relating the diagenetic history of the sandstones to the preservation of primary porosity and the formation of secondary porosity. Techniques included structural and isopach mapping, thin-section analysis, scanning electron microscopy.

Britt sandstones record regressive-transgressive couplets in response to deltaic progradation, abandonment, and subsidence in the southeastern Anadarko Basin, during the Late Mississippian. Four principle facies compose the sequence: 1) deltaic bar-finger sands, 2) delta-destructive sand bars, 3) shelf sand-ridges, and 4) storm deposits. These facies record the transition from the deltaic to the shelf regime. Except for storm deposits, sandstones are quartzitic with fossils and ooids abundant locally. Detrital clay matrix is a major constituent of some sands. Numerous

episodes of diagenetic activity have altered extensively the mineralogical character of these sands. Chlorite, silica, and carbonates are the primary authigenic minerals.

CHAPTER I

INTRODUCTION

General Characteristics and Location of Thesis Area

The study area is located in the southeastern portion of the Anadarko Basin, which extends across southern Oklahoma and into the Texas Panhandle (Figures 1, 2). Data used in this study are derived from wells drilled within the petroliferous Watonga-Chickasha Trend of Oklahoma (Figure 1). This giant field is a gas-prone accumulation well-known for production from overpressured Morrowan (Early Pennsylvanian) and Chesterian (Late Mississippian) clastic reservoirs. Although this field was discovered more than twenty years ago, completions by Woods Petroleum and Apexco, Inc. in 1974 extended the limits southeastward, creating a period of intense development that reached its maximum during the drilling boom of the late 1970's and early 1980's.

The area of investigation consists of twenty townships; T. 9 N. through T. 12 N., and R. 9 W. through R. 13 W. (Figure 2). The total area involved is approximately 720 square miles which, includes portions of Caddo and Canadian Counties of Oklahoma.

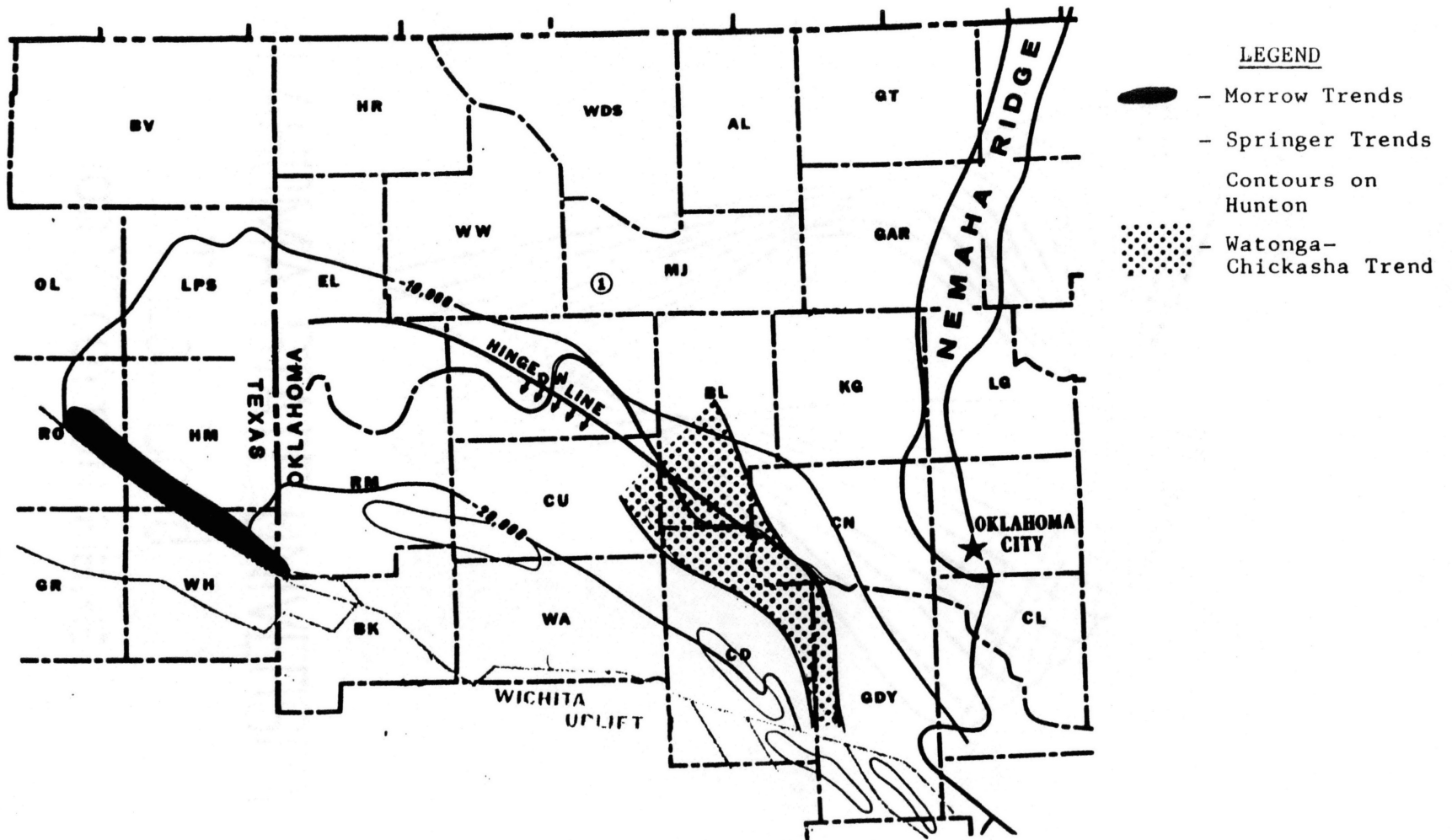


Figure 1. Morrow- Springer Trends (After Evans, 1979)

STATE OF OKLAHOMA

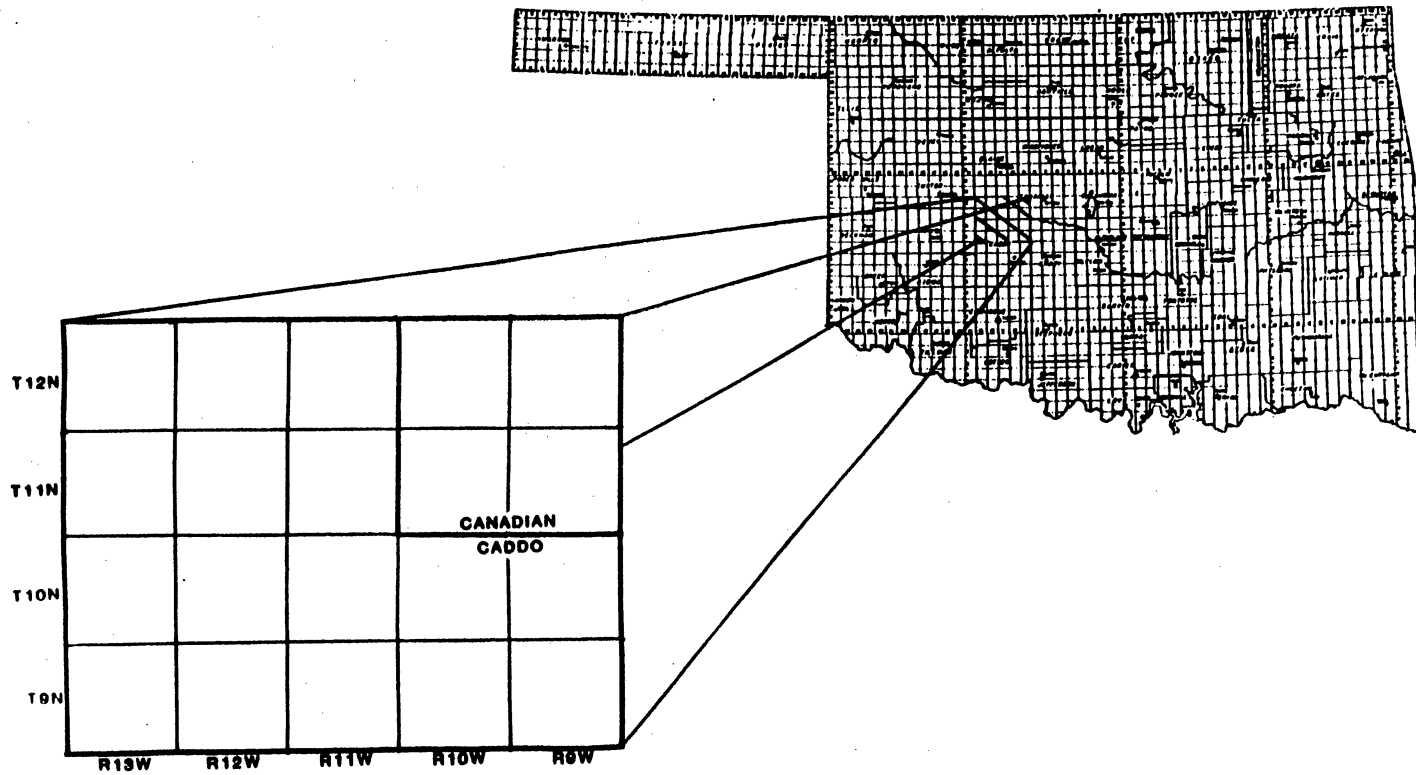


Figure 2. Location of Study Area

This study primarily is concerned with documenting the importance of the Upper Mississippian Britt interval, a shale- and sand-dominated sequence. Numerous sands within this interval are important hydrocarbon reservoirs.

Purpose of Investigation

The purpose of this investigation was four-fold involving examination of the sedimentologic, stratigraphic, petrologic, and diagenetic aspects of the Britt sandstones and shales in the Canadian and Caddo County portions of the Watonga-Chickasha Trend. Specific objectives of this research include: 1) characterizing Upper Mississippian and Lower Pennsylvanian stratigraphy, 2) defining the setting in which Britt strata were deposited, 3) presenting an in-depth analysis of the Britt petrological character, 4) defining and describing the diagenetic events that affected the Britt sandstones, and 5) relating the diagenetic history of the rocks to the preservation of primary porosity and the formation of secondary porosity.

Methods and Procedures

Six maps were constructed using more than 450 well logs (Plates I - VI). Well logs and cores were used exclusively due to lack of outcrop within the boundaries of the thesis area. All well logs released by MJ Systems and Riley's Electric Logs as of June, 1986 were used. Three gross sand isopach maps (Plates III - V) were constructed in an effort

to demonstrate accurately the trends of sand bodies. One gross interval isopach map (Plate VI) was constructed for the purpose of determining regional depositional strike. Two structural contour maps (Plates I and II) were constructed for the following purposes: 1) to establish regional structural trends, 2) to determine if significant faulting had occurred, and 3) to assess the effects of structure on hydrocarbon accumulation within the thesis area. Methods used in the construction of each map type are presented in Appendix A.

Five regional stratigraphic cross-sections (Plates VII - XI) were constructed across the thesis area. Three of these cross-sections are dip-oriented and two strike-oriented, with reference to regional structure. Locations of these regional cross-sections are presented in Figure 3. Several localized cross-sections were constructed to illustrate lateral variation in the stratigraphic succession and to determine geometries of individual sand bodies. These sections are presented within the body of the thesis.

Eight cores with total footage of 491 feet were logged in order to: 1) establish type and sequence of sedimentary structures and textures, 2) relate lithologic units to specific depositional environments, and 3) correlate megascopic features noted in the cores to features noted during thin-section analysis. Data derived from core analysis include lithology, sedimentary structures, textures, and mineralogical constituents. Descriptions of cores are presented in

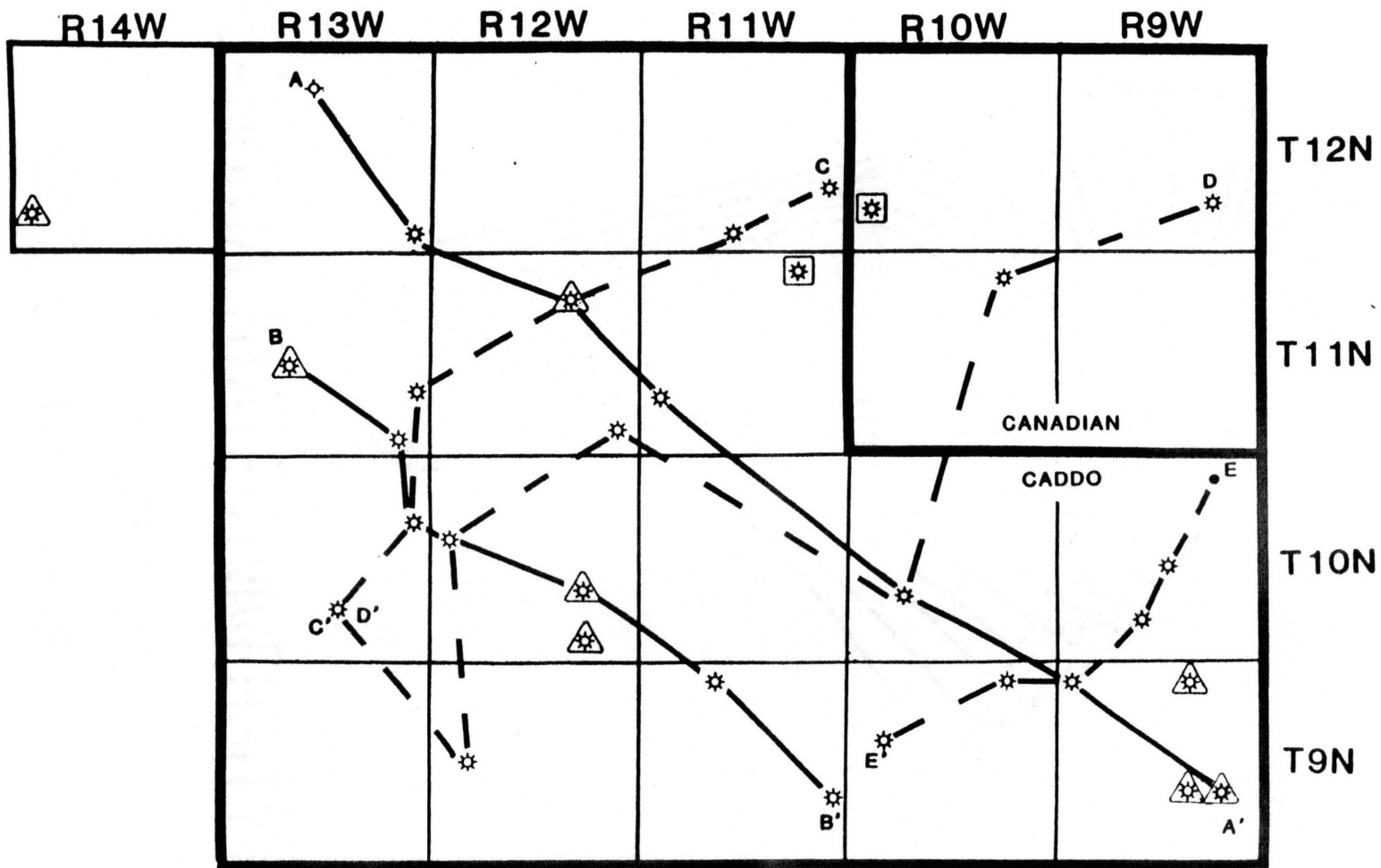


Figure 3. Cross-section, Core, and Drilling-cutting Location Map.

△ - Core Location

□ - Drill-cutting Location

Appendix B. Drill cuttings from two wells were analyzed in an effort to interpret vertical variations within the Britt interval. Locations of cores and drill cuttings are presented in Figure 3.

Analysis of thin sections yielded much of the petrologic and diagenetic data presented in this research. Fifty-eight thin sections were analyzed for the purpose of 1) establishing the general petrologic character of the various lithologic types represented, 2) observing the effects of diagenesis on Britt sands, and 3) determining the origins of porosity within the reservoir sands. Each thin section was point-counted to a minimum of 400 points. Two grain mounts were made from drill cuttings. These thin sections were analyzed solely for observing their mineralogical content and were not point-counted.

In addition to routine thin-section analysis, scanning electron microscopy (SEM) was employed. SEM analysis permits the visual inspection of the rock fabric, observation of the morphology of diagenetic minerals, and the opportunity to analyze the geometry of pore spaces and pore throats, all at high magnification. Three samples were analyzed in this manner.

Previous Investigations

Previous articles pertaining to Upper Mississippian clastic deposits of the Anadarko Basin are uncommon. Reasons for the lack of research concerning these sediments are

many. Primarily, sedimentologic similarities between Upper Mississippian clastic rocks and those of the overlying Lower Pennsylvanian Morrow Formation have led to confusion in stratigraphic terminology. While numerous published works exist covering aspects of Morrowan clastic sedimentation and petrology (e.g., Adams, 1964, Khaiwka, 1968, Bloustone, 1975, Shelby, 1980, and many others) few exist concerning any aspect of Upper Mississippian clastic sediments. Secondly, data from successful well completions in Chesterian clastics, including well logs, cores, and drill cuttings, may not be released for proprietary reasons. Thirdly, financial, geological, and engineering constraints do not allow for abundant cores to be taken from Upper Mississippian clastic reservoirs. The loss of this data source has slowed the development of depositional models and thereby reduced published research.

Several articles concerning Chesterian clastic deposition in southern Oklahoma have been published within the last thirty years. Peace (1965) presented the structural geology of the southeastern Anadarko Basin and its influence on Chesterian sedimentation. Extensive regional mapping was undertaken by Peace along with the measurement of numerous sections where Chesterian clastic strata crop out in association with exposed folds. In a self-proclaimed controversial paper, Beckman and Sloss (1959) postulated the existence of an unconformity underlying Chesterian clastic sediments in the Ardmore Basin. These authors also

discussed the petrologic aspects of these exposed sandstones and shales. Jacobsen (1959) reviewed the role of Chesterian clastics as reservoirs and implied a direct link between sedimentation and tectonism in the deposition of thick Chesterian sandstones paralleling the southwestern limbs of many large anticlines of southern Oklahoma.

Mid-Continent Pennsylvanian paleogeology was reviewed by Moore (1979). Evans (1979), Feinstein (1981), Brewer et al. (1983), and Garner and Turcotte (1984) attempted to unravel the complex structural geology of the Mid-Continent.

Various works have been published in attempts to establish the age of the Springer Group. Westheimer (1956), Elias (1956), Waddel (1966), Dunn (1966), and Straka (1972) argued the age of these strata and placement of systemic and formational boundaries on the basis of various faunal assemblages including, conodonts, ammonoids, and foraminifers.

Several published articles have been written concerning the hydrocarbon potential of Chesterian clastic deposits in the southeastern Anadarko Basin. Authors promoting such plays include Riley (1966), Wroblowski (1966), Swanson (1968), and Davis (1978). Rasco and Adler (1983) presented an in-depth review of hydrocarbon production from reservoirs of various ages across the Mid-Continent.

CHAPTER II

STRATIGRAPHIC FRAMEWORK

Introduction

The stratigraphic unit of interest, the Britt, is an ad hoc member of the Upper Mississippian Goddard Formation (Peace, 1965). The Goddard Formation is one of two formations that compose the Springer Group, a basinward-thickening clastic sequence. This group overlies the Mississippian Caney Formation and is overlain by the Pennsylvanian Morrow Formation. Carbonate deposition prevailed from Ordovician through the Late Mississippian in the southern Mid-Continent. The Springer Group represents the change to clastic-dominated sedimentation which prevailed through the remainder of the Paleozoic. The regional Upper Mississippian-Lower Pennsylvanian stratigraphy is presented in Figure 4.

The purpose of this chapter is two-fold: 1) to outline the general stratigraphic succession from the Upper Mississippian Caney Formation to the Lower Pennsylvanian Morrow Formation, and 2) to demonstrate the existence of the pre-Pennsylvanian unconformity that interrupts the normal stratigraphic succession.

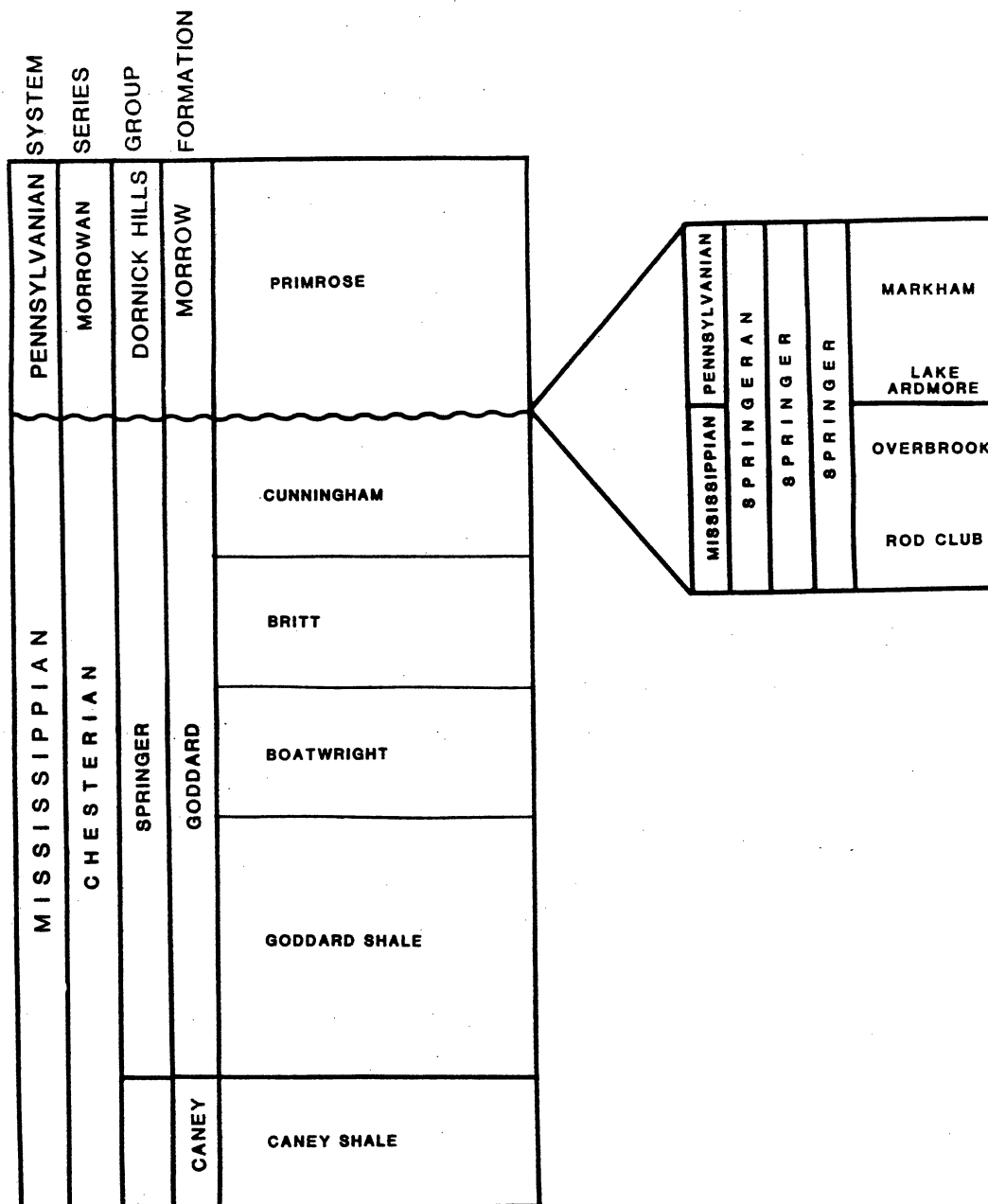


Figure 4. Stratigraphic Column (Modified from Westheimer, 1956, Peace, 1965, Waddel, 1966, and Straka, 1972)

Upper Mississippian-Lower Pennsylvanian Stratigraphy

Regional Attributes

Various authors have investigated the Upper Mississippian-Lower Pennsylvanian stratigraphic succession in southwestern and south-central Oklahoma. Major works have been published by Elias (1956) who merged various faunal assemblages to design his stratigraphic column, Waddel (1966), who used fusilinids as the basis for his study, and Straka (1972) who based his stratigraphic scheme on conodonts.

Tomlinson (1959) first proposed that the term "Springer Group" be used to define the strata that lie above the Mississippian Caney Formation but below the Pennsylvanian Morrow Formation (Figure 4). Peace (1965) first proposed that the Springer Group be divided into the Springer and Goddard Formations (Figure 4). The boundary between these rock units is the base of the Rod Club Sandstone (Westheimer, 1956). Within the study area, the top of the Springer Group (the top of the Goddard Formation) is represented by an unconformity. The Springer Formation is not present within the boundaries of the thesis area. This formation is shown in the Stratigraphic Column (Figure 4) solely for the purpose of understanding the regional stratigraphy.

One of the most debated issues concerning the stratigraphy of southwestern Oklahoma is the age of the Springer

Group. Based on evidence presented by Elias (1956), Waddel (1966), Dunn (1966), and Straka (1972), the Springer Group is transitional Mississippian to Pennsylvanian in age; thus portions of southwestern Oklahoma represent one of few places on the North American craton where continuous sedimentation has occurred across this systemic boundary (Gordon and Mamet, 1978). Each of the authors previously cited considers the base of the Lake Ardmore Member of the Springer Formation to be the boundary between Mississippian and Pennsylvanian strata (Figure 4).

Local Attributes

In the thesis area, the Goddard Formation, can be divided into four mappable ad hoc members. In ascending order these are the Goddard, Boatwright, Britt, and Cunningham (Figure 4). With the exception of the Goddard, these members are sand-shale packages. The Goddard Member is a shale-dominated sequence generally devoid of all but very localized sandy units (as interpreted from well logs). The local stratigraphic terminology is adopted from the Springer Group of southern Grady County, Oklahoma (Figure 2). The Cunningham, Britt, and Boatwright members take their names from the well in which each originally was found productive (Jordon, 1957). Type logs for the thesis area were provided by geologists of Union Oil of California, who correlated from southern Grady County to the study area. On the basis of scout-ticket "calls" it is evident that a large

majority of exploration companies working this region have adopted similiar nomenclature for these intervals. Equivalent strata are hydrocarbon-productive in other portions of south-central and southwestern Oklahoma, but locally they are known by other names (Peace, 1965).

The Britt Member encompasses strata between the base of the "Britt Marker" and top of the "Boatwright Marker" (Figure 5). Both of these boundary units are regionally extensive and typically thin. They are characterized on well logs by high resistivity. During the course of this investigation two distinct traceable depositional systems were found within the Britt Member. On the basis of this observation the Britt was divided into upper and lower submembers. Such a division has not been noted in any known published articles. No regionally consistent stratigraphic marker separates these genetic intervals.

Cross-Section Network

A network of three NE-SW (dip-oriented) and two NNW-SSE (strike-oriented) stratigraphic cross-sections was constructed within the thesis area (Figure 3) for the purpose of: 1) insuring reliable correlations, 2) illustrating the electric log character of the various members of the Goddard Formation, 3) demonstrating variation in the stratigraphic position of the pre-Pennsylvanian unconformity, and 4) establishing the regional stratigraphic framework utilized throughout the study. Logs from cored wells commonly were

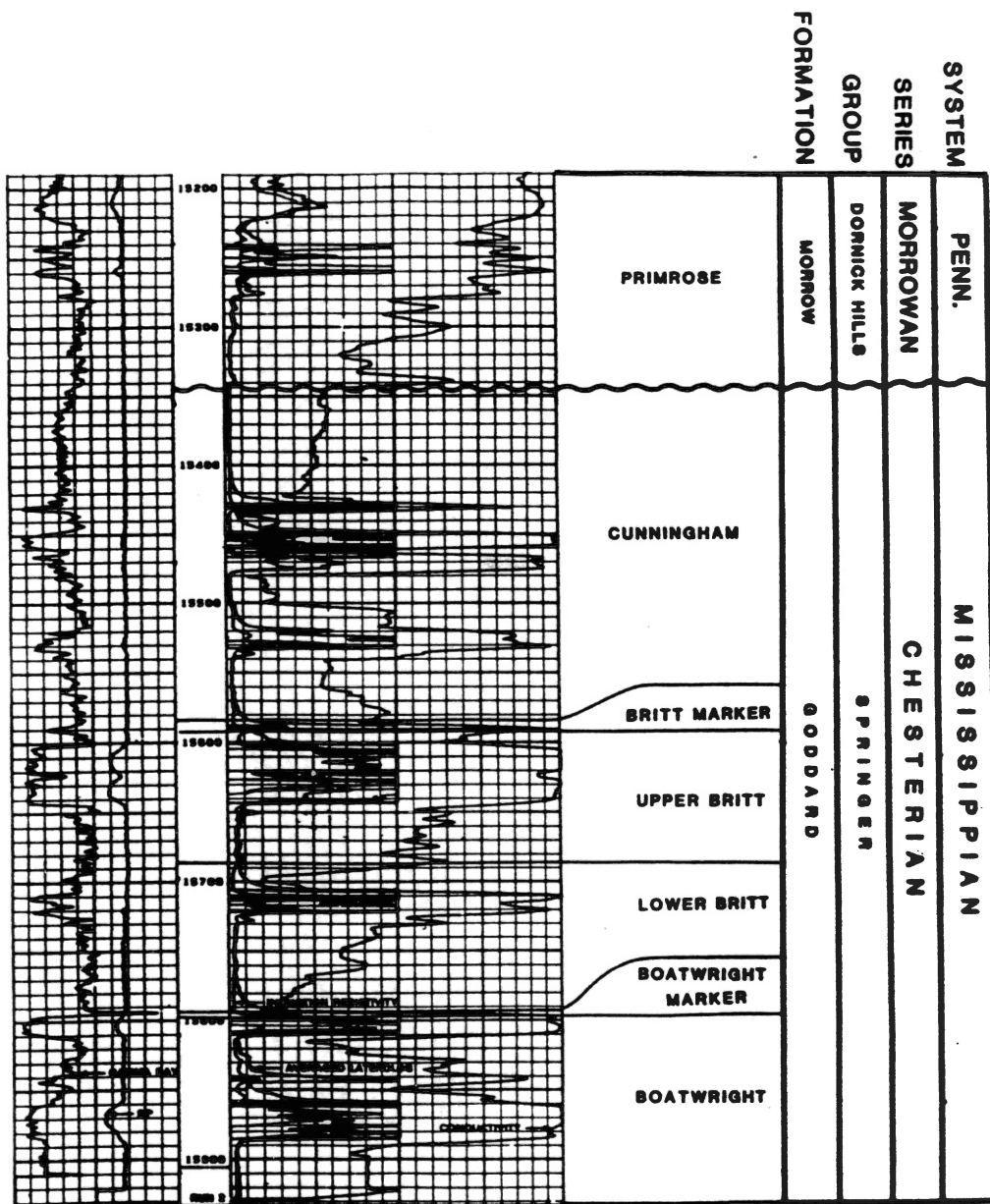


Figure 5. Type Log. well Log from the Berexco, Inc. Larson No. 1-14. Section 34-T10N-R12W. Caddo County, Oklahoma.

utilized, thus making it possible to compare well-log signatures to data from cores and thus to fit them into a reliable characterization of Chesterian lithology and facies. The reference datum for each of these cross-sections is the top of the Springer Group, which corresponds to the pre-Pennsylvanian unconformity within the study area. Stratigraphic intervals correlated in each cross-section include the Goddard, Boatwright, Britt, Cunningham, and Morrow. Cross-section D - D' (Plate X), a dip-oriented section, demonstrates the boundary between the Caney Formation and Goddard Shale. This contact is readily recognizable on well logs because of the increased resistivity and decreased gamma-ray intensity associated with the Caney Formation. Cross-section D - D' also demonstrates the basinward thickening of the Goddard Shale.

Mississippian-Pennsylvanian Unconformity

Regional Attributes

The Mississippian-Pennsylvanian systemic boundary is considered to be unconformable in most areas on the North American craton, inclusive of the Mid-Continent. Gordon and Mamet (1978) recognized a portion of southwestern Oklahoma as one of few places on the craton where continuous sedimentation has occurred across this systemic boundary. Pre-Pennsylvanian subcrop maps constructed in shelf areas of the Anadarko Basin show pinching-out of successively older

strata shelfward, suggesting that erosion was more intense north of the study area (Lyons, 1970). The effects of intense Late Paleozoic erosion in the Mid-Continent are most evident in central Kansas, where Pennsylvanian clastics overlie PreCambrian igneous rock. Paleogeologic mapping (Figure 6) indicates that much of the Mid-Continent was subaerially exposed during the Late Mississippian.

Local Attributes

Continuous sedimentation across the Mississippian-Pennsylvanian systemic boundary did not occur in any portion of the study area. Evidence supporting this statement may be found in the dip-oriented cross-sections (Plates IX - XI) where progressively older members of the Goddard Formation are truncated shelfward beneath the pre-Pennsylvanian unconformity. As previously noted, the author does not consider the Springer Formation to be present in the region. Peace (1965) indicates the Springer Formation exists basinward (south) of the study area.

Method for Interpreting Systemic Boundary from Well Logs

Recognition of the contact between the Pennsylvanian Morrow Formation and underlying Mississippian Goddard Formation on well logs is possible using the conductivity curve generally found associated with the small scale (1" per 100') resistivity (dual induction) log. Correlation between

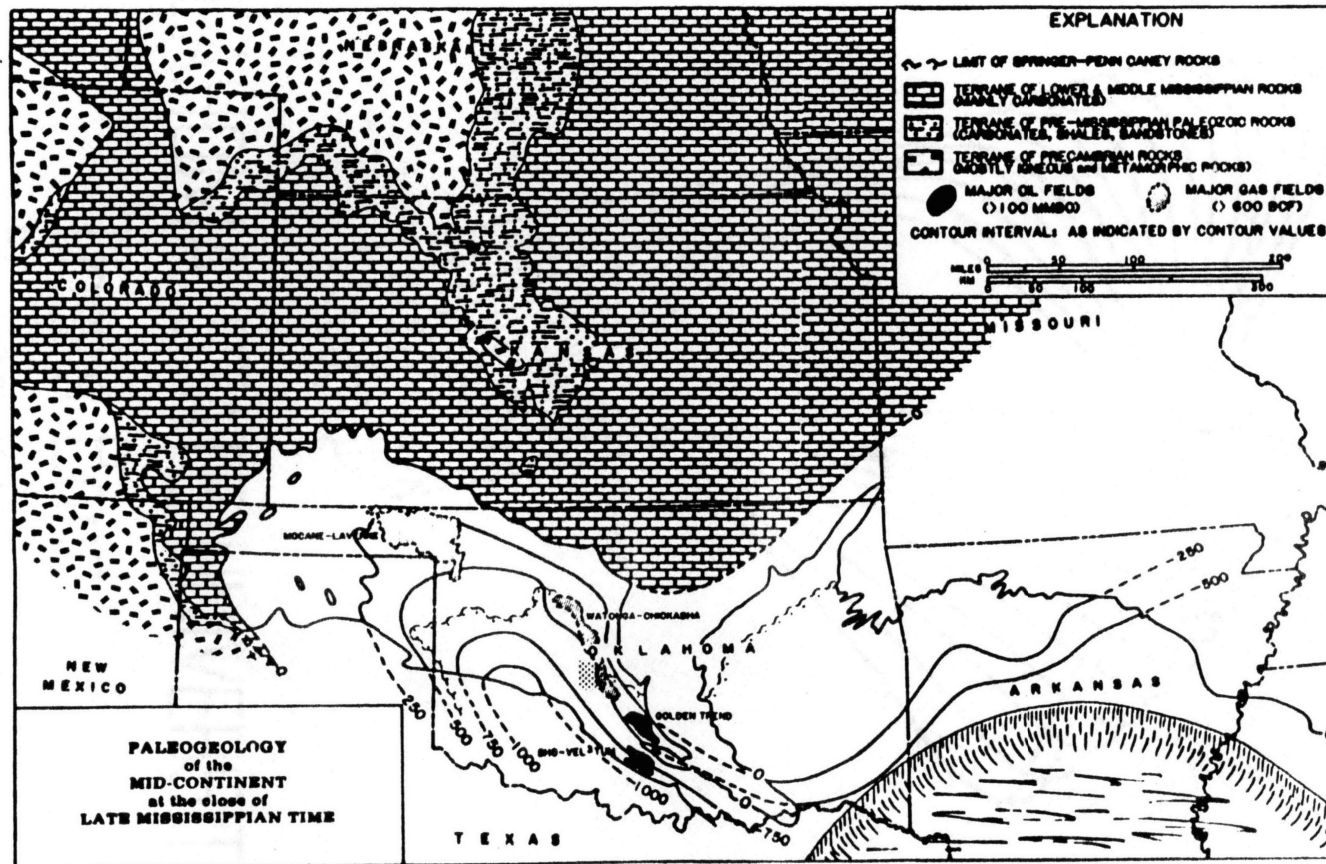


Figure 6. Paleogeology of the Mid-Continent at the Close of the Mississippian (After Rascoe and Adler, 1983)

[Dotted pattern] - Study Area

well logs from the Apexco, Inc. Buell No. 1-A (Section 10-T11N-R12W) and a lengthy core taken from this well suggests that shales of the Springer are much more conductive to electric current than the overlying shales of the Morrow.

This difference in conductivity allows for recognition of the Goddard-Morrow formational boundary, which corresponds to the Mississippian-Pennsylvanian systemic boundary in the thesis area. The relatively poor conductivity of the Morrow shales is attributed to the presence of thinly interbedded sandstones within the shaly intervals. In comparison, shales of the Springer generally are devoid of sand.

The first leftward deflection of the conductivity curve below correlatable lower Morrow sand units that is greater than 650 millimhos-m was chosen to represent the boundary between the Mississippian Goddard Formation and the Lower Pennsylvanian strata. Due to variations in the calibration methods of logging tools among service companies the 650 millimhos-m cutoff point was used with discretion. This method was used throughout the study.

Evidence supporting the use of the conductivity curve to differentiate between these two systems is shown in the dip-oriented cross-sections (Plates IX - XI). Successively older members of the Goddard Formation pinch out shelfward against the inferred contact in each cross-section. Additional evidence was contained within a core from the Apexco, Inc. Buell No. 1-A. The pre-Pennsylvanian unconformity is within two stacked sand bodies, the upper of the Penn-

sylvanian Morrow Formation and the lower of the Mississippian Goddard Formation. The contact between these units was erosional with load casts immediately underlying the boundary. The Morrow sand was clay-rich and not well-sorted in comparison to the underlying sand body of the Goddard Formation. After correcting the core to well-log depth the unconformity was found to be seven feet high to the boundary inferred on well logs.

The small amount of variation between the actual and inferred systemic boundaries of the Apexco, Inc. Buell No. 1-A demonstrates the error inherent in use of the previously described technique. The unconformity in the Buell No. 1-A was chosen on well logs at the point where the conductivity value surpassed 650 millimhos, which corresponds to the base of the Goddard Formation sand unit. The systemic boundary could not be chosen from well logs at the exact point within the stacked sand units. In Figure 7, the Apexco, Inc. Buell No. 1-A well log shows positions of the actual and inferred systemic boundaries.

Well logs from the regional cross-sections (Plates VII-XI) also serve as examples of the inherent error involved when choosing the stratigraphic position of the pre-Pennsylvanian unconformity from the conductivity curve. A review of the five regional cross-sections indicates that in 15 of 26 well logs the Mississippian-Pennsylvanian contact was chosen at the base of a sandstone, suggesting that the boundary is within a sequence of stacked sandstones. Most

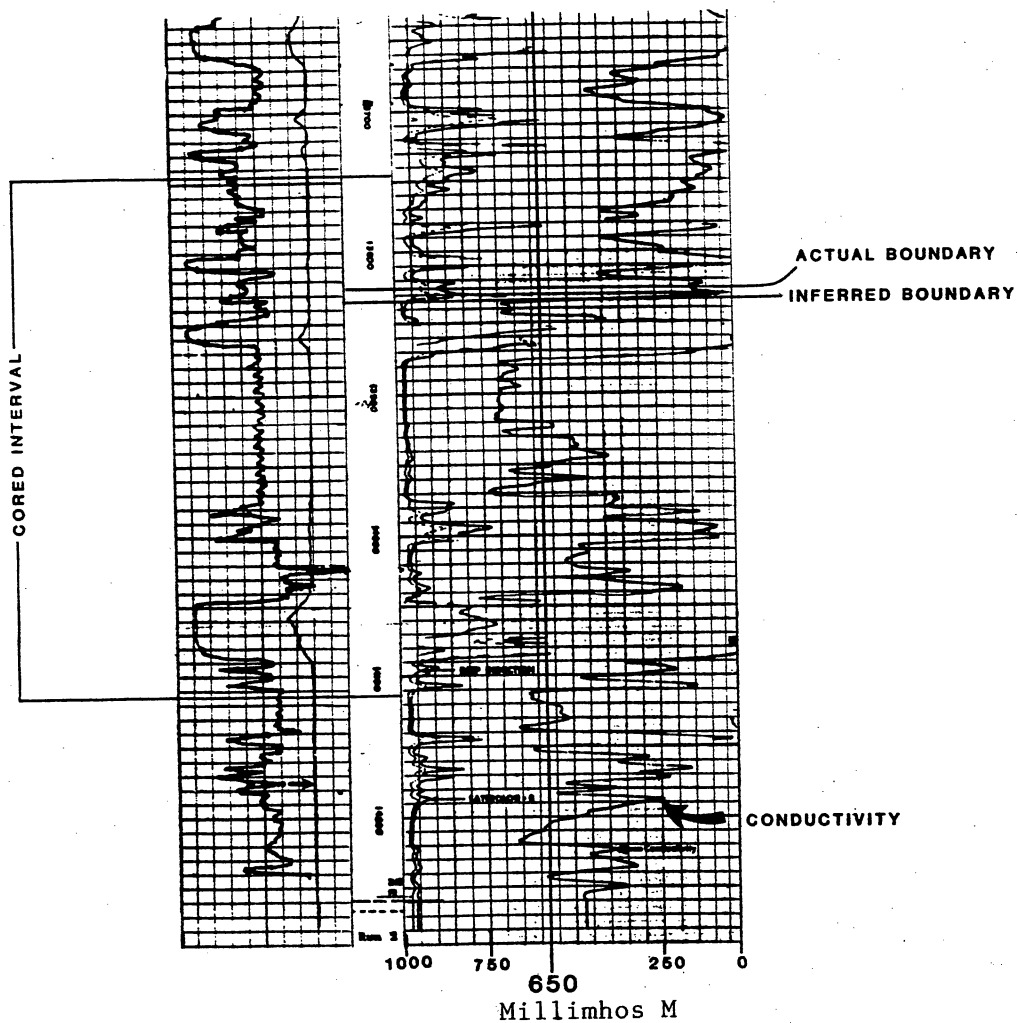


Figure 7. Interpretation of Mississippiian-Pennsylvanian Unconformity from Well Logs. Well Log from Apexco, Inc. Buell No. 1-A, Section 10-T11N-R12W, Caddo County, Oklahoma

of these sandstone bodies are less than twenty feet thick. The margin of error is small and one that is acceptable operationally, considering the fact that within the area of investigation, the average thickness of the Springer Group (Goddard Formation) is more than 400 feet.

Conductivity can be calculated from resistivity logs by the use of this simple formula:

$$\text{Conductivity} = 1000/\text{Resistivity}$$

Although resistivity may also be used to differentiate between Pennsylvanian and Mississippian strata the scale used to present conductivity shows a more pronounced difference and thus, the boundary is more readily recognizable.

Jacobsen (1959) is believed to be the first author to use the conductivity curve for the purpose of distinguishing between Mississippian and Pennsylvanian clastic sediments in the southeastern part of the Anadarko Basin. The described method was used to select the systemic boundary on type logs for the thesis area. This includes the logs of Apexco Inc. Buell No. 1-A. Scout-ticket "calls" by various petroleum exploration companies active in the thesis area indicate that usage of the conductivity-curve method in some form is widely accepted.

Depositional Hiatus Between Cunningham and Britt Members

Analysis of regional dip-oriented cross-sections

(Plates IX - XI), gross-sand maps of the Upper and Lower Britt submembers (Plates III - V), and the Apexco, Inc. Buell No. 1-A core suggests that a break in deposition is shown in the normal stratigraphic succession between the Britt and Cunningham members of the Goddard Formation. Evidence for the existence of this stratigraphic feature is as follows:

- 1) The Upper Britt submember is of an offlapping nature. Dip-oriented cross-sections (Plates IX - XI) show pinchout of the Upper Britt to the northeast.

- 2) The Upper Britt submember is absent in the Apexco, Inc. Buell No. 1-A, as determined from incorporation of data from the regional stratigraphic cross-sections and core from this well. The contact between a massive fine-grained Lower Britt sandstone and the overlying, sparsely fossiliferous, black, fissile Cunningham shale is sharp, with load features and evidence of scouring (Figure 8).

Two hypotheses have been developed regarding the nature of the anomalous section. (1) Assuming that the nature of the contact is truly erosive, Upper Britt strata were removed by erosion over much of the study area, leading to the offlapping geometry observed on dip-oriented cross-sections (Plates IX - XI). (2) A sediment-bypass system deposited marine Upper Britt sediments parallel to the paleoshoreline. Lower Britt deposits shelfward of the area of active Upper Britt deposition were exposed subaerially but subjected to little erosion. The source of these sediments was located



Figure 8. Core from the Apexco, Inc.
- Buell No. 1-A demonstrating erosional contact between Lower Britt sandstone and black, laminated, sparsely fossiliferous Cunningham shale.

outside the area of investigation. The second explanation does not account for the sharp contact and scouring noted between the Lower Britt sandstone and Cunningham shale in the Apexco, Inc. Buell No. 1-A core.

Additional evidence from cores and from mapping of the Britt member basinward of the study area is needed for a more complete analysis. The approximate shelfward extent of Upper Britt strata is demonstrated in gross-sand isopach maps (Plates IV and V).

CHAPTER III

STRUCTURAL FRAMEWORK

Introduction

The area of interest is located within the Anadarko Basin, an ultra-deep, asymmetric, intracratonic basin. The Anadarko Basin is the largest element of several north-northwesterly trending basins and uplifts located between the Ouachita Fold Belt of southeastern Oklahoma and Sierra Grande Uplift of northeastern New Mexico (Figure 9). Tectonically-related fragmentation of a single large basin with origins in the Late Precambrian began during the latest Devonian and continued into the Pennsylvanian (Feinstein, 1981). A series of smaller basins was created, which includes the Anadarko, Ardmore, Marietta, and numerous smaller basins.

Major positive features delineating boundaries of this petroliferous basin are the northwest-trending Central Kansas Uplift to the north, the Amarillo - Wichita Uplift to the south, the Arbuckle Uplift and Nemaha Ridge to the east, and the Apishapa Uplift of southeastern Colorado to the northwest (Figure 9).

The Nemaha Ridge (Figure 9), a positive structural

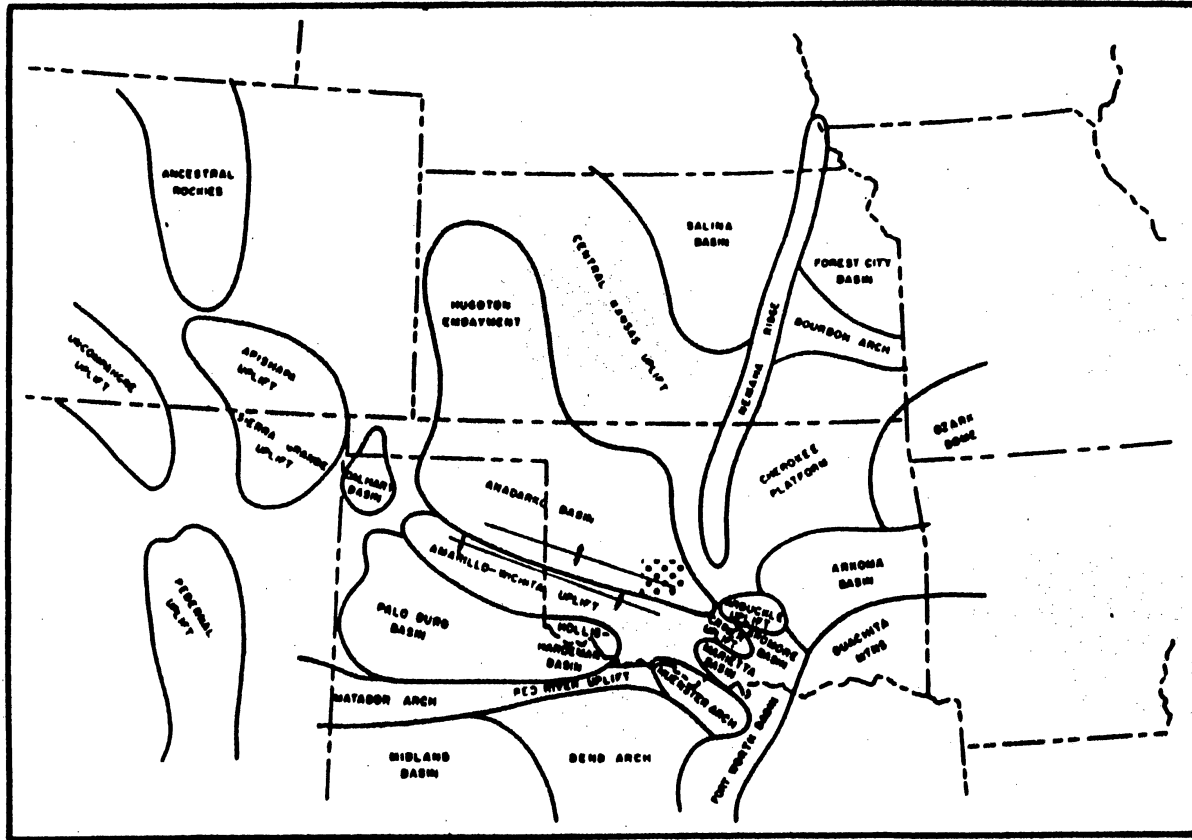
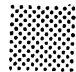


Figure 9. Principle Pennsylvanian Physiographic Features of the Southern Mid-Continent (After Moore, 1979)

 - Study Area

feature extending from southeastern Nebraska to south-central Oklahoma, may have influenced directly deposition of Morrowan and Chesterian clastic sediments. Rocks of the Upper Mississippian through Lower Pennsylvanian are absent across this element as a result of non-deposition or erosion. Therefore, timing of initial movement of the Nemaha Ridge is questionable.

Episodes of Structural Activity in the Anadarko Basin

Two major episodes of structural activity affected the southeastern Anadarko Basin after the Middle Mississippian. The onset of rapid subsidence and the change from carbonate- to clastic-dominated sedimentary facies during the Late Mississippian reflect a distinct change in the structural style of the region (Evans, 1979; Garner and Turcotte, 1984). During this time the initial phase of the Amarillo-Wichita orogenic episode began involving southwestern Oklahoma and the Texas Panhandle. Compression, resulting in vertical block uplifting (down-to-the-basin normal faulting) with displacements in excess of 20,000 feet characterized this orogenic event, which continued through the Middle Pennsylvanian (Evans, 1979; Garner and Turcotte, 1984). An idealized cross-section (Figure 10) demonstrates vertical block uplift associated with the Amarillo-Wichita Uplift.

Additional information regarding the initiation of the

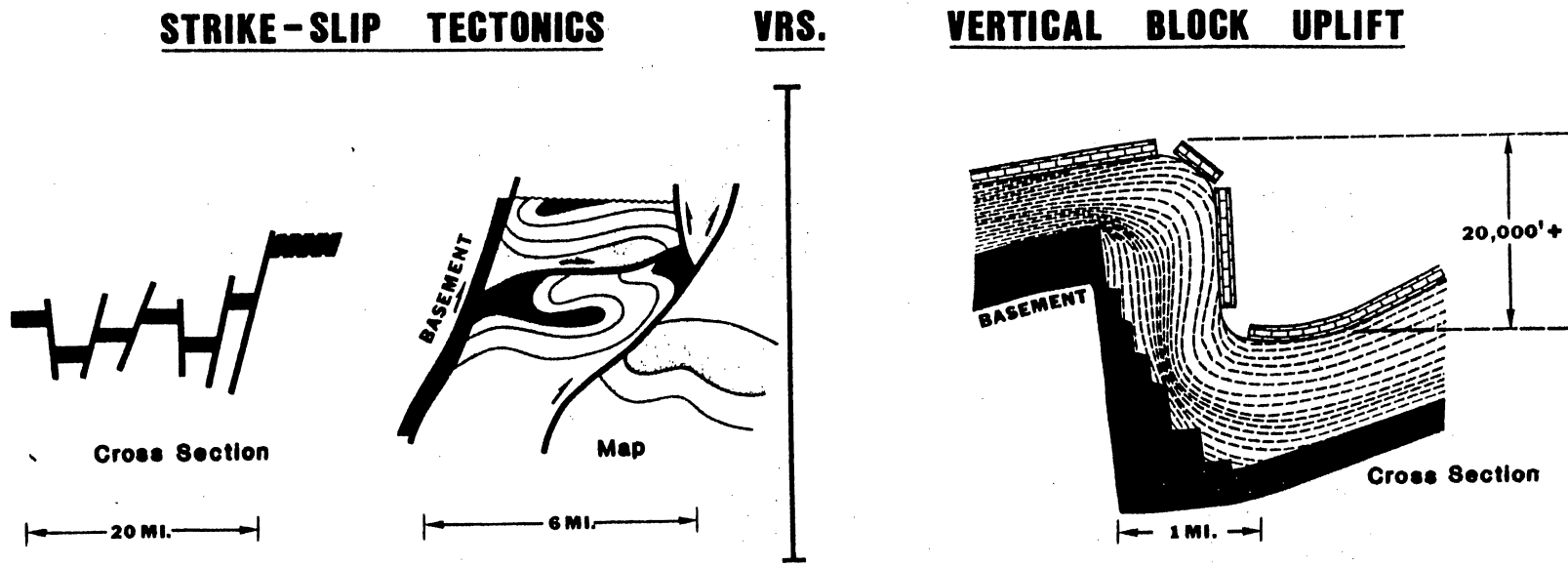


Figure 10. Types of Deformation Along the Wichita Mountain Front (After Evans, 1979)

Amarillo-Wichita Orogeny is inferred by unique changes in the sedimentation pattern. Jacobsen (1959) reported beds of conglomerate in the lower portions of the Goddard Shale (Figure 4) in the Anadarko Basin. Similiar conglomeratic units were noted by Beckman and Sloss (1959) in the Ardmore Basin in strata equivalent to the Goddard Shale. Each of these authors interpreted the conglomerates to represent the beginning of uplift. Well-known examples of conglomerates recording uplift include the Fountain Formation of central and south-central Colorado and the highly-productive hydrocarbon-bearing Atokan "granite wash" deposits of Beckham County, Oklahoma, and Hemphill County, Texas.

A second major orogenic episode, the Arbuckle Uplift, began during the Middle Pennsylvanian. This tectonic event greatly affected the structural composition of the Mid-Continent, especially that of southern Oklahoma (Rascoe and Adler, 1983; Garner and Turcotte, 1984). A left-lateral shear component developed along faults created during previous tectonic activity (Figure 10) (Evans, 1979; Donovan, 1985). This uplift is characterized by narrowing of the depositional trough and is responsible for creating the Arbuckle Mountains of south-central Oklahoma. Maximal downwarping in the Anadarko Basin was recorded during this tectonic cycle by an extremely thick section of Morrowan and Atokan sedimentary rocks (Evans, 1979; Garner and Turcotte, 1984). The Arbuckle Orogeny ended in the Permian.

Local Structural Geology

Local structural geology reflects the influence of basinal downwarping and both the aforementioned tectonic events. Two structural contour maps of the thesis area were constructed; the "Britt Marker" and the Mississippian-Pennsylvanian unconformity served as datums. The "Britt Marker" is an excellent stratigraphic marker discernible in logs of virtually every well-bore in the study area that is of sufficient depth. Two structural contour maps (Plates I and II) were necessary to interpret the horizontal component of the normal faults that are in the thesis area.

The regional structural style characteristic of the Anadarko Basin is represented in Plates I and II. Structure is represented by gentle warping with strike N50 - 60 W. Structural dip is southwestward. Dip steepens basinward; in the northeastern portions of the region (T12N-R10W) dip is approximately 2.0°, increasing to about 3° in central areas (T10N-R12W), and is as much as 4° in the southeastern part (T9N-R12W).

At least two faults are present within the study area. Both the faults that are mapped are down-to-the-basin normal faults, oriented subparallel to the hingeline of the Anadarko Basin (Figure 1). The attitude and orientation of the fault plane suggests that these faults were created by vertical block movement relating to the Amarillo-Wichita Uplift. Structural-contour mapping indicates closure

associated with both faults. These faults will be discussed in greater detail in following paragraphs.

A minor fault is located within the Canadian County portion of the thesis area (T11N-R10W). The trend of this fault is approximately N75° W with maximal throw of 250 feet (Plate I - Section 15-T11N-R10W). A comparison of Plates I and II indicates that the fault plane is essentially vertical, a characteristic of faulting associated with the Amarillo-Wichita Uplift (Evans, 1979).

A major fault with maximal throw of 1,400 feet (Plate I - Section 25-T10N-R13W) is located in the southwestern portions of the thesis area (T10N-R13W through T9N-R11W). The nature of this fault is similar to that of the fault described previously, except for magnitude and trend. The strike of N60° W more closely follows regional depositional strike. Executive Reference Map 311 (GeoMap, 1981) indicates that this fault extends northwestward outside the study area. A review of the literature yielded no reference to this tectonic feature. Henceforth, the term "Eakly Fault" shall be used in reference to this normal fault.

A comparison of well logs in the vicinity of the Eakly Fault to those located more shelfward (north) indicates that the Cunningham Member (Figure 4) thickens significantly basinward. Thickness of the Cunningham increases abruptly on the downthrown side of the fault. Such an observation suggests that upper portions of the Springer Group were eroded extensively prior to deposition of the Morrow Formation.

These additional strata were classified as part of the Cunningham member because they lie below the Mississippian-Pennsylvanian unconformity and above older Cunningham strata correlated from the upthrown side (north) of the Eakly Fault. The stratigraphic position of the additional section is illustrated diagrammatically in Figure 11.

Pre-Pennsylvanian erosion removed the Springer Group in far east-central and northeastern portions of the thesis area (Plate VI). Lower Pennsylvanian clastics lie directly upon the Mississippian Caney Formation. The line of truncation of the Springer Group extends in a north-north-westerly direction, whereas depositional strike of the Springer Group is more west than north. This observation suggests that erosion occurred not only as a result of the withdrawal of the epicontinental sea into the depositional trough, but may have been initiated also by uplift east of the study area. Two positive structural elements are east and northeast of the study area; They may be related to this truncation pattern. Peace (1965) suggested that the Pauls Valley Uplift of central Grady County (Figure 2) could have led to the elevation of the area of investigation. Another alternative is uplift of the Nemaha Ridge (Figure 9) with initial movement during the Late Mississippian or Early Pennsylvanian. The southern end of this element is located northeast of the study area. Further regional investigation beyond the scope of this study is needed to establish timing of initial movement of the aforementioned

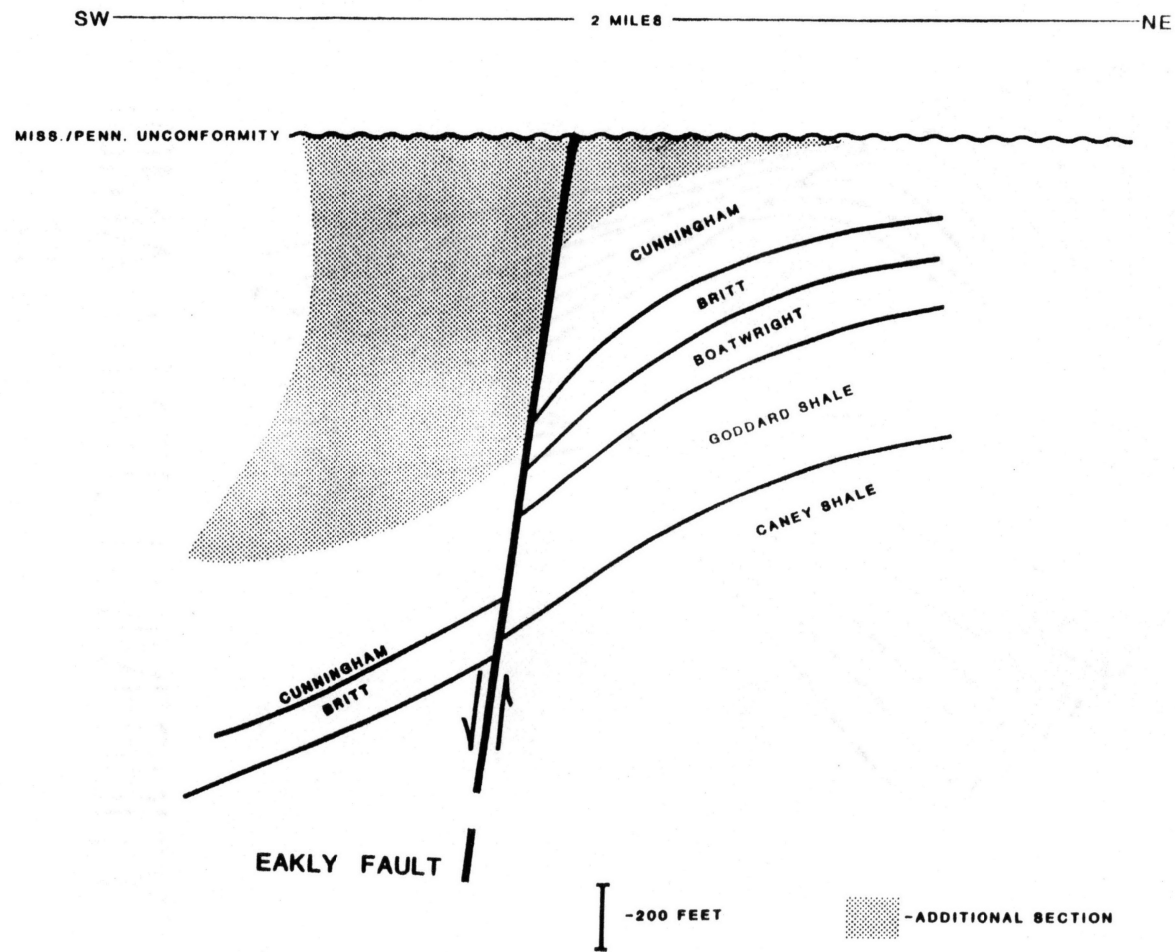


Figure 11. Stratigraphic Position of Additional Cunningham Strata on Downthrown Side of Eakly Fault

structures.

The Fort Cobb Anticline, the axis of which extends through the southwesternmost portions of the study area (T9N-R13W), is one of a series of four anticlines (Fort Cobb, Cordell, Sayre, Mobeetie) interpreted by Evans (1979) to have formed as a result of the Arbuckle Orogeny. Evans (1979) suggested these folds represent the classic sinusoidal pattern of folding associated with strike-slip tectonics; they have nearly parallel axes, which intersect the preserved shear plane at an angle of approximately 30° . In this instance, the shear plane would have been the Atokan reactivation of near-vertical faults that formed during the Amarillo-Wichita Uplift (Evans, 1979). Locations of the Fort Cobb and Cordell Anticlines within the regional structural framework are illustrated in Figure 12. Although the axis of the Fort Cobb structure passes through the southwesternmost portions of the thesis area, a lack of deep wells curtailed mapping of this element at depth.

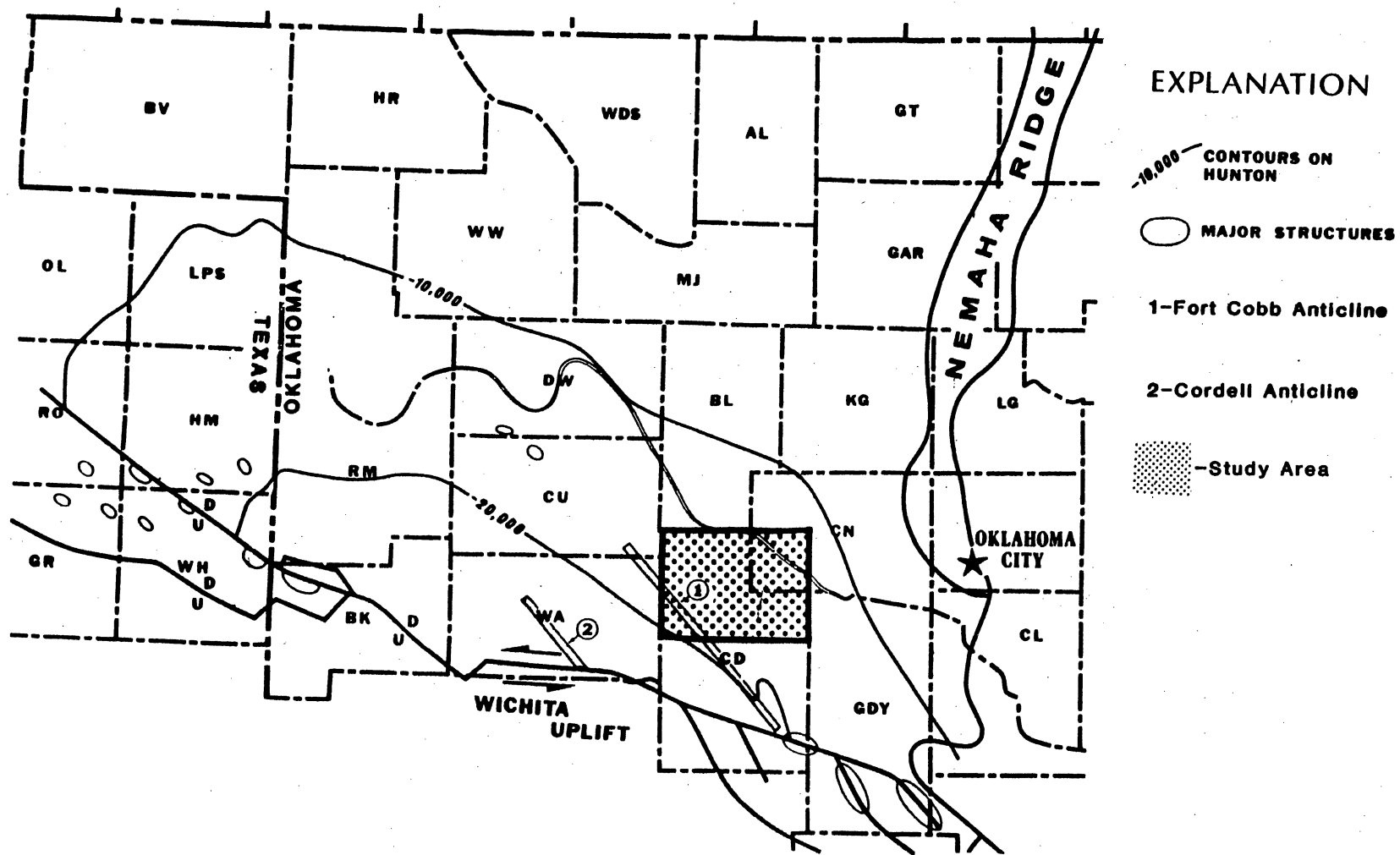


Figure 12. Major Structural Features of Western Oklahoma
(After Evans, 1979)

CHAPTER IV

PETROLOGY, DIAGENESIS, AND POROSITY

Introduction

Britt sandstones are predominantly quartzitic with bioclastic debris and ooids the dominant components, locally. Britt "sands" contain trace amounts of feldspar, rock fragments, heavy minerals, and glauconite. Detrital clay matrix, dependent on the environment of deposition, was found in abundance. Numerous episodes of diagenesis have altered extensively the mineralogical character of these sands. The interrelationship between the detrital components of Britt sands and shales and the chemical reactions that occurred at depth has resulted in the partial preservation of original porosity and the creation of secondary porosity. Mechanical compaction of these sediments has resulted in the ductile deformation, suturing, and fracturing of grains.

Techniques employed in the petrologic and diagenetic study of Britt sandstones included use of standard petrographic microscopy, staining of thin sections with Alizarin S, potassium ferricyanide, and sodium cobaltinitrite, and scanning electron microscopy (SEM). Types and percentages of constituents in sandstones of the Britt are presented in

Tables I through VIII in Appendix C.

Pertaining specifically to Britt sandstones, the primary purposes of this chapter are to: 1) describe the detrital and authigenic constituents, 2) relate the presence of authigenic minerals to processes responsible for their formation, 3) establish the chronologic order of diagenetic events which have affected Britt sandstones and, 4) describe those factors which contributed to the preservation of primary porosity and to the formation of secondary porosity.

Detrital Constituents in Britt Sandstones

Britt sandstones are quartzitic, generally lacking all but trace amounts of feldspar, rock fragments, heavy minerals, and glauconite. Detrital clays and siliceous matrix were abundant in many samples of sandstones. The purpose of this section is to describe briefly the detrital components found in Britt sandstones. Constituents will be described in order of abundance.

Quartz

Quartz is the primary component in Britt sandstones. Plutonic, volcanic, and metamorphic varieties were recognized in thin section; plutonic quartz is the dominant type. Volcanic and metamorphic varieties were found only in trace amounts. Recognition of these three varieties was based on criteria proposed by Krynine (1946) and Folk (1974).

Plutonic quartz is monocrystalline with sub- to anhedral crystals. This type possesses low birefringence under crossed polarizers, few microlites and vacuoles, and straight to slightly undulose extinction. Volcanic quartz in Britt sandstones is idiomorphic with straight extinctions. Grain embayments are the prominent diagnostic feature. Microlites and vacuoles are rare in volcanic quartz but can be diagnostic when concentrated in bands paralleling the margins of individual grains (Scholle, 1979). Metamorphic quartz is polycrystalline with extinction ranging from straight to undulose. Many crystals are elongated, possessing straight to crenulated boundaries.

Detrital Clay Matrix

Detrital clay matrix was found in abundance in Britt sands that were deposited in relatively low-energy environments. Distinguishing between authigenic and detrital clay is difficult in some thin sections. One criterion for recognizing detrital clay is the presence of grains "floating" in a clay matrix. This implies that the clays were deposited at the same time as the grains. This was the case in Britt sandstones (Figure 13). Clays in the Britt possess a greenish tint under plane-polarized light and appeared to "flow" around grains. Minor amounts of detrital clay are associated with sedimentary rock fragments.

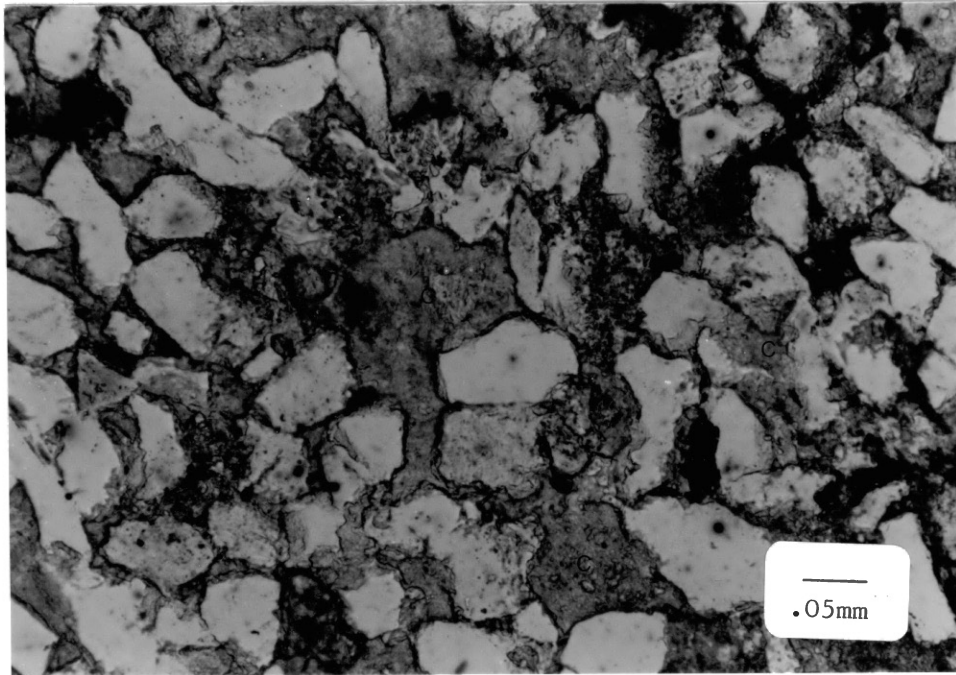


Figure 13. Photomicrograph of authigenic chlorite (C), recrystallized from detrital clay matrix, supporting detrital grains. This evidence indicates that the clay originally was allogenic.

Fossils

Fossils are the primary constituent in some Britt sandstones. Sands composed of bioclastic material admixed with as much as 70% quartz have been termed "coquinoid sandstones" (Brenner and Davies, 1973). Bioclastic material was found in virtually every thin section analyzed. Major types of fossils, in decreasing order of abundance, included echinoderms, brachiopods, and pelecypods. Other varieties included corals, ostracods, bryozoans, and trilobites. Bivalved shells were generally disarticulated with many fragmented or fractured.

Varieties of echinoderms present within Britt sandstones include echinoids and crinoids with the former more abundant. These types of echinoderms may be distinguished by the arrangement of pores on their plates. In crinoids, pores are arranged in a random fashion. Echinoids show an ordered arrangement with rows of pores aligned in parallel. Echinoderm tests were composed originally of calcite. Some are as large in diameter as 2 mm.

Brachiopods of the Britt have a low-angle fibrous wall structure and are impunctate to pseudopunctate. Rare forms possess a thin, prismatic outer wall in association with the fibrous wall. Brachiopod shells were originally calcitic and were as large as 3 cm, although average length is less than 8 mm. Bored shells were noted in thin section.

Pelecypods were recognized only by the characteristic

shapes of their shells. The originally aragonitic shells have inverted to calcite or dolomite, thus obliterating all shell structure. Pelecypod shells in Britt sandstones are much more fragmented than the brachiopod shells with which they were associated; this suggests that brachiopod shells were stronger and more resistant to abrasion. This characteristic may be attributed to the original composition or structure of the shell.

Ooids and Coated Grains

Ooids compose more than 75% of the constituents in certain lithologic units in the Britt. Such units were applicably termed limestones, and more specifically, oosparites (Folk, 1962). Although ooids were the primary component of these sediments, quartz was the dominant mineral at some places. This was due to the presence of fine- to medium-grained quartz, which served as the nuclei for the majority of the ooids (Figure 14). Fragments of fossils also commonly served as nuclei (Figure 14) along with rare rock fragments and feldspar grains. Ooids typically are medium-grained in the Britt, attesting to the high energy of their environment of formation.

Coated grains are defined in this research as detrital grains possessing a thin micritic coating (less than .1 mm), which may or may not completely cover the grain. Grains with micritic coatings that exceeded .1 mm were classified as coated grains if the coating did not completely cover

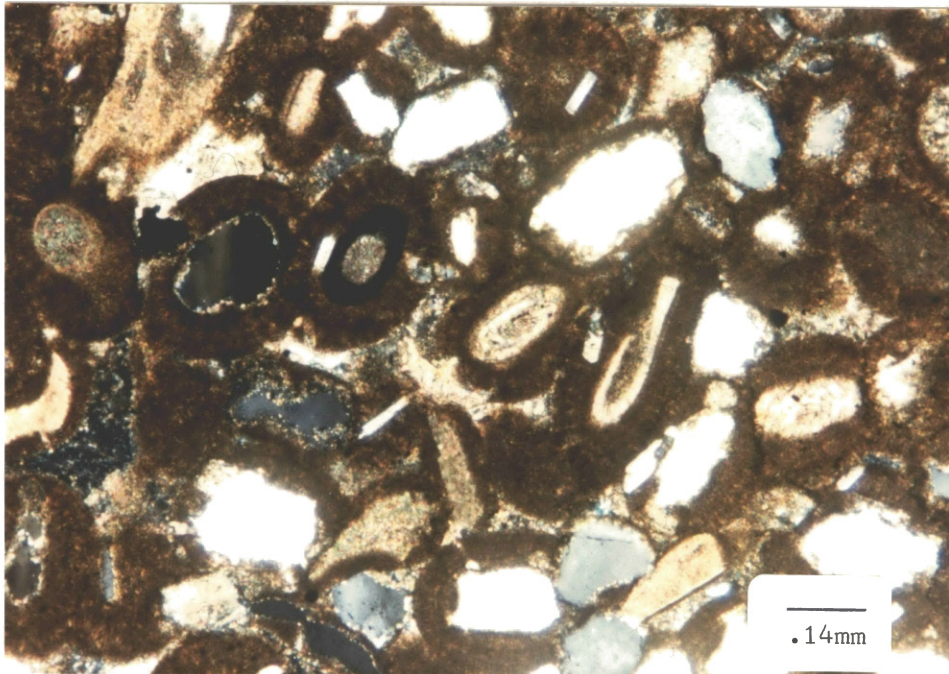


Figure 14. Photomicrograph of oolitic limestone unit with medium-grained detrital quartz grains (Q) and fossils (F) serving as ooid nuclei.

the nucleus. In comparison, ooids possess micritic coatings in excess of .1 mm which completely cover the nucleus. Coated grains commonly are associated with oolitic units. Coated grains were included with ooids during point-counting.

Siliceous Detrital Matrix

Siliceous detrital matrix is composed of silt-sized quartz grains. This constituent commonly was found in immature Britt sands and along stylolites where they originated from partial disintegration of detrital quartz.

Feldspars

Trace amounts of plagioclase and potassic feldspars were found in Britt sandstones with the former the dominant variety. Plagioclase feldspars exhibited albite twinning. Potassic varieties were recognized by diagnostic grid twinning. Several slides were stained with sodium cobaltinitrite solution. Sanidine, a untwinned potassic feldspar, then was readily recognizable.

Rock Fragments

Rock fragments in Britt sandstones occur in trace amounts and are of sedimentary or volcanic origin. Sedimentary rock fragments (SRF) are composed of shale or siltstone, generally, and are well-rounded. These grains are dull brown under plane polarized light and exhibit low

birefringence under crossed nichols. Volcanic rock fragments (VRF) are recognized by their aphanitic texture. These grains are very rare.

Other Detrital Grains

Other detrital grains in Britt sandstones include zircon, muscovite, hornblende, and biotite, with each in trace amounts. Zircon was observed in nearly every thin section and was the most abundant heavy mineral. The relative abundance of this grain type can be attributed to its low solubility (i.e. resistance to weathering). Zircon grains are well-rounded, exhibit extremely high relief in thin section, and demonstrate strong to extreme birefringence. They commonly are concentrated along bedding planes. Muscovite is much more common than biotite due to greater chemical stability. Muscovite grains are elongated or blade-like and show high birefringence. Hornblende is also rare in Britt sandstones. This mineral was recognized by its pleochroic nature and variation in grain color from the grain margin inward, under crossed polarizers. Biotite grains are elongated, show excellent cleavage, and are pleochroic. Color varies through shades of yellow, brown, and green.

Glauconite

Glauconite is a phyllosilicate that generally is rare. However in certain units of the Britt it is abundant. Both brown and green varieties were observed in thin section with

40

brown the dominant type. Variation of color is due to the difference in the oxidation state of iron in the crystal structure of glauconite. Oxidized iron (ferrous - Fe²⁺) is in the crystal structure of brown glauconite whereas the reduced state of iron (ferric - Fe³⁺) is associated with the green variety (Al-Shaieb, 1986). Glauconite grains are well-rounded and may be of fecal origin. They commonly are concentrated along bedding planes.

Authigenic Constituents in Britt Sandstones

Britt sandstones have been subjected to numerous episodes of diagenesis. Volumetrically, silica and carbonate cements, along with chlorite, are the more important authigenic minerals. The purpose of this section is to describe the authigenic minerals in Britt sandstones.

Authigenic Clays

Authigenic chlorite, kaolinite, and illite were found in Britt sandstones. Chlorite is very abundant with only trace amounts of kaolinite and illite present. Chlorite was recognized in thin section by its greenish tint under plane polarized light. Analysis of Britt sandstones by scanning electron microscopy indicated chlorite to have a platy or bladed appearance with an edge-to-face relationship with detrital grains (Figure 15). Chlorite filled pores or coated grains (Figure 15). Kaolinite also filled pores in

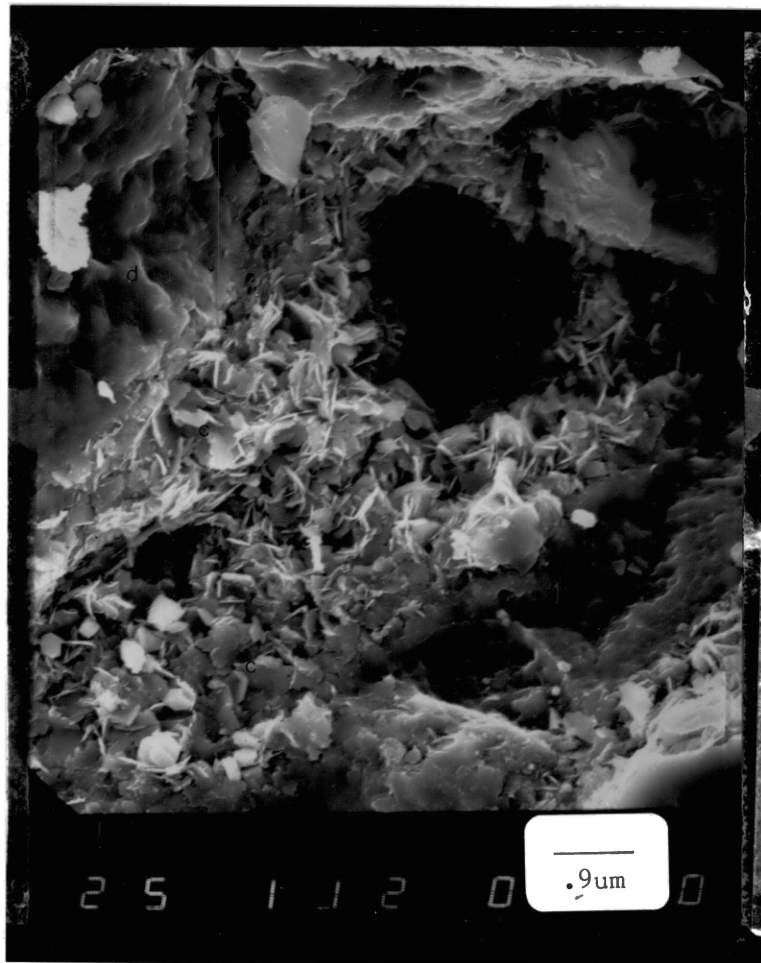


Figure 15. SEM Photomicrograph. Platy authigenic chlorite (C) shows edge-to-face relationship with detrital grains (D). Magnification - 2000X.

Britt sandstones. This authigenic constituent possesses well-developed pseudohexagonal crystals in a stacked vermicular or "worm-like" arrangement. Illite occurred as a by-product of the alteration of feldspars in Britt sandstones. Many feldspar grains were completely altered to illite, retaining the original shape of the feldspar (as observed with the scanning electron microscope).

Siliceous Cements

Four types of authigenic siliceous cements were recognized in Britt sandstones. Syntaxial quartz overgrowths are very common with chert cement abundant locally. Chalcedony and drusy megaquartz are extremely rare. Stages of syntaxial quartz-overgrowth cementation range from early to advanced. This variety of silica cement accounts for as much as 25% of the rock by volume (Figure 16). Detrital quartz grains subjected to this type of cementation show well-developed idiomorphic overgrowths (Figure 17), which form in optical continuity with quartz grains. Unlike many sandstones, the percentage of syntaxial quartz overgrowths in Britt sandstones can be attained by point counting, due to the thin, chloritic dust rims between overgrowths and detrital grains (Figure 16).

Chert is either pore-filling cement (Figure 18) or an alteration of siliceous detrital grains. This authigenic cement composes as much as 20% of the rock by volume. Chert was recognized in thin section by its polycrystalline habit

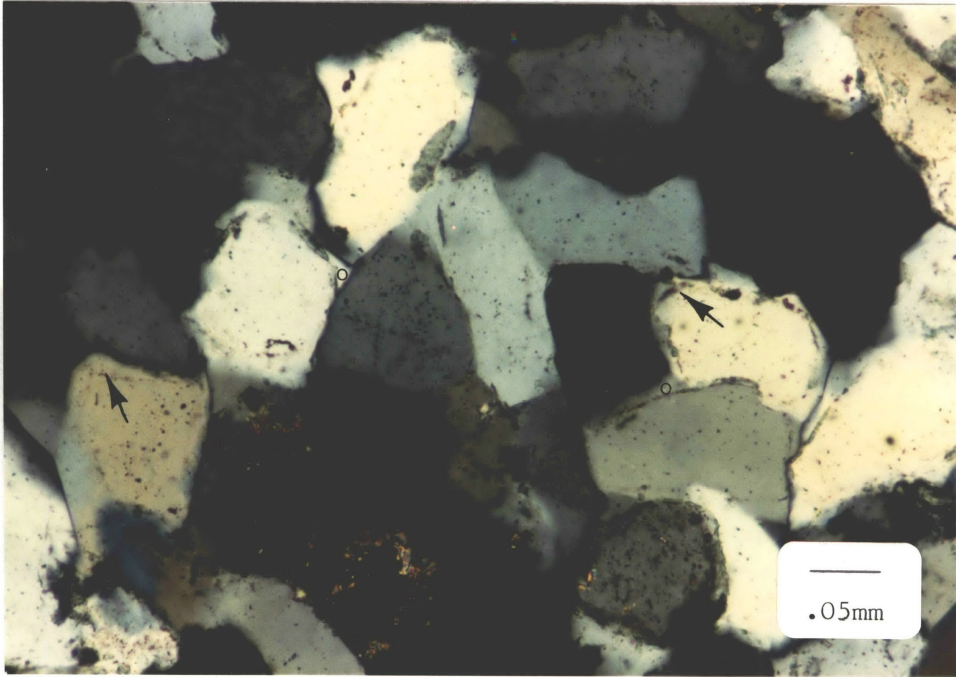


Figure 16. Photomicrograph illustrating advanced syntaxial-quartz-overgrowth cementation (O). Note chlorite dust rims (arrows) between detrital grains and overgrowths.



Figure 17. SEM Photomicrograph. Syntaxial quartz overgrowths in a quartzitic sand. Magnification-3000X.

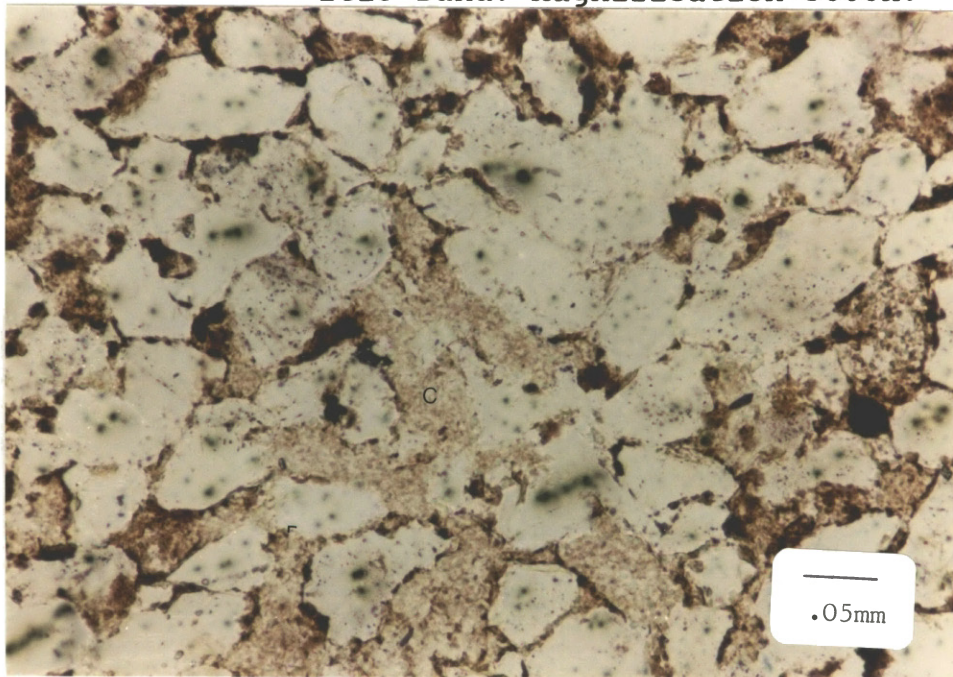


Figure 18. Photomicrograph. Chert cement (C) fills pores between detrital grains. Chert characteristically is light brown under plane polarized light.

and typical light brown color under plane polarized light.

Drusy megaquartz was found as a grain lining in Britt sandstones with the long axis of individual crystals perpendicular to the margins of detrital quartz grains, on which individual crystals were precipitated. In rare instances, megaquartz was found as a replacement fabric associated with chert.

Chalcedony was recorded in only one thin section. It precipitated as a pore-filling cement in a highly quartzitic sand. Chalcedony has a fibrous, radiating habit.

Carbonate Cements

A variety of carbonate cements was found in Britt strata. This includes siderite, aragonite, calcite, and ferroan and non-ferroan varieties of dolomite. Dolomite was the dominant carbonate cement, generally occurring as a pseudomorphous replacement of calcite.

Siderite was found as thin, elongated nodules in shales of the Britt (Figure 19). These authigenic nodules have reddish brown color and they distorted the laminated shales in which they precipitated. No siderite was found in Britt sandstones.

Aragonite has been altered to more stable calcite or dolomite in Britt sandstones. Crystals are acicular; they precipitated as isopachous rims around fossil fragments. The long axes of individual crystals were perpendicular to margins the grains on which they grew. This cement occur-

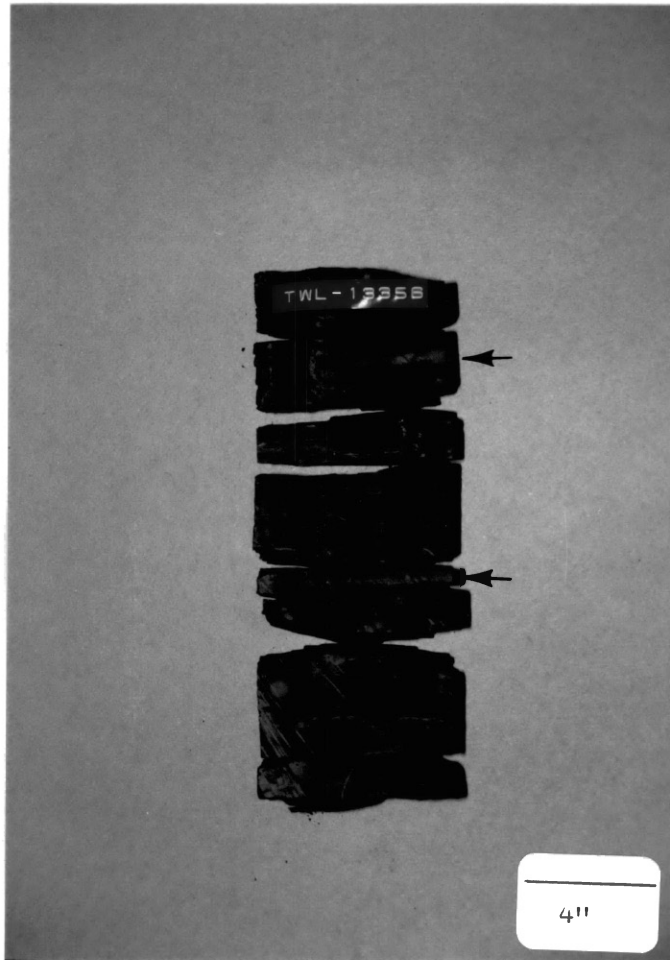


Figure 19. Core photograph demonstrating elongated siderite nodules (arrows) in a prodeltaic shale.

red only in minor amounts and was restricted to highly-fossiliferous (coquinoid) sands.

Several morphological varieties of authigenic calcite are present in the sandstones. Poikilotopic, blocky, drusy, and syntaxial forms were well represented. Each of these cements is pore filling. Poikilotopic calcite cement was found in quartz-dominated sandstones. In this variety, single calcite crystals nucleated from a fossil fragment cement large volumes of the rock (Figure 20). The cement is in optical continuity with the nucleus. Poikilotopic cement composes as much as 40% of the rock by volume in rare instances.

Blocky calcite cement precipitated as numerous crystals, giving it a mosaic appearance where viewed under crossed polarizers. Blocky calcite was found only in highly-fossiliferous (coquinoid) sands. Drusy calcite is a variety of blocky cement. This type is often indicative of void-filling. Crystal size increasing toward the center of the cavity is the diagnostic feature of this carbonate cement. Syntaxial calcite overgrowths are most common on echinoderm plates in sandstones. This cement is in optical continuity with the fossil nucleus; it completely destroyed porosity in echinoderm-rich sediments.

Dolomite occurred extensively as an alteration of calcite cements and fossils. Dolomite was identified by staining thin sections with Alizarin S. Ferroan and non-ferroan varieties are present, with two types of dolomite

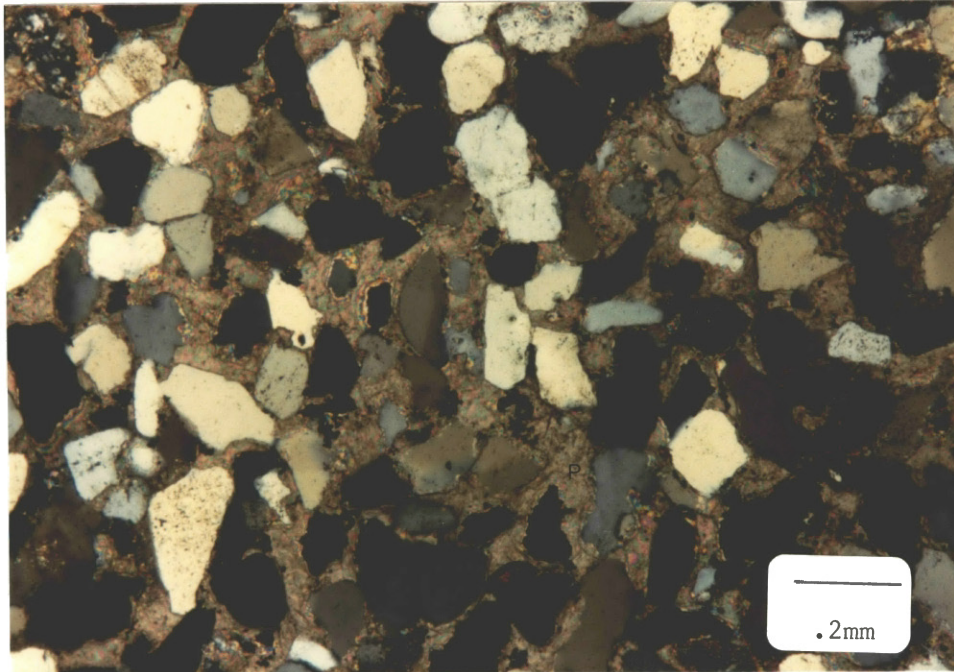


Figure 20. Photomicrograph. Poikilotopic carbonate cement (P) is an early diagenetic mineral. This cement was originally calcite but has been altered to ferroan dolomite.

recognized by crystal shape and extinction pattern. Small, euhedral non-ferroan dolomite crystals (Idiotopic-P) occurred as isolated rhombohedra associated with fossil fragments or carbonate cement. Individual crystals had straight extinctions and were found in only minor quantities. Baroque or "saddle" dolomite replaced fossils and calcite cements (Figure 21). Both ferroan and non-ferroan varieties were recognized in thin section with the aid of potassium-ferricyanide staining. Diagnostic characteristics of baroque dolomite include curved crystal boundaries and sweeping extinction (Xenotopic-C).

Collophane

Collophane is an authigenic phosphate mineral that is the predominant cementing agent of Britt sandstones in rare instances. This mineral is characteristically light brown under plane polarized light. It is isotropic and shows low birefringence. Collophane was found as a replacement of carbonate cements, clays, and the micritic coatings of ooids. Fossils associated with collophane have been altered to apatite. This mineral was not present as a void-filling cement in Britt sandstones.

Pyrite

Pyrite commonly is found in association with organic material and precipitates under reducing conditions. Pyrite

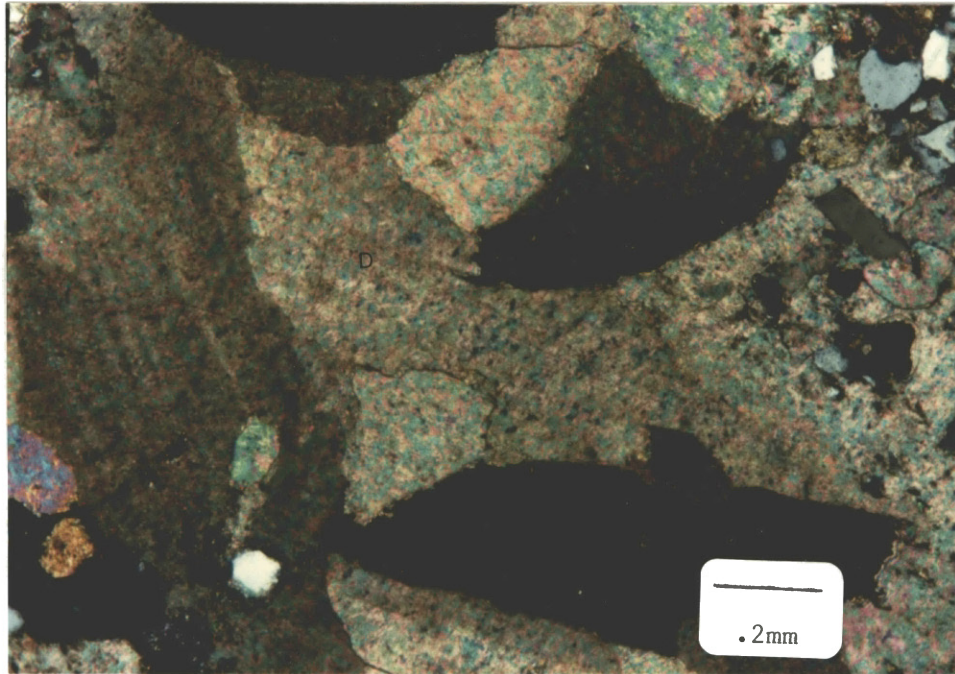


Figure 21. Photomicrograph. Saddle or "baroque" dolomite (D) replaces both fossils and calcite cements. Curved euhedral crystals and undulose extinction are diagnostic of this variety of dolomite. Slide is stained with potassium ferricyanide and Alizarin S.

was observed both as a replacement of detrital and authigenic constituents and as pore-filling cement. This authigenic sulfide mineral was recognized by its yellow-gold color under reflected light. Crystals generally are euhedral when observed under extreme magnification, suggesting a diagenetic origin.

Organic Material

Bitumen and oil are the organic materials in Britt sandstones. These soluble residues are amorphous and brown to black. Bitumen commonly is associated with stylolites. Oil either lines or fills pores. Organic material composed as much as 5% of the rock in localized areas but typically was found in only trace amounts.

Origins of Authigenic Constituents

Numerous articles have been published concerning the origins of authigenic minerals such as those found in Britt sandstones (e.g. Heald and Larese, 1973, Hayes, 1979, Franks and Forester, 1984, and many others). On the basis of mass balance equations, ions that react to form authigenic minerals in many sandstones must be derived, in part, from sources other than the sandstones themselves (Pittman and Larese, 1986). The purpose of this section is to discuss briefly the possible origins and environments of formation of authigenic minerals in sandstones of the Britt.

Several parameters influence greatly the formation of

Detrital Constituents

Quartz

Monocrystalline
Polycrystalline

Clay Matrix

Recrystallized to chlorite in many specimens. Minor detrital illite associated with sedimentary rock fragments.

Skeletal Fragments

Echinoids, Brachiopods, Pelecypods, Corals
Bryozoans, Trilobites

Feldspars

Potassic varieties include microcline and sanidine.
Plagioclase variety is albite.

Rock Fragments

Sedimentary Rock Fragments
Volcanic Rock Fragments

Siliceous Matrix

Commonly associated with stylolites.

Glauconite

Brown and green varieties were recognized.

Other Constituents

Zircon, Muscovite, Hornblende, Biotite

Figure 22A. Detrital Constituents in Britt Sandstones. Abundance decreases from the top.

Authigenic Constituents

Clays

Chlorite
Illite
Kaolinite

Silica

Syntaxial Overgrowths
Chert
Drusy Megaquartz
Chalcedony

Carbonate Cements

Dolomite
 Ferroan baroque dolomite (Xenotopic C)
 Non-ferroan dolomite (Idiotopic E)
Calcite
 Poikilotopic
 Blocky
 Drusy
Siderite
Aragonite
 Acicular

Other Constituents

Pyrite, Organic Material, Collophane

Figure 22B. Authigenic Constituents in
Britt Sandstones. Abundance
decreases from the top.

authigenic minerals in sandstones. These factors include time, temperature, pressure, chemistry of formation water, composition of detrital grains, and the generation of hydrocarbons. For this research, diagenetic environments are categorized as either shallow or deep.

Shallow diagenesis occurs at or near the surface, in water influenced by the surface environment. Deep-burial diagenesis occurs in strata not affected by surficial influences. It is beyond the scope of this research to give a detailed account of all factors specifically influencing the formation of each authigenic mineral.

Authigenic Clays

Authigenic clays formed in the deep-burial environment. Authigenic chlorite was determined to have recrystallized from detrital clay matrix. The common occurrence of detrital grains "floating" in a chloritic matrix in Britt sandstones attests to the allogenic origin of this clay (Figure 13). Sharp x-ray diffraction peaks (Appendix D) and the edge-to-face (cardhouse) morphology (Figure 15) were criteria on which this type of clay was judged to be authigenic. Illite formed as an alteration product of feldspars. Altered grains possessed sharp-angled corners and alignment of illite crystals along what appeared to be cleavage planes, where observed under extreme magnification. Kaolinite was well-crystalline in Britt sandstones. This authigenic clay is most closely associated with the maturation of

kerogen and the formation of secondary porosity via dissolution of metastable constituents (Moncure et al., 1984; Al-Shaieb, 1986). The thermal dissociation of kerogen provides the organic acids and CO₂ which are important in dissolution of metastable constituents such as carbonates, feldspars, and various rock fragments (Al-Shaieb and Shelton, 1981; Surdam et al., 1984; Moncure et al., 1984). Ions from the dissolution of these constituents may be precipitated as authigenic minerals, such as kaolinite.

Siliceous Cements

Cementation by syntaxial quartz overgrowths and chert was extensive in portions of Britt sandstones. Initiation of this type of cementation occurs at approximately 80 °C (Al-Shaieb, 1986; Leder and Park, 1986). This temperature suggests a deep-burial environment of formation. One of the most important factors to consider in sandstones with high authigenic silica content is the origin of the silica. Pittman (1980) has suggested several sources, including dissolution of detrital quartz grains via pressure solution, replacement of silicates with carbonates, and clay-mineral diagenesis, which includes shale diagenesis. Dissolution of feldspars may be an important contributor of silica in feldspathic sands. Extensive silica cementation in Britt sandstones suggests that an abundance of silica was available and that the sands were sufficiently permeable to allow the flow of silica-concentrated formation waters. Moncure

et al. (1984) emphasized shale diagenesis as a main source of silica in relatively impermeable Tertiary sands of the Gulf Coast. Silica cement was found to compose as much as 25% of the rock near the sand-shale contact but was not found in percentages greater than 5% in the central portions of the sands. This suggests that low permeability in these sands restricted flow of silica-rich formation waters. The opposite was observed in quartzitic Britt sandstones as evidenced by the presence of silica cement throughout. The author recognizes that other sources of silica also may have supplied a substantial amount of the silica that cemented Britt sandstones.

Carbonate Cements

Based on the morphology and relationship with other diagenetic constituents, calcite cements precipitated early in the diagenetic history of Britt sandstones. Acicular, blocky, drusy, poikilotopic and syntaxial cements form in the shallow marine or phreatic environment (Flügel, 1982).

Acicular cement was the earliest to precipitate. This variety surrounds fossil fragments. Syntaxial and poikilotopic cements were next to precipitate, followed by drusy and blocky varieties. Timing of precipitation of these cements is inferred directly from thin-section analysis. Calcite cements composed up to 40% of the rock at some places in Britt sandstones. Detrital grains appear to

"float" in the cement, indicating that no significant compaction took place prior to cementation (Figure 20). Additionally, other diagenetic minerals were not commonly associated with calcite cements. These observations suggest early precipitation of calcite, which destroyed virtually all porosity and permeability in affected areas.

Pittman (1980) and Al-Shaieb and Shelton (1981) have proposed several sources of ions for carbonate cements. Sources in the shallow diagenetic regime include sea water. Deep-burial sources include carbonate skeletal grains and by-products of Redox reactions. Two other sources, connate water and the mixing or diluting of brines, may be associated with either shallow or deep burial diagenesis.

Dolomite ($\text{CaMg}(\text{CO}_3)_2$) commonly is a pseudomorphous replacement of calcite cement and fossil fragments in Britt sandstones. Two important criteria must be met before such replacement will occur. (1) A source of magnesium must be available. (Mg^{2+} replaces Ca^{2+} in the calcite crystal lattice during the alteration to dolomite.) Sources of Mg^{2+} include shale diagenesis, dissolution of feldspars and rock fragments, and the recrystallization of detrital clay matrix. (2) The $\text{Ca}^{2+}/\text{Mg}^{2+}$ ratio must be suitable for the replacement of Ca^{2+} by Mg^{2+} . This ratio is variable and is dependent on the concentration of other free ions in the formation water (Al-Shaieb, 1986).

Collophane

Collophane generally is associated with areas of upwelling (Blatt, 1982). Cold, deep, phosphate-rich ocean water rises up against the landmass with phosphatic sediments (e.g. bones, teeth, shells) subsequently deposited in the shelf regime. Very slow rates of sedimentation are necessary to concentrate phosphatic sediments. The environment in which calcite cement and certain detrital constituents were replaced by collophane could not directly be ascertained. By direct relationship, it is known that collophane precipitated after calcite cement. The lack of other authigenic minerals associated with carbonate cements precluded judgment of the relative timing of precipitation.

Pyrite

Formation of authigenic pyrite is related directly to the maturation of kerogen and so is associated with the deep-burial diagenetic regime. Criteria which must be met for the precipitation of pyrite include a reducing environment and a source of sulfur and iron. The reducing environment is in the subsurface. A source of sulfur is the thermal maturation and subsequent dissociation of kerogen. Possible sources of iron include shale diagenesis, feldspar or rock fragment dissolution, and the release of iron during recrystallization of detrital clay matrix to chlorite. Iron is abundant in sediments of the Anadarko Basin.

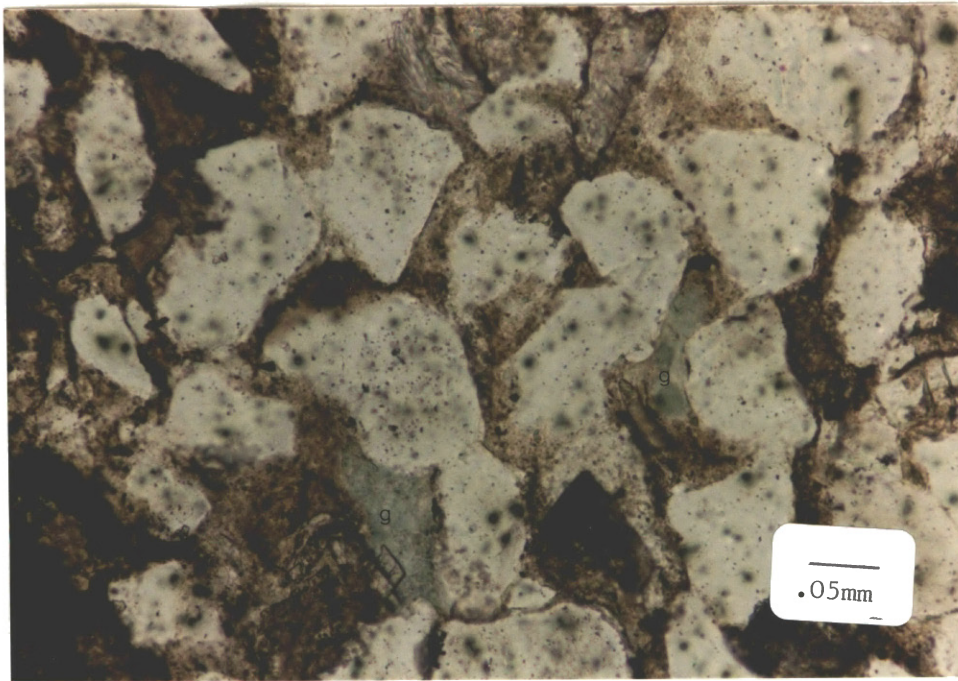
Organic Material

Oil and bitumen are derived from the thermal maturation of kerogen. This process is related to heat, pressure, and time. Types of kerogen include vitrinite, alganite, inter-nite, and extrinite. These varieties are directly related to the environment of deposition of the host sediments (Al-Shaieb, 1986). The type of kerogen controls the relative amounts of CO_2 and CH_4 derived from maturation and thus has an influence on diagenesis.

Deformation Fabrics

Britt strata are buried to depths between 11,000 and 20,000 feet in the thesis area. The weight of overlying strata has deformed ductile grains (e.g. glauconite, micas, shale clasts - Figure 23A). Rigid grains, such as quartz, commonly show sutured grain-to-grain contacts indicative of pressure solution. The presence of stylolites in rocks has been attributed to overburden stresses, in part. Pressure solution with resulting dissolution of detrital constituents along stylolite seams may provide a source of silica for quartz cementation (Pittman, 1979). Warped parallel to subparallel lines also were commonly found on quartz grains in Britt sandstones (Figure 23B). These have been interpreted as Boehm strain lamellae and result from excessive strain on rigid detrital grains (Scholle, 1979).

A.



B.

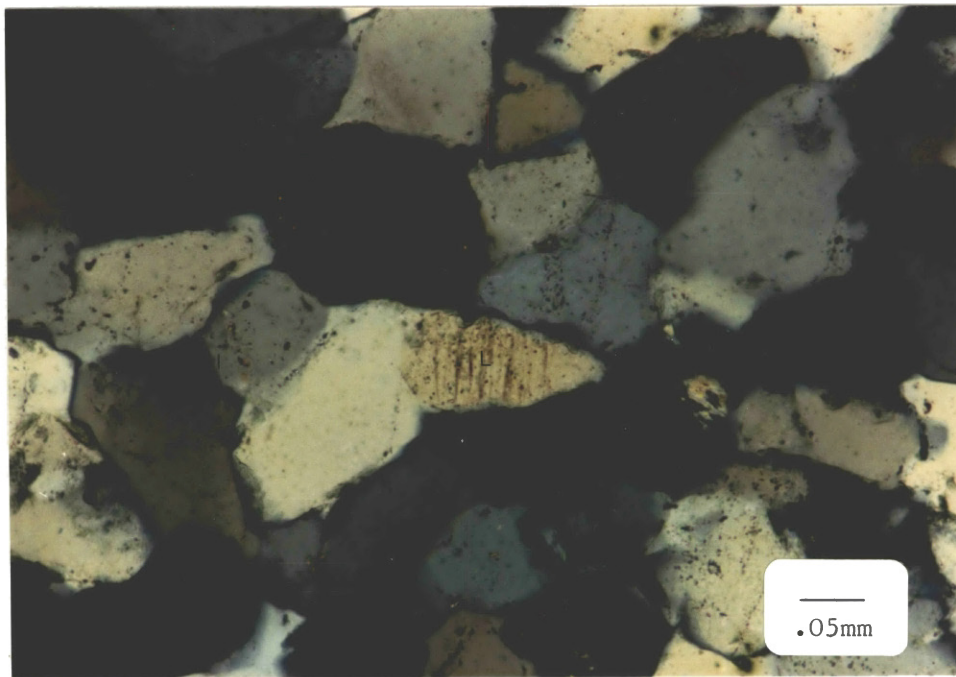


Figure 23. Photomicrographs demonstrating deformation fabrics in Britt sandstones. (A) Deformation of glauconite (G). (B) Bohm strain lamellae (L) resulting from stress on a rigid quartz grain.

Porosity

Porosity in Britt sandstones is either primary or secondary. Diagenesis has modified the original porosity extensively. Sands of the Britt Member produce more natural gas than any rock unit in the thesis area (Figure 24). A discussion of the origins of porosity in these sandstones is relevant for this reason.

Primary Porosity

Types of primary porosity may be classified as interparticle, which is the most common, intraparticle, and intercrystalline (Choquette and Pray, 1970). Primary porosity has been modified diagenetically in Britt sandstones. Terms proposed by Choquette and Pray (1970) to describe modified porosity include the following: 1) preserved, 2) enlarged, 3) reduced, and 4) filled. Primary porosity retained in diagenetically-altered sandstone may be referred to as "preserved." "Filled" porosity refers to pores filled by authigenic cements. Destruction of porosity in this manner was very common in Britt sandstones, especially by silica and carbonate cements. Cementation and compaction were responsible for destruction of much of the original porosity.

Partial filling of pores results in "reduced" porosity. Clays, organic material, and pyrite most commonly reduced porosity in the sands of the study area, without completely

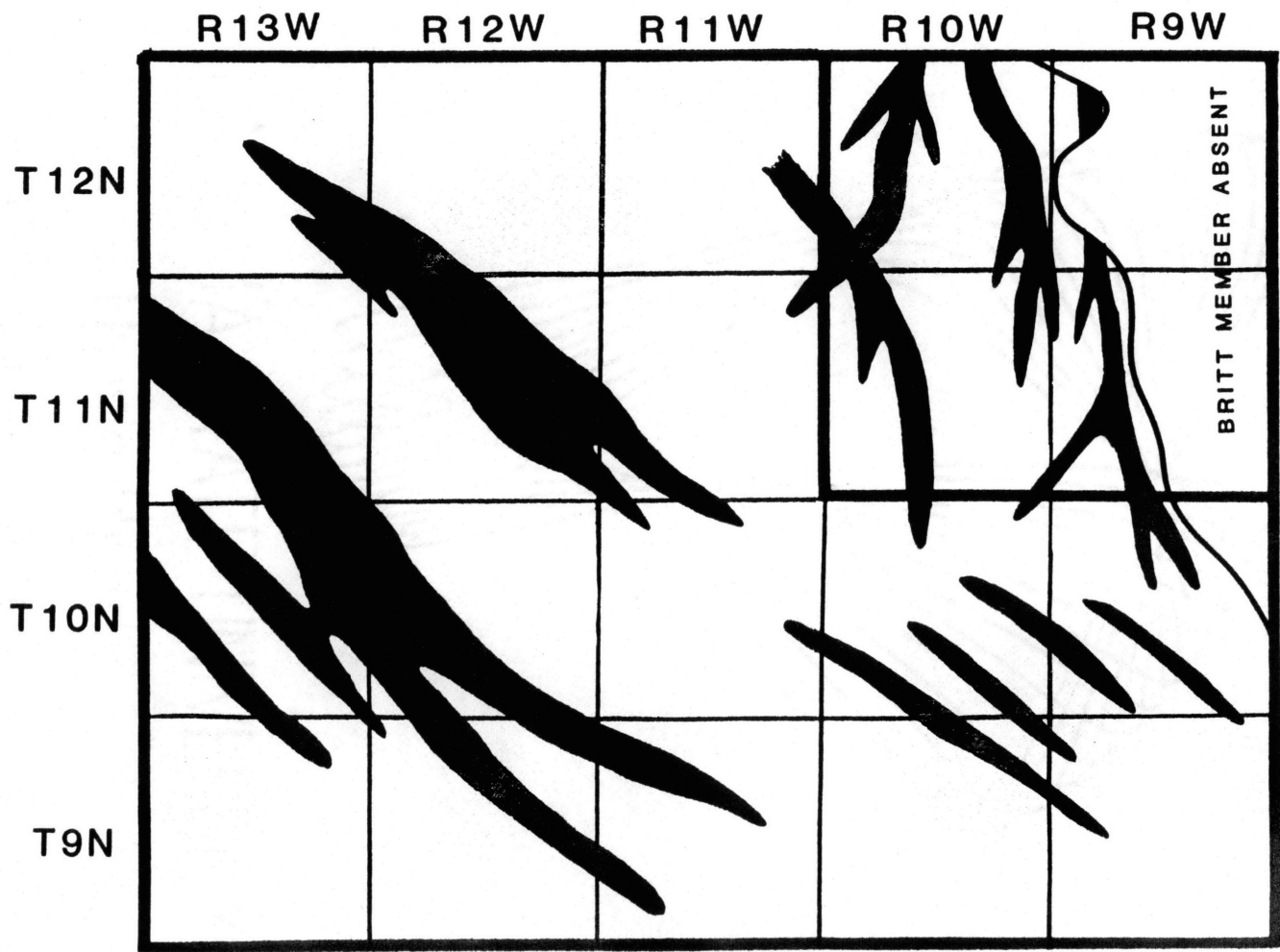


Figure 24. Trends of Productive Britt Sandstones

filling pores. Partial filling by carbonate and silica cements was atypical. "Reduced" porosity is the most common type of primary porosity. Chlorite, which precipitated from detrital clay matrix, partially filled many pores. Mechanical compaction of sediments, resulting in flowage of ductile grains and rotation of grains, was also a significant factor in loss of primary porosity.

Enlargement of primary pores resulted largely from dissolution of detrital quartz and clay matrix. Preserved primary porosity and associated permeability allowed the flow of formation water through Britt sands. The chemical disequilibrium between the detrital constituents and formation water resulted in partial dissolution of the former. Etching of quartz grains was common in Britt sandstones (Figure 25).

Secondary Porosity

Schmidt and McDonald (1979) proposed that the processes of generation of secondary porosity in clastic sediments be classified into five categories including: 1) dissolution of detrital constituents, 2) dissolution of authigenic cements, 3) dissolution of authigenic replacement minerals, 4) shrinkage, and 5) fracturing. Criteria suggested by these authors for recognition of secondary porosity include partial dissolution of grains, molds of detrital grains, inhomogeneity of packing, oversized or elongated pores, and corroded, fractured, or honeycombed grains.

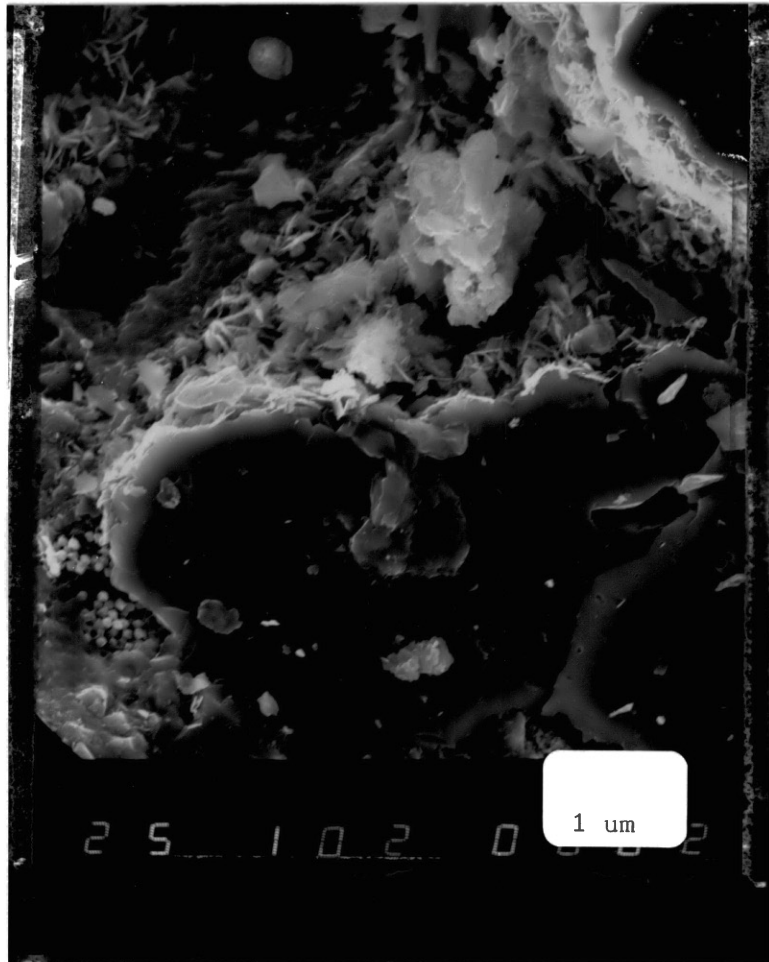


Figure 25. SEM photomicrograph. Secondary porosity resulted from the partial dissolution of detrital quartz. Note etching of grain (arrow). Magnification - 1000X.

Dissolution of quartz and detrital clay matrix were responsible for most of the secondary porosity (Figure 25, 26). Minor porosity resulted from dissolution of other detrital constituents such as feldspars, rock fragments, fossils, heavy minerals and glauconite. Such porosity may be important locally. Evidence of dissolution of authigenic replacement minerals, such as dolomite and pyrite, and shrinkage of grains was not observed in Britt sandstones.

Dissolution of authigenic constituents contributed only minor amounts to the total porosity of the sandstones. Etched calcite and syntaxial quartz overgrowths were observed. The lack of advanced dissolution of these cements may be attributed, in part, to the low permeability of tightly-cemented portions of the rock. Flow of formation water in such areas was restricted. This impeded flow did not allow for chemical reactions between the rock and formation water, which might have resulted in advanced dissolution of the cements.

Fracturing of Britt sandstones was noted in cores. Fractures typically were "vertical." Petrographic analysis of a single fracture showed that kaolinite filled the void. Carbonate and silica cements were found in the rock but not as fracture-fillings. This observation suggests that this fracture opened late in the diagenetic history of the rock. Although fracturing was minor in Britt sandstones, it may have had a significant role in the transmission of fluids and natural gas through the rock.

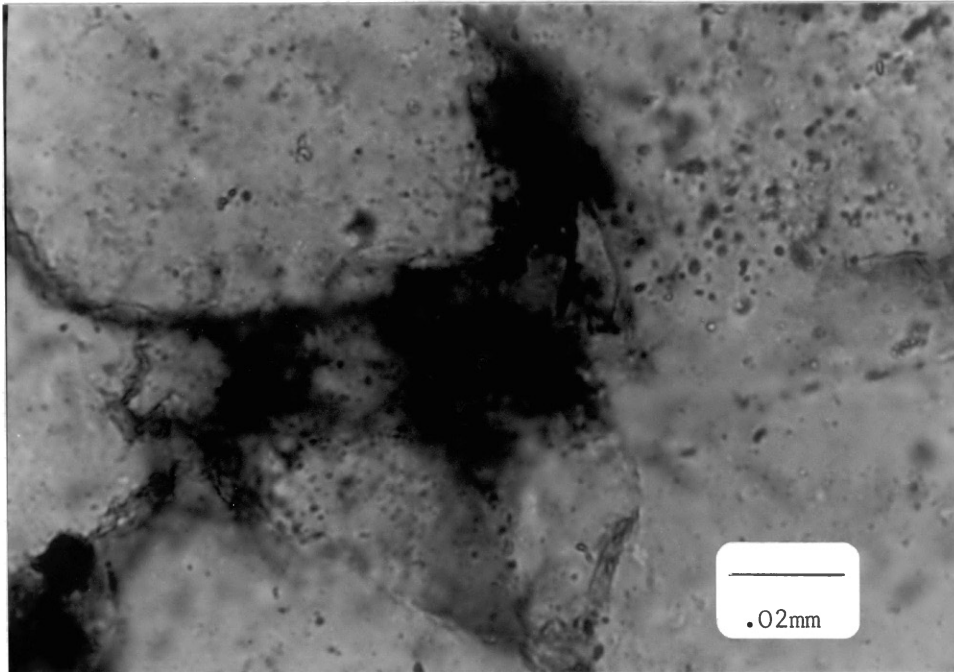


Figure 26. Photomicrograph demonstrating dissolution of detrital clay matrix (C). Porosity is in blue.

Microporosity

For this research, the term "microporosity" is defined as minute voids between crystals of authigenic clays that have filled or lined pores. Due to the abundance of authigenic chlorite in the study sandstones, this porosity type was abundant. Microporosity may be either primary or secondary in origin, dependent on the site of authigenic-clay precipitation. Primary microporosity was associated with clays formed in primary pores. Secondary microporosity was associated with clays precipitated in voids of secondary origin, such as grain molds or fractures. Microporosity associated with alteration of detrital grains to clays (e.g. plagioclase feldspar to illite) was classified as secondary. Both primary and secondary varieties of microporosity were well represented in sandstones of the Britt with primary microporosity the more abundant.

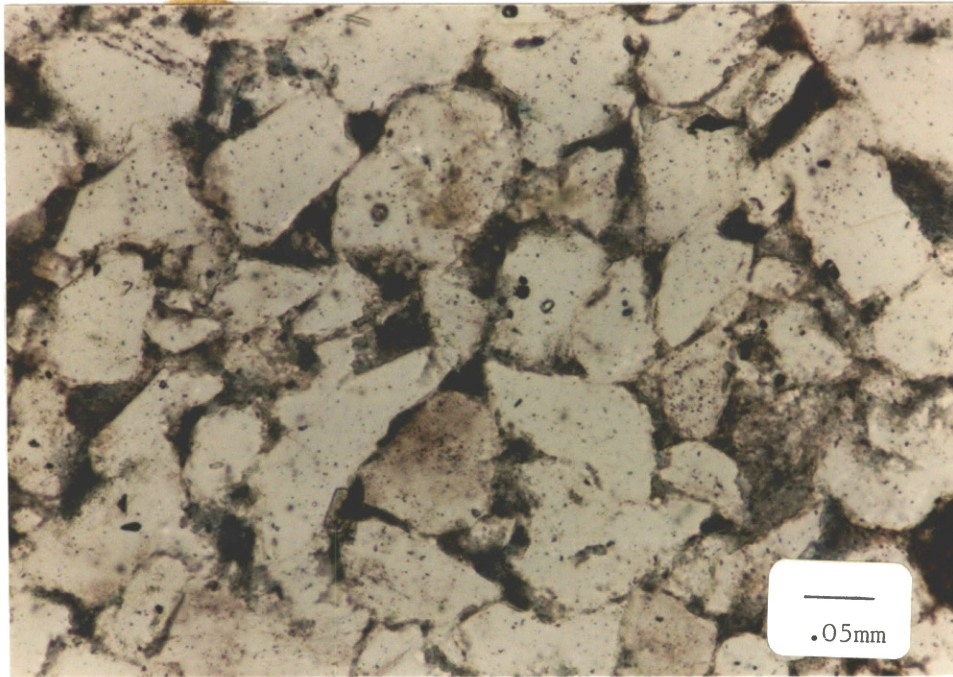
Microporosity associated with chlorite in sandstones led to significant problems when determination of total porosity from thin-section analysis was attempted. Total porosity was underestimated in rocks with abundant microporosity, as determined from a comparison of point-counted thin-section porosity to the porosity observed with the scanning electron microscope. The small pores typical of microporosity cannot be observed under a conventional petrographic microscope in most instances, especially the microporosity associated with authigenic chlorite. The reader

should be aware that porosity-values presented in Appendix C and used to construct Figure 28 were based on point-counting of thin sections and that porosity can be significantly larger where chlorite is present.

Relationship Between Porosity, Silica
Cement, Authigenic Clay, and Depo-
sitional Environments

Authigenic chlorite, which precipitated from detrital clay matrix, is abundant in specific sand units in the Britt Member. An inverse relationship between authigenic clays and silica cement has been noted in reservoir sands such as the Upper Mississippian Berea Sandstone in the Appalachian Basin, the Cretaceous Tuscaloosa Sandstone in Louisiana, and the Pennsylvanian Morrow Sandstone of the Anadarko Basin (South, 1983; Pittman and Larese, 1986). Based on petrographic analysis, silica cementation is inhibited on grains with clay coatings, especially chlorite-coated grains (Pittman and Larese, 1986). Authigenic chlorite in Britt sandstones can be attributed directly to the depositional environment. Detrital clay matrix is winnowed in high-energy environments (Spearing, 1976). Quartzitic Britt sandstones deposited in high-energy regimes lack appreciable amounts of chlorite. These sands are tightly cemented with authigenic silica (Figure 27A). In contrast, sands with at least 4% to 8% chlorite demonstrated limited silica cementation (Figure 27B). Inhibiting precipitation

A.



B.

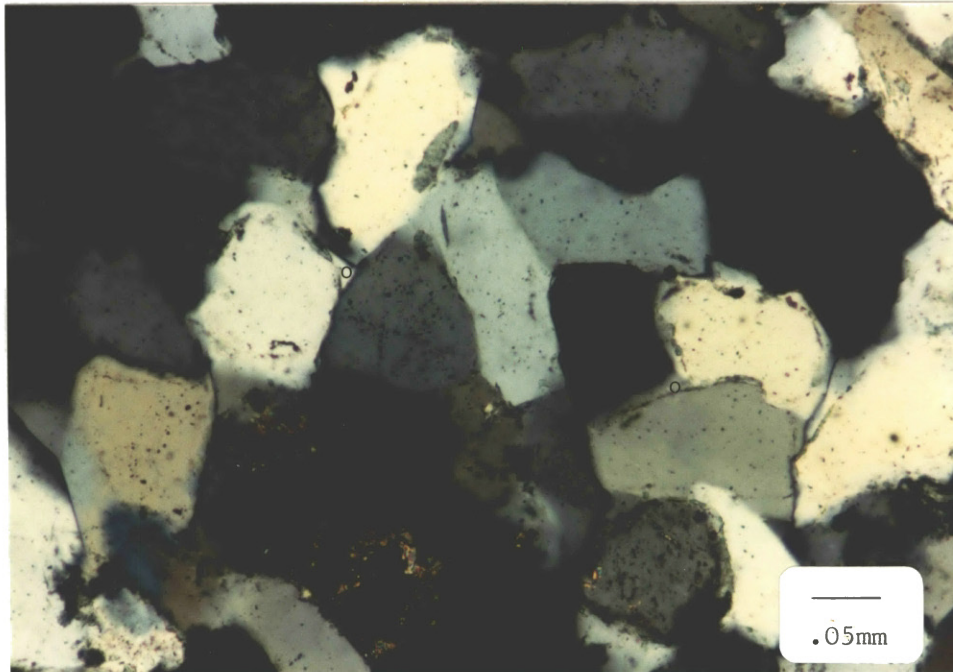


Figure 27. Photomicrographs for comparison of the extent of silica cementation (S) in quartzitic sands. (A) Advanced silica cementation occurred in sands with minor chlorite. (B) In contrast, sands with chlorite percentages in excess of 4% show limited evidence of silica cementation.

of syntaxial quartz overgrowths preserved porosity in Britt sandstones. It is hypothesized excessive amounts of chlorite have destroyed significant porosity and permeability. Porosity was not observed where the rock was matrix-supported.

Analysis of Britt sandstones indicated that the optimal chlorite percentage for preserved primary porosity is between 4% and 14% (Figure 28). Advanced silica cementation occurred in rocks where chlorite is less than 4%. Amounts in excess of 14% led to filling of pore spaces by clay matrix during compaction. Permeability was diminished greatly where chlorite percentages exceed 14% (based on thin-section analysis). The relationship between chlorite and authigenic silica is illustrated graphically in Figure 29.

Relationship Between Silica and Carbonate Cements

An inverse relationship exists between silica and carbonate cements in Britt sandstones. The difference in environments of formation and the lack of permeability are the most significant factors to consider. Calcite, much of which was later converted to dolomite, precipitated in the shallow diagenetic regime where surficial water influenced diagenesis. Virtually all porosity and permeability were destroyed in portions of the rock subjected to this type of early cementation. Lack of sufficient porosity and permeability in these areas prevented fluid movement through the

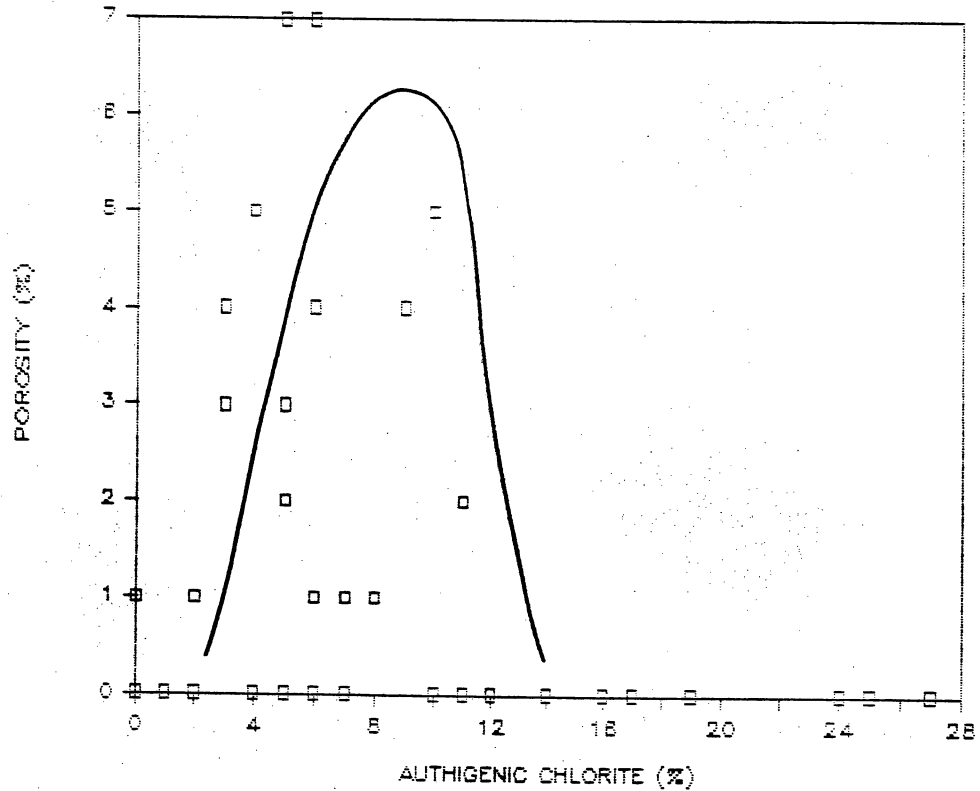


Figure 28. Relationship between authigenic chlorite and porosity. The curve illustrating the relationship was generated empirically from analysis of thin sections. As demonstrated by the graph, porosity is associated with chlorite percentages between 4% and 14%. It should be remembered that porosity was mostly likely underestimated where chlorite ranged between the previously cited values. The lack of porosity in thin sections where chlorite percentages were between 4% and 14% can be attributed to early calcite cementation which generally was associated with fossiliferous sandstones. Calcite cements commonly were minor in sands with chlorite percentages in excess of 14%.

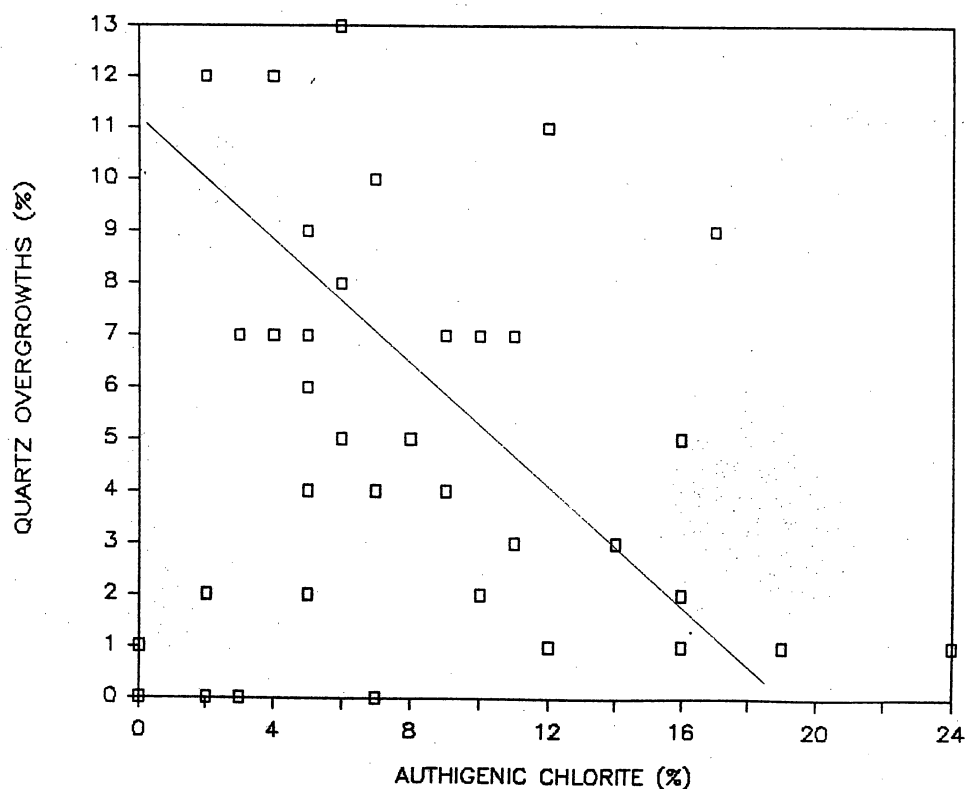


Figure 29. Relationship between authigenic chlorite and syntaxial quartz overgrowths. Based on analysis of thin sections it was determined that the relationship between chlorite and silica overgrowths is inversely proportional in Britt sandstones. Chlorite inhibited the growth of silica. A similar relationship was noted in the Pennsylvanian Morrow Sandstones by South (1983) and in the Mississippian Berea Sandstone and Cretaceous Tuscaloosa Sandstone by Pittman and Larese (1986). High silica content associated with high chlorite values resulted from "averaging" during point counting. Areas of certain thin sections contained abundant silica overgrowths whereas other portions of the thin section were devoid of authigenic silica but abundant in chlorite.

rock during later diagenetic phases, such as precipitation of authigenic silica. Portions of the sandstones not subjected to early calcite cementation and lacking appreciable amounts of chlorite were cemented extensively with silica (Figure 16). The relationship between carbonate cement and authigenic silica is illustrated in Figure 30.

Paragenetic Sequence

The number of diagenetic minerals observed illustrates the complexity of reconstructing a diagenetic history for Britt sandstones. Additionally, the variety of morphologies of calcite cements suggests precipitation in several shallow diagenetic regimes including the shallow marine or phreatic. To simplify explanation of the paragenetic sequence, the relationship among various types of calcite cements will not be discussed. Calcite cementation will be discussed as a single event, inasmuch as interpretation of early carbonate diagenesis is not the emphasis of this portion of the study. A summary of the paragenetic sequence is given in Figure 31.

The earliest phase of diagenesis involved the beginning of compaction with the consequent expulsion of pore water. Significant loss of sediment volume can occur in the shallow diagenetic regime (Pittman, 1979). Total volume loss is dependent on lithology with muds much more susceptible to compaction due to water loss than are sands.

Calcite cementation was the second phase of diagenesis

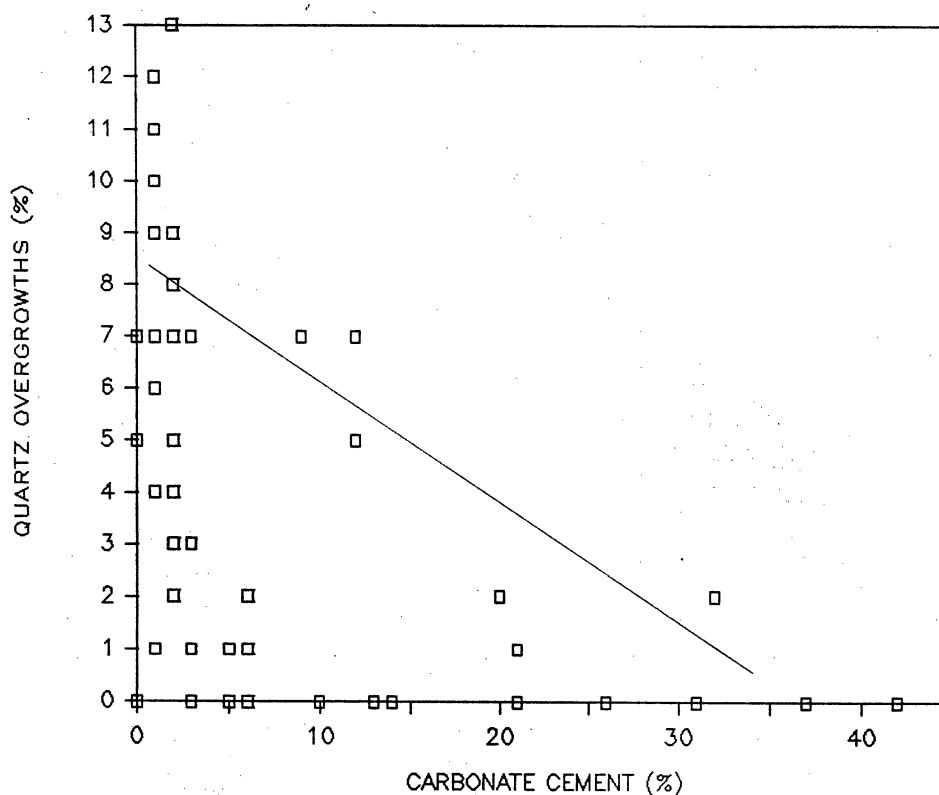
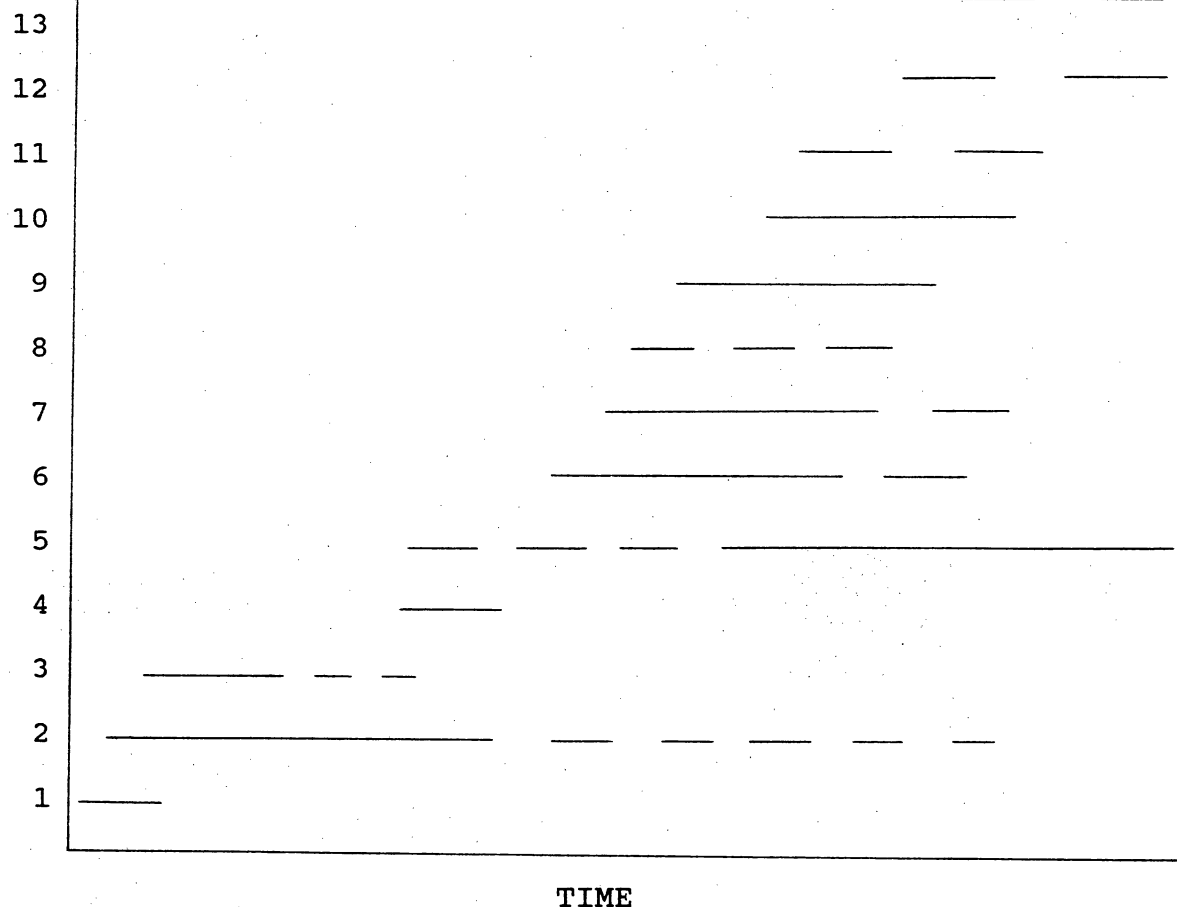


Figure 30. Relationship between carbonate and silica cements. The relationship between these authigenic constituents was determined empirically. Morphology of the carbonate cements suggests they precipitated early in the diagenetic history of Britt sandstones resulting in the destruction of primary porosity in certain portions of the sand. Scatter of data points suggests other factors such as the presence of chlorite or the lack of uniformity of an authigenic mineral in a thin section, have influenced the relationship. Low authigenic silica content in association with low carbonate values is a result of chlorite inhibiting the precipitation of quartz overgrowths.



DIAGENETIC EVENTS

1. Deposition of Sediments
2. Compaction of Sediments
3. Precipitation of Calcite Cements
4. Collophane Replacing Calcite and Clays. Carbonate-shell Fossils Converted to Apatite
5. Maturation of Kerogen
6. Recrystallization of Clay Matrix to Chlorite
7. Precipitation of Silica Cements
8. Dissolution/Alteration of Feldspar, Rock Fragments
9. Conversion of Calcite Cements and Fossils to Dolomite
10. Dissolution of Quartz
11. Precipitation of Kaolinite
12. Generation of Oil.
13. Precipitation of Pyrite

Figure 31. Paragenetic Sequence of Britt Sandstones

in the study sandstones. The morphological varieties previously discussed suggest a shallow depth of formation, as does the relationship with other diagenetic minerals. Replacement of calcite cement and various detrital constituents by collophane also occurred at a relatively shallow depth. The lack of a direct relationship between collophane and other diagenetic minerals precluded confident judgement as to the the relative timing of replacement.

Attempts to interpret the diagenetic sequence became more complex during analysis of minerals that precipitated in the deep-burial regime. This was due to the occurrence of "simultaneous" diagenetic events and the lack of direct relationships between certain authigenic minerals.

Authigenic chlorite was observed as thin dust rims between detrital quartz and syntaxial overgrowths. Precipitation of authigenic silica is generally associated with acidic or slightly basic conditions (Al-Shaieb, 1986; Leder and Park, 1986) as is the alteration or dissolution of detrital clay matrix. These events are interpreted to have occurred contemporaneously in Britt sandstones. Calcite cements and fossils were also susceptible to dissolution during this phase. In part, organic acids derived from the thermal maturation of kerogen are responsible for the acidity (Surdam et al., 1984; Moncure et al., 1984). Dissolution of calcite was minor; this can be attributed to the lack of acidic formation water flowing through these tightly-cemented rocks. Dissolution of fossil fragments in

Britt sandstones which had only small percentages of carbonate cement was common.

Dissolution of feldspars and rock fragments or their alteration to chlorite or illite occurs in acidic conditions (Moncure et al., 1984). This event may have provided a source of iron and magnesium ions for ferroan dolomite to replace calcite. They also may have provided a source of silica for syntaxial overgrowths and chert. Dissolution of the aforementioned constituents, along with diagenesis of shales, provide a source of ions for the precipitation of kaolinite, chlorite, and illite. Kaolinite appears to have formed as feldspars and rock fragments were being dissolved or altered. This mineral was found filling pores lined with authigenic chlorite (Figure 32).

The next stage of diagenesis involves dissolution of quartz resulting in the formation of secondary porosity or enlargement of primary porosity. Etching was evident when viewed under extreme magnification (Figure 25).

The final stage of diagenesis involved the precipitation of euhedral pyrite crystals and the generation of oil from kerogen which filled or lined primary and secondary pores in most Britt sandstones. Pyrite was found precipitated on kaolinite booklets which filled pores (Figure 32).

Alternative interpretations are possible from the relationships observed among various authigenic constituents. The interpretation given is the simplest, involving the fewest number of inferred changes in the chemistry of the



Figure 32. SEM Photomicrograph. Kaolinite (K) filled pores. This authigenic clay had a vermicular morphology and euhedral pseudo-hexagonal crystals. Note authpyrite (arrow) which has precipitated on kaolinite booklets. Magnification - 3000X.

formation water. Based on research by various authors (e.g. Al-Shaieb and Shelton, 1981; Moncure et al., 1984, and Pittman and Larese, 1986) maturation of kerogen seems to have had a significant, if not controlling, influence on the chemistry of formation waters in petroliferous basins such as the Anadarko Basin.

CHAPTER V
DEPOSITIONAL ENVIRONMENTS AND SEDIMENT-
OLOGICAL CHARACTER

Introduction

The Britt sandstones record regressive-transgressive couplets in response to progradation, abandonment, and subsidence of deltas during the Late Mississippian. Four principle facies compose the depositional sequence: 1) bar-finger sands, 2) delta-destructive sand bars, 3) shelf sand-ridges, and 4) storm deposits. Two distinct depositional cycles were recognized, leading to division of this interval into upper and lower submembers. Each of the aforementioned facies is represented in the Lower Britt Submember. The Upper Britt Submember is represented only by shelf sand-ridges. Principle purposes of this chapter include: 1) defining and describing the principle facies, 2) describing the depositional regime in which each Britt facies was deposited, and 3) developing a depositional model for the Britt genetic interval.

Analysis of Britt facies was conducted in three phases. Phase I involved description of individual facies. Sedimentologic character, trend, and geometry of individual

sandstones was determined via core data and subsurface mapping from well logs. Interpretation of the depositional setting of each facies was made in Phase II. Knowledge of regional structural geology and stratigraphy was essential. Phase III involved integration of data from Phases I and II in an effort to reconstruct the depositional history of the Britt genetic interval.

The thesis area represents only a portion of the area covered by Britt strata. Britt fluvial, deltaic, transitional marine, and marine sediments composed a regionally extensive depositional system. Consolidation of maps constructed by geologists of Ward Petroleum Corporation with those for this study, demonstrate the areal extent and trends of Britt sandstone deposits (Figure 33).

A review of modern shelf regimes and sediment movement from the terrestrial environment into these regimes is presented within this chapter. Such a discussion was necessitated by the variation in depositional environments among facies of the Britt.

Shelf Depositional Regimes and Sediment Movement

Study of the sedimentary processes which result in the formation of shelf bedforms in the modern marine environment has allowed for the comparison of relict bedforms to modern ones. Prior to discussion of individual facies that compose the Britt Member, it is relevant to describe the regimes

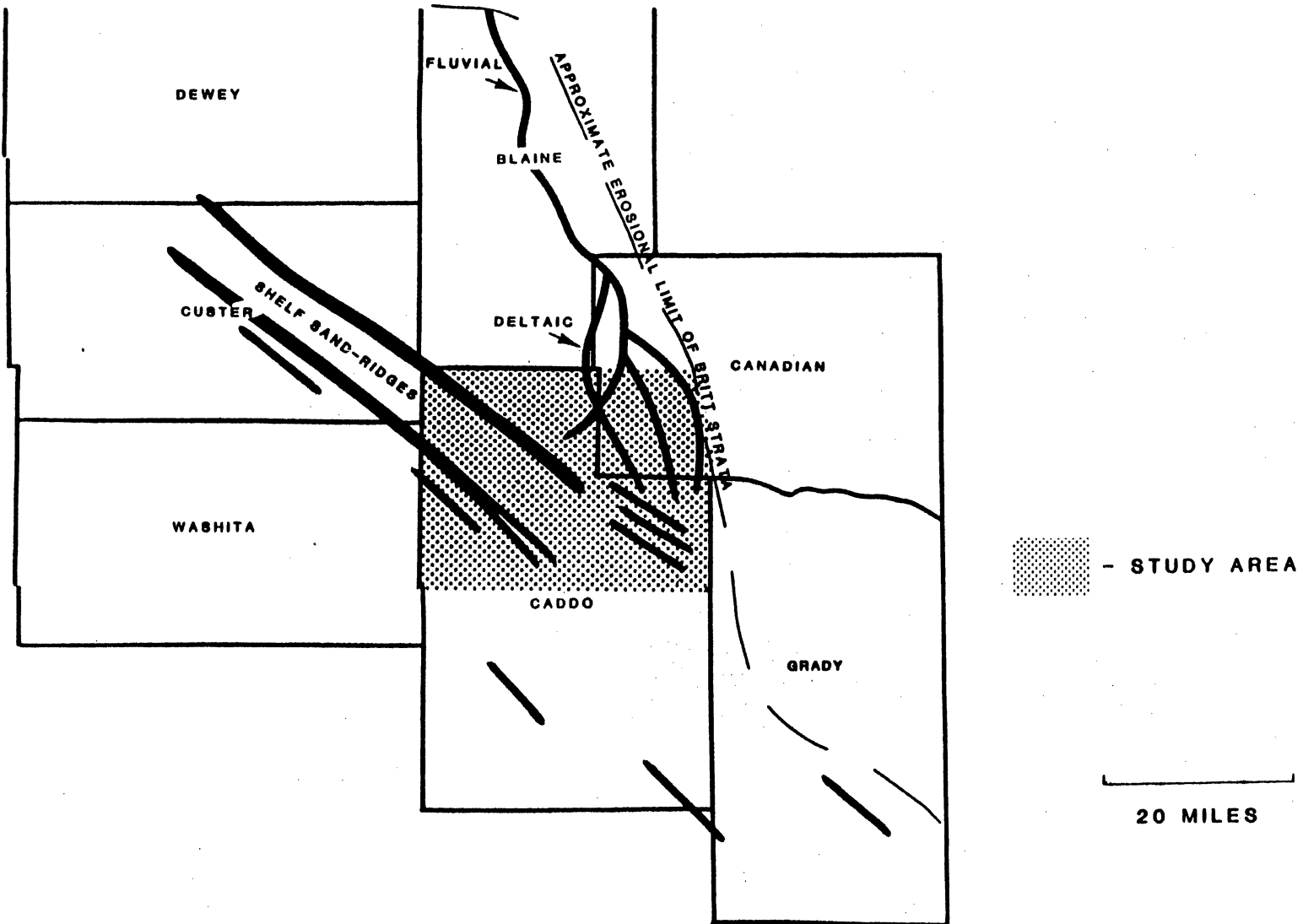


Figure 33. Known Extent of Britt Sandstones in Western and Southern Oklahoma

of the modern ocean and to briefly discuss the various modes of sediment transport into the marine environment.

Mooers (1976) recognized four regimes in the modern oceanic environment. Division of each regime was based on differing interactions of waves, tides, and currents with sediments.

1) Nearshore regime: This regime extends from the shoreline to the edge of the shoreface (0 to approximately 60 feet deep). It is characterized by strong surf-zone influence. Waves break constantly, creating longshore and transverse currents which move sediments laterally along the coastline. This process is partly responsible for redistribution of deltaic sediments that enter the near-shore environment, leading to formation of barrier bars and subaqueous sand-ridges which parallel the shoreline.

2) Inner-shelf regime: This regime extends from the shoreface to water depths of 150 to 650 feet. The inner-shelf represents the transition from the high-energy near-shore environment to the quiet waters of the deeper shelf. With the exception of areas within a high tidal range, storms are the dominant mechanism for moving sediment and water. Water movement within this regime is greatly affected by seasonal climate variations.

3) Outer-shelf regime: Water depths may exceed 1,600 feet in the outer shelf. This regime represents the transition from shelf to oceanic environments. Outer-shelf waters are characterized by strong density stratifications.

Current convergences, turbidity flows, and mud plumes off deltas have been suggested by Drake (1976) as possible mechanisms for sediment movement within this regime.

4) Oceanic regime: This environment includes the deep ocean and continental slope. It is characterized by nearly constant winds that result in coastal upwellings or downwellings, which may move large amounts of sediment.

A summary classification of offshore regimes and environments is presented in Figure 34.

A marine depositional setting is inferred for three of the four Britt facies. Sediment movement from a terrestrial source into the marine environment played an essential part in the formation of each unit.

Three modes of transport have been proposed to move sediments into the shelf and near-shore environments:

1) River-mouth bypass - This type of movement consists of seaward-moving currents generated by rivers, primarily at flood-stage (Swift, 1976). Sediments bypass coastal areas as strong river currents jet fine clastics seaward. Such deposits are derived from outside the basin of deposition (exogenic).

2) Shoreface bypass - Erosional retreat of the shoreline during a marine transgression causes reworking of the transgressed surface with formation of a residual sand sheet over the recently flooded area (Swift, 1976). Sediments are derived from within the basin (endogenic).

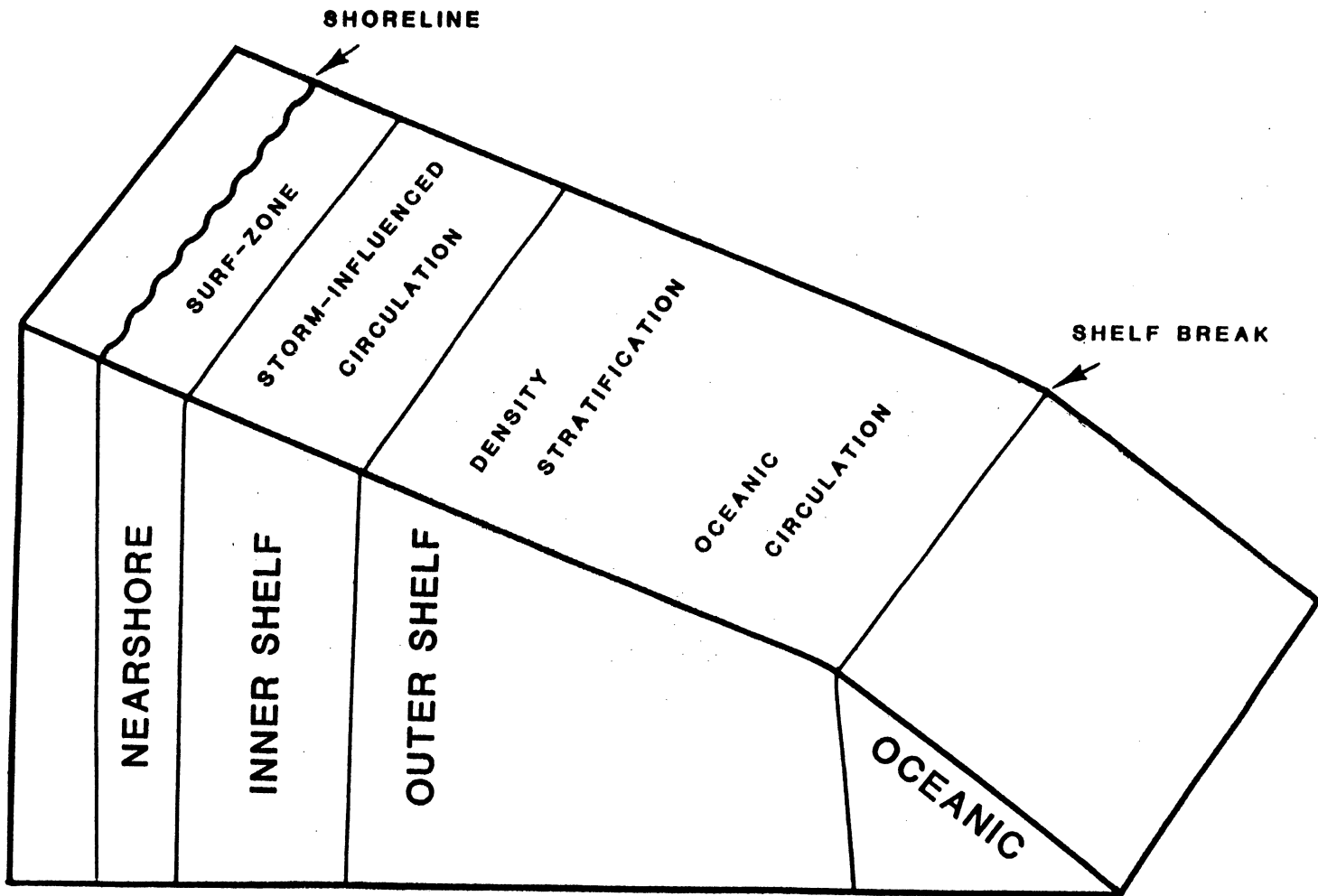


Figure 34. Summary Classification of Offshore Regimes
 (After Mooers, 1976)

3) Storm surges - Hayes (1967) and Morton (1981) studied recent marine storms that affected coastal areas. Their work indicated that significant amounts of sediment can be moved during a single storm event. Walker (1979) proposed that fossil-debris and sand are carried seaward by strong unidirectional bottom currents that occur ahead of storms. A 400% increase in the suspended-sediment load was noted after a recent hurricane off the United States' Pacific coast (Drake, 1976). With storms having been an "everyday occurrence" in terms of geologic time, it is evident that these events may have been a dominant mechanism in the seaward transport of sediments, especially in areas with high storm frequency.

Phase I: Description of Principle Facies

The purpose of this section is to describe the sedimentologic and geometric aspects of the four sandstone facies that compose the Britt genetic interval. Cores, isopach maps, and stratigraphic cross-sections were the principle sources of information.

Bar-Finger Sands

Bar-finger sands were recorded exclusively in the Lower Britt genetic interval, in the northeasternmost portions of the thesis area (T11-12N, R9-11W) (Plate III). Individual sand bodies trend in a general NNE-SSW direction, normal to depositional strike of the Springer Group (Plate VI) and to

the hingeline of the Anadarko Basin (Figure 1).

Lower Britt bar-finger sands possess low sinuosity. Individual sand bodies are approximately one-half to five-eighths of a mile in width. Average maximum thickness of individual units is 55 feet as inferred from isopach mapping (Plate III). Based on inferences from isopach maps and localized cross-sections, sandstone units in this facies are lenticular (Figure 35). Lack of data from cores precluded description of sedimentologic features.

Delta-Destructional Sand Bars

Delta-destructional bars exclusively in the Lower Britt genetic interval are thin, elongated units that trend essentially parallel to depositional strike of the Springer Group (Plate VI) and to the hingeline of the Anadarko Basin (Figure 1). This facies is in the northeastern one-half of the study area. Delta-destructional bars commonly are stacked, with as many as four individual units encountered in a single well-bore.

Delta-destructional bars were not included during construction of the Lower Britt Gross Sand Isopach Map (Plate III). Inclusion of this facies masked the trend and thickness of associated sandstone facies in the Britt genetic interval, although individual bars rarely exceed 20 feet in thickness. They were excluded because of the multi-storied nature of these sand bodies. A gross sand isopach map of the delta-destructional bar facies would have had little value

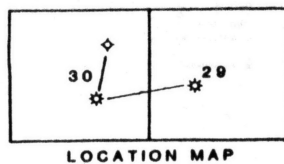
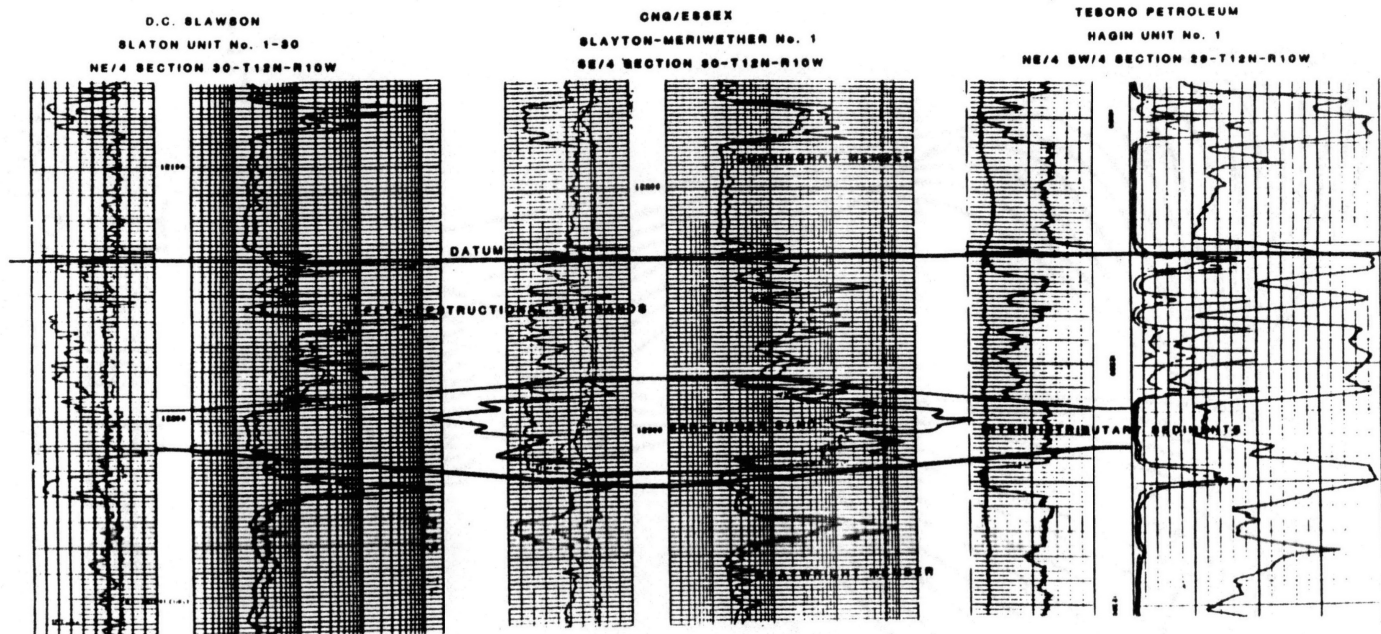


Figure 35. Stratigraphic Cross-section Illustrating Various Facies in the Lower Britt Submember. Datum: Base of "Britt Marker"

in the interpretation of geometry of these units, due to their multi-storied nature. One extraordinarily continuous bar system was traceable in the subsurface. A gross sand isopach map demonstrating trend and geometry of this bar system is presented in Figure 36.

Two available cores contain evidence of delta-destructive bars. (Tenneco Grant Rumley No. 1-22; Section 22-T9N-R9W; Apexco, Inc. Buell No. 1-A; Section 10-T11N-R12W). In addition, drill cuttings from this facies were examined in two wells; the CNG/Essex Hollis No. 1 (Section 2-T11N-R11W) and the CNG/Essex Slayton-Meriwether No. 1 (Section 30-T12N-R10W).

The delta-destructive bar in the Grant Rumley No. 1-22 is 16 feet thick. The basal four feet are classified as a medium-grained oosparite (Folk, 1962); small-scale planar cross-bedding is the dominant sedimentary structure. Quartz and fossil fragments most commonly serve as ooid nuclei. This unit grades into a fine-grained, quartzitic sand containing numerous thin, highly-fossiliferous laminae. Few ooids are present. Convolute and irregular bedding are the dominant structures in the middle portions of the unit. Fossil content decreases upward significantly. The uppermost four feet are also fine-grained and quartzitic. Only trace amounts of fossils and ooids are present. Bioturbated rock and rare small-scale trough cross-beds are common. Sandy and oolitic units are well-sorted throughout the entire unit. The upper contact of the bar is gradational with

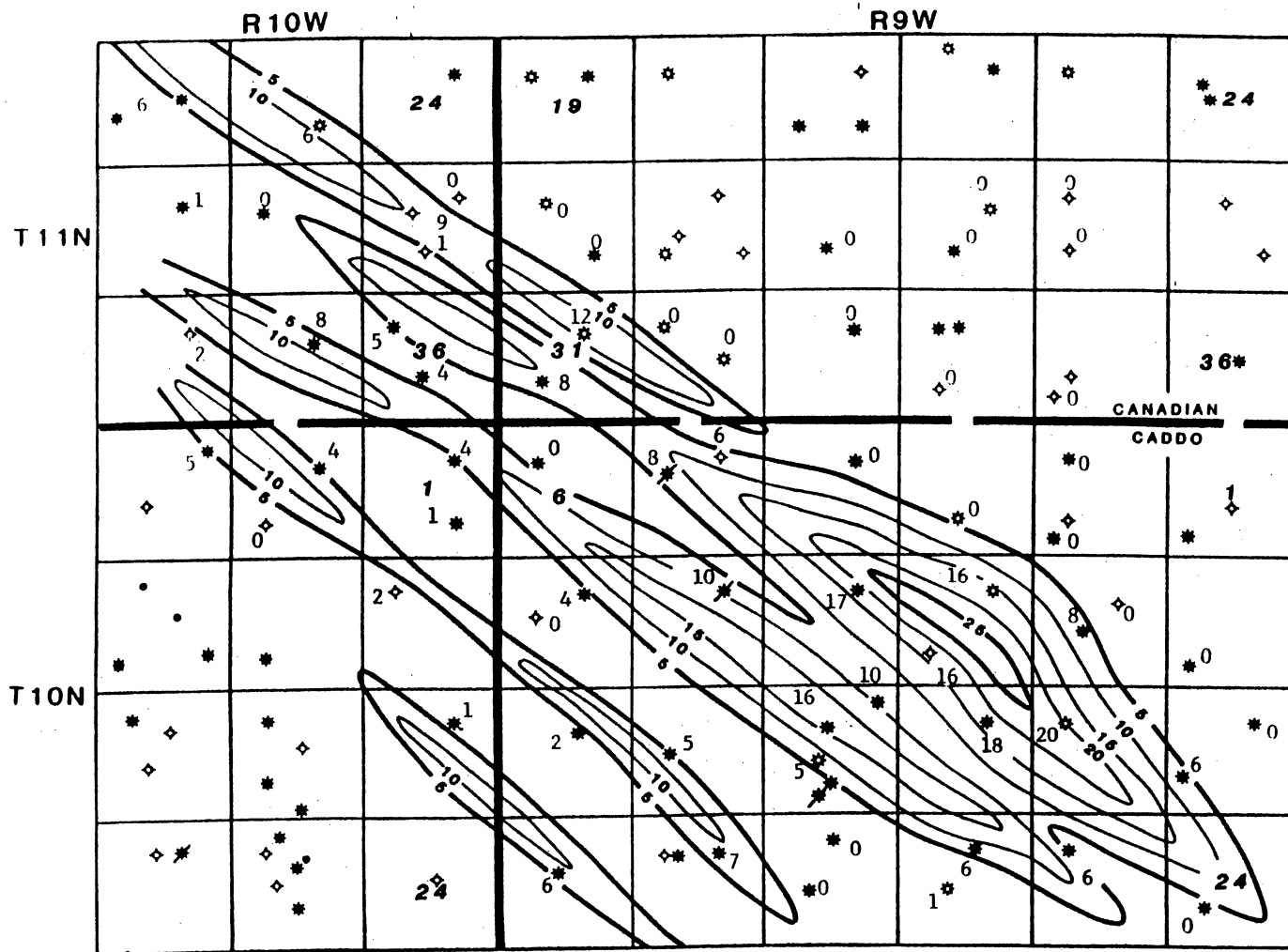


Figure 36. Lower Britt Delta-Destructional Bar Complex
Gross Sand Isopach Map (After O'Donnell, 1986)

overlying sediments, typically lenticularly-interbedded sandstones, siltstones, and shales.

The delta-destructive bar in the Apexco, Inc. Buell No. 1-A is 13 feet thick; it contains up to 10% ooids in the lower portions, within a well-sorted, fine-grained, fossiliferous, quartzitic sandstone. Fossil and ooid content decrease upward significantly with the sandstone remaining well-sorted throughout. For the most part, sedimentary structures within this unit are distorted beyond recognition. The distorted bedding resulted from compaction. Possible small-scale cross-bedding and bioturbated beds are present. Both the upper and lower contacts of this bar are gradational. Lenticular-bedded and laminated sandstones, siltstones, and shales underlie the bar. The upper contact is recognized by an abrupt change from fine- to very fine-grained sand.

Glauconite was found exclusively in the delta-destructive bar facies. This detrital sediment commonly is concentrated at the bases of small-scale trough cross-beds. Glauconite in drill-cuttings can aid the well-site geologist in distinguishing among the facies of the Britt.

Shelf Sand-Ridges

Shelf sand-ridges are regionally extensive, marine sandstones, present in both the Upper and Lower Britt Submembers (Plates III-V). These sands "parallel" depositional strike of the Springer Group (Plate VI) and the hingeline of

the Anadarko Basin (Figure 1). Shelf sand-ridge systems in both the Upper and Lower Britt genetic intervals extend distances in excess of 60 miles, paralleling one another (Figure 33). Smaller sand-ridges are associated with the two major trends (Plates III - V). Due to their limited extent and a lack of sufficient well control, smaller ridges not associated with major trends were excluded from isopach mapping.

Maximum sand thickness is approximately 60 feet with average sand-ridge width of one to one and one-half miles (as inferred from isopach mapping - Plates III - V). Smaller ridges are less than one-quarter of a mile wide. Interpretation of the geometry was difficult, because of sparse well control. Based on limited areas with adequate well control, Britt shelf sand-ridges appear to have relatively flat bases and convex-upward upper surfaces.

Shelf sand-ridges are represented in five of the eight cores used in this research; three in the Upper Britt and two in the Lower Britt. Detailed core descriptions are presented in Appendix B.

Strata underlying shelf sand-ridges are dominated by wavy and lenticular bedding (Figure 37). These strata are composed of interbedded sandstones, siltstones, and shales with fossils being rare to common. Rare microfaulting is present. Basal contacts of shelf-sand ridges are gradational. Middle and lower portions of shelf sand-ridges are moderately fossiliferous, fine-grained, well-sorted, and



Figure 37. Core photograph showing wavy lenticularly-interbedded sands, silts, and shales typical of strata underlying Britt shelf sand-ridges.

quartzitic. These units are very fine-grained in basalmost portions. Fossils commonly are small due to breakage. Intraclasts, composed primarily of shale, are common but do not exceed trace amounts. Bedding typically is massive but small-scale trough cross-beds, parallel laminations, and bioturbated layers are also present. Bioturbation was extensive in middle and lower portions of sand-ridges but was limited to intervals presently less than six inches thick. Compaction features, including disrupted bedding, micro-faulting, and stylolites are rare to common. The upper portions of sand-ridges are typified by decrease in fossils, intraclasts, and grain size. This section is very fine-grained, well-sorted, sparsely fossiliferous, and quartzitic. Bioturbation was extensive; it destroyed virtually all primary sedimentary structures. Disrupted bedding is common with parallel laminations and stylolites rare to common. Authigenic chlorite, which recrystallized from detrital clay matrix, is abundant throughout these sand-ridges. Ooids are rare. The upper contact of shelf sand-ridges is gradational. Strata that overlie sand-ridges are either laminated, dark gray to black, sparsely-fossiliferous shales or wavy interbedded sandstones, siltstones, and shales. These strata commonly show evidence of moderate bioturbation.

Storm Deposits

Storm deposits are thin units composed primarily of

bioclastic debris and quartzitic sand. They are within marine depositional units in the Lower Britt Submember. Brenner and Davies (1973) defined coquinoid sandstones as bioclastic sediments admixed with as much as 70% sand. This description adequately describes the petrologic nature of storm deposits in the Britt. Due to the thin, discontinuous nature of storm deposits, isopach mapping was not attempted.

Storm deposits are represented in two cores. Individual units are between four and eighteen inches thick with abrupt upper and lower contacts. The lower portion of these units is coarse-grained and poorly-sorted. Cross-beds and parallel laminations are rare to common. The dominant constituent is bioclastic debris, which commonly was mixed with medium- to fine-grained quartzitic sand (Figure 38B). At some places the lower portions of storm deposits are composed entirely of bioclastic material, with echinoderms and brachiopods the most common fossil types. Rare corals, trilobites, bryozoans, and ostracods also are present. Coquinoid sandstones, dominant in lower portions of storm deposits, grade rapidly into sparsely- to moderately-fossiliferous, quartz-dominated sandstone (Figure 38C). Sandstones are fine- to very fine-grained and moderately-sorted. Bioturbated strata are common along the upper contacts of storm deposits.

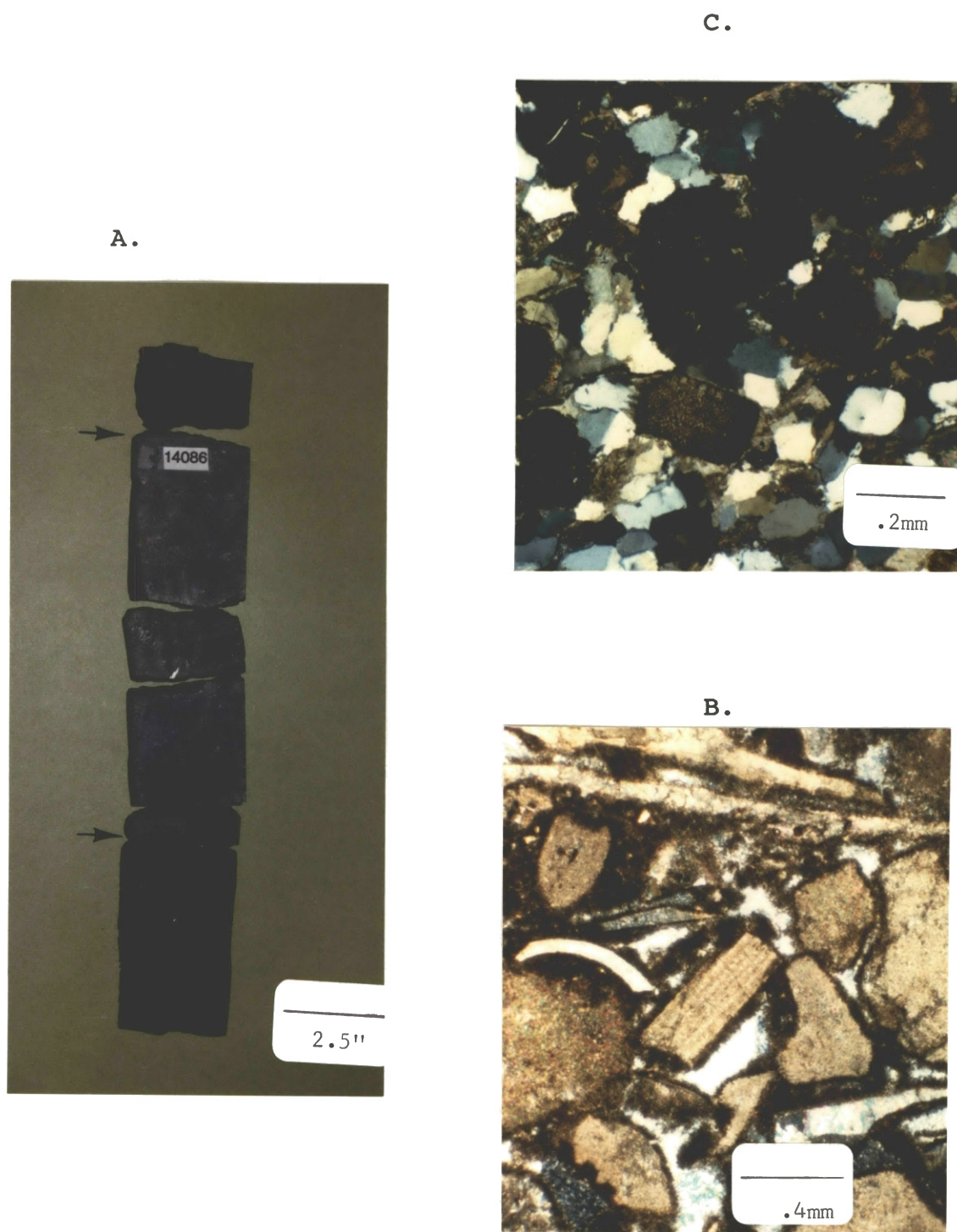


Figure 38. Petrologic nature of Britt storm deposits. Boundaries of storm deposit are denoted by arrows. (A) Core photograph of an 11" storm deposit. (B) Photomicrograph of lower portion of storm deposit. Fossils are dominant constituent. (C) Photomicrograph of upper portion of storm deposit. Note increase amount of quartz grains.

Phase II: Paleoenvironmental Interpretation
of Principle Facies

The primary purpose of this interpretative section is to describe the depositional setting of each facies and those processes that operated within each regime.

Bar-Finger Sands

Bar-finger sands in the Lower Britt were deposited as individual distributary channels that advanced basinward within a prograding deltaic complex. Henceforth, this complex shall be referred to as the Lower Britt deltaic system. Interpretation of the depositional environment in which these sands were deposited was made exclusively from isopach maps and stratigraphic cross-sections.

Bar-finger sands and channel-mouth bars are the dominant reservoir facies in river-dominated deltaic complexes. These sand bodies commonly are encased in impermeable deltaic or marine muds, resulting in stratigraphic hydrocarbon traps. Important deltaic subfacies are illustrated in map and cross-section view in Figure 39.

A complete, idealized depositional sequence representing high-constructive river-dominated deltaic progradation is given in Figure 40. Prodelta muds mark the initial phase of deltaic encroachment into an area. Delta-front silts and fine-grained sands overlies prodelta muds as progradation of the deltaic system continues. Overlying delta-front

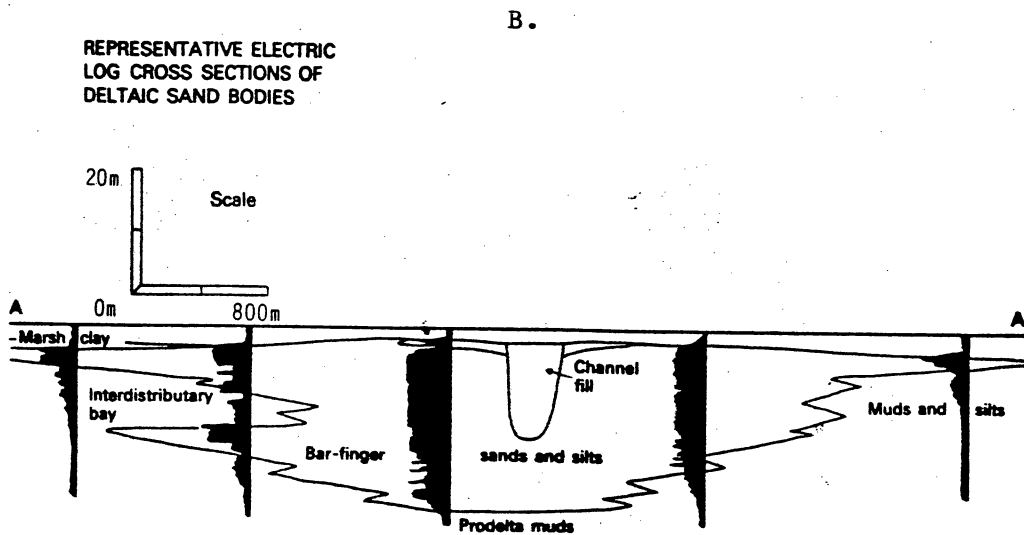
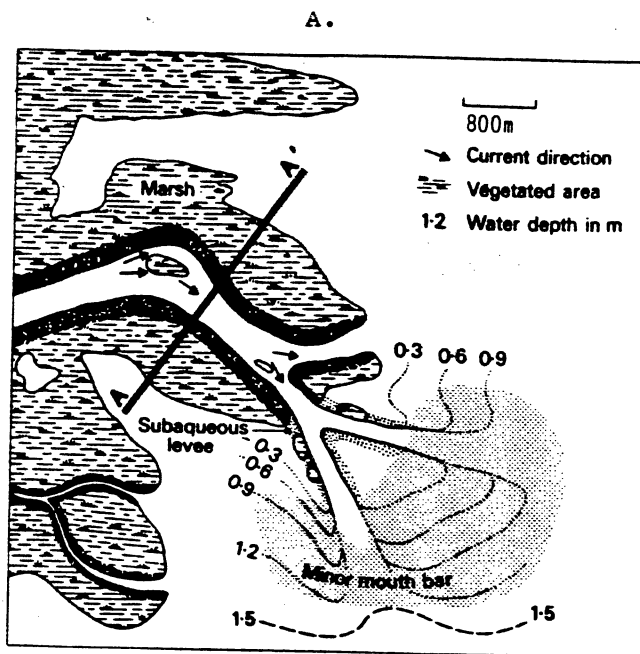


Figure 39. Significant Subfacies of the River-Dominated Delta:
 (A) Map View (B) Cross-sectional View (After Elliott, 1981)

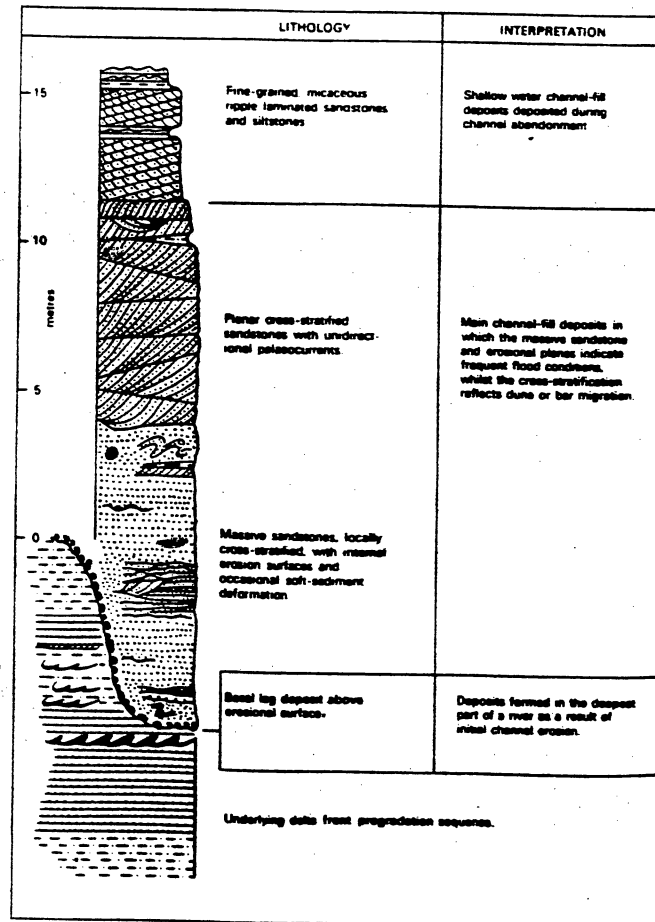


Figure 40. Idealized Vertical Sequence of Distributary-Channel/Bar-finger Sandstone (After Elliot, 1981)

sediments are bar-finger sands, many of which are primary reservoirs in the delta. In the absence of this facies, time-equivalent sediments are interdistributary-bay sediments. Within the Lower Britt deltaic system, prodelta and delta-front sediments are thin, and evidence of scouring and partial removal of these units by bar-finger-sand channels is common. Scouring of channels into the underlying Boatwright Member also was common.

Bar-finger sands were the distal end of the Lower Britt deltaic system as made evident by the basinward termination of these sands within the boundaries of the study area (Plate III). The shoreline-parallel orientation of Britt delta-destructive bars suggests that some sediments were reworked laterally by longshore currents, formed by waves breaking in the near-shore regime (Elliot, 1981).

Based on the geometry of the delta, the presence of bar-finger sands, and the position of the delta on the craton, the Lower Britt delta has been classified as a cratonic, river-dominated deltaic system based on the classification scheme for deltas proposed by Brown (1979). The geometry of the delta is controlled primarily by fluvial processes; there is minimal influence of basinal processes. The presence of shoreline-parallel delta-destructive bars associated with this depositional cycle suggest other processes such as waves and storms have laterally reworked some of the sediments entering the basin. Deltaic complexes

on Mid-Continent shelves were generally river-dominated due to the minimal affects of wave and tidal processes (Brown, 1979).

An equivalent fluvial facies has been identified north of the thesis area (Figure 33) (O'Donnell, 1986). This relationship implies that a point source to the north supplied sediments to the Anadarko Basin via the Lower Britt delta. This parent river system can be traced 40 miles northward in the subsurface to the area of truncation at the Mississippian-Pennsylvanian unconformity (O'Donnell, 1986).

The full areal extent of the Lower Britt deltaic system could not be ascertained because of pre-Pennsylvanian erosion (Plate III). Removal of Britt strata to the east of the study area limited mapping of this depositional system.

Delta-Destructional Sand Bars

Delta-destructional sand bars form in the near-shore regime in response to abandonment of entire deltas or individual lobes. As seas transgress over subsiding deltaic lobes, reworking of sediments may occur (shoreface-bypass). Elliot (1981) suggested that sediments which compose delta-destructional bars are derived from the upper portions of deltas. Active deltaic lobes in the vicinity may also supply some of the sediment. The shoreline-parallel orientation of Lower Britt delta-destructional bars suggests that storm or wave processes reworked the sediments.

Evidence of the high-energy depositional environment of

these bars is present in cores. Core analysis shows ooids to be common to abundant in lower portions of delta-destructive bars. The presence of oolitic beds suggests that the water was clear, warm, and agitated, with pH conducive to the precipitation of inorganic CaCO_3 . Precipitation of inorganic CaCO_3 generally is restricted to shallow water lacking significant suspended material (Flugel, 1982). Suspended clays and other fine material, commonly found in association with active deltaic lobes, inhibit algal growth. Algae have an indirect but very important control on the precipitation of CaCO_3 in that CO_2 in water inhibits CaCO_3 precipitation by lowering the pH (Al-Shaieb, 1986). Algae removes CO_2 during photosynthesis thus allowing pH to rise and precipitation of CaCO_3 to occur. The presence of inorganic CaCO_3 in delta-destructive bars suggests that no active deltaic lobe was in the immediate vicinity at the time these units were deposited. Micritization of ooids in the shallow marine environment was very common. This process destroyed much of their internal structure.

Further evidence implying a high-energy depositional setting for Britt delta-destructive bars is the large sizes of detrital grains that serve as ooid nuclei. Individual nuclei are as much as .20 mm in diameter. Fossils are abundant in the lower portions of the bars. Commonly broken, fossils were recognized only by shell pattern, not by outline. Oolitic and associated fine-grained clastic sediments are well-sorted.

Decreasing energy conditions are reflected by the lack of ooids in the upper portions of delta-destructive bars. Micrite-coated grains are common. Coatings are interpreted to form in a manner similar to that of the ooids' coatings, but under lower energy conditions. This interpretation is made on the basis of identical grain-coating material on ooids and coated grains, concentric growth lines of the coatings of both grain types, and the close association of the two. Fossils are larger and more easily recognizable in upper portions of the bars. The quartzitic sand is fine-grained and well-sorted. This apparent decrease in energy is attributed to continued subsidence of the delta. However, energy was sufficient to maintain growth of these units in slightly deeper water. Oolitic belts formed concurrently to the north in the most recently transgressed areas of the abandoned delta. Delta-destructive bars were covered with fossiliferous silts and shales or, in rare instances, by shelf sands. This reflects a change to a relatively quiet-water marine environment.

The multistoried nature of delta-destructive bars indicates that several minor transgressive-regressive events have occurred during deposition of this facies. Worldwide sea-level fluctuations, subsidence of the abandoned delta, or structural activity that was beginning to reshape the Mid-Continent may have been responsible for minor changes in sea level.

Delta-destructive bars are of little economic value.

With the exception of restricted areas, these sand bodies lack sufficient porosity to make them attractive exploration targets.

Shelf Sand-Ridges

Shelf sand-ridges were defined as longitudinal bedforms deposited in the inner- or outer-shelf regime that can attain thicknesses of greater than 30 feet (Brenner, 1980). Multiple sand-ridges can form concurrently on the shelf with individual ridges spaced thousands of feet apart (Figure 41). Sand bodies of this facies extend "normal" to the coastline in tide-dominated seas or "parallel" to the coast in wave- or storm-dominated basins (Brenner, 1980). The latter was the case in Britt seas. Shelf sand-ridges are the most regionally extensive of the sandstone facies in the Britt Member. The abundance of data (cores, well logs) from sand-ridges can be attributed to the economic viability of these gas-prone reservoirs. Success of future exploration may hinge on correctly interpreting the conditions that influenced deposition of sand-ridges.

Analogous bedforms have been described from Jurassic and Cretaceous strata deposited in shelf areas of the Western Interior Seaway of North America. Detailed analyses of the geometry, internal structure, and lateral facies relationships of these Mesozoic sand bodies have been undertaken by numerous authors, including Berg (1975), Spearing (1976), Brenner (1980), and Tillman and Martinson (1984). Extensive

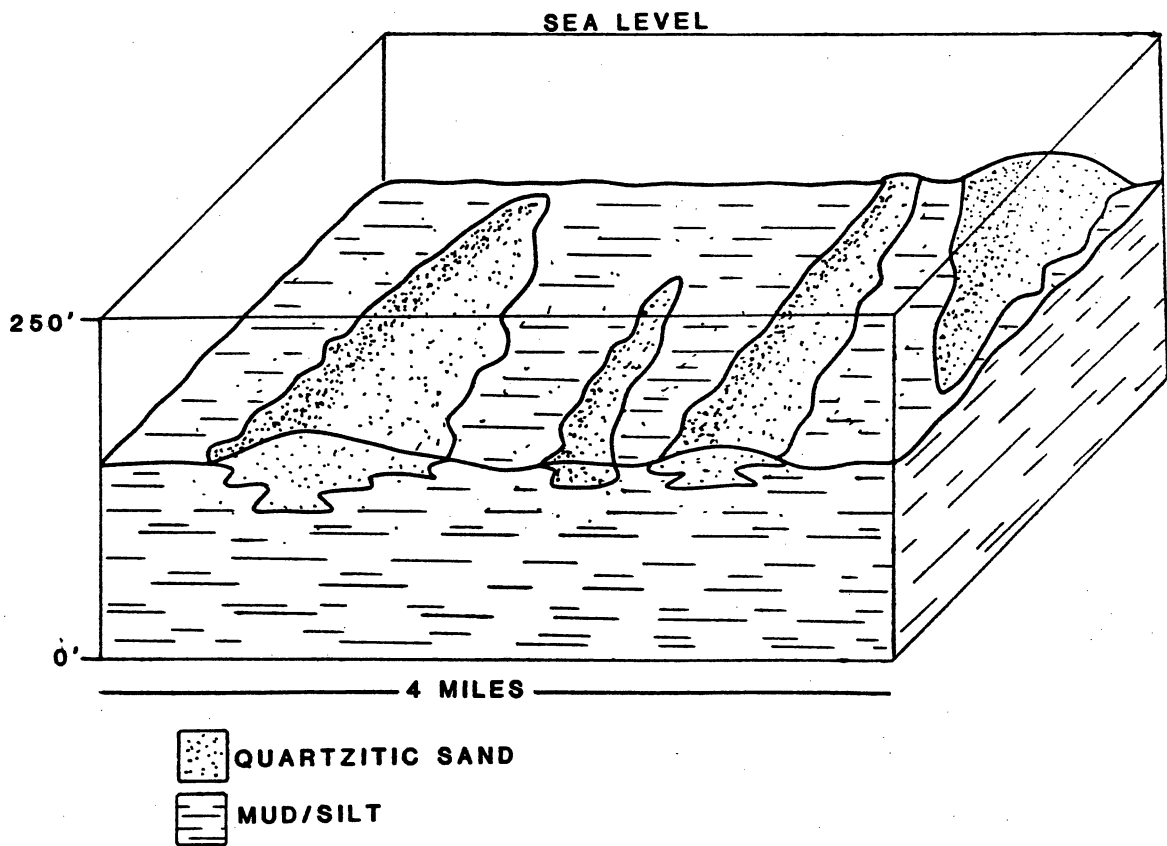


Figure 41. Block Diagram Illustrating Idealized Geometry and Relationships Among Shelf Sand-Ridges. Dimensions are Approximate (After Brenner and Davies, 1973)

research by these authors provided the data necessary for comparing the origins and morphologies of these units to shelf sand-ridges of the Britt.

Two hypotheses have been developed concerning the presence of sand-ridges on ancient and modern shelves. (1) Caston (1972) interpreted linear sand bodies on the North Sea shelf to have formed during the transgression that occurred after the last Ice Age from relict glacial features. Ridges in the North Sea are an example of relict structures, covered and modified by encroaching seas. Barrier islands commonly are modified in this manner. (2) The other mechanism of development involves direct formation of sand-ridges in the shelf environment. Jurassic and Cretaceous sand-ridges of the Western Interior Seaway are interpreted to have formed in this manner (Berg, 1975; Spearing, 1976, and others).

Keys to delineating the mode of formation of a particular sand-ridge system are the lateral facies relationships, geometry, and internal features. Correct interpretation of the depositional environment of lateral facies equivalent to sand-ridges can aid greatly in determining the origin of sediments that compose sand-ridges, whether endogenic or exogenic. Drowned barrier bars, an example of relict features that may be reworked into shelf sand-ridges, represent a source of endogenic sediments. Landward of barrier bars, lagoonal or back-bar sediments could be expected. Basinward, shales of the normal marine shelf should be found. In

contrast, sand-ridges formed directly in the shelf regime would be totally encased in marine shales. Adjacent equivalent facies both basinward and shelfward would virtually be identical. Lack of data from cores precluded judgment about the origin of Britt shelf sand-ridges based on associated facies.

Judgment of the origin of Britt shelf sand-ridges was made from observing their geometries and internal structures. Although not an absolute determining factor, the apparent absence of tidal channels cut through Britt sand-ridges suggests deposition in deep water. In addition, it is possible that Britt shelf sand-ridges were completely reworked from relict features with all original features destroyed. If once present, tidal channels may have been filled by reworked sediments.

The internal structure of the shelf sand-ridges, including sedimentary structures and grain size variation, provided the most evidence suggestive of the origins of these bedforms. Comparison of cores from sand-ridges to those of delta-destructive bars attested to the lower energy conditions in which sand-ridges were deposited. Ooids, abundant in portions of destructive bars, are rare in shelf sand-ridges. Bioturbated rock commonly is extensive, especially in the upper portions of sand-ridges. Burying organisms usually cannot tolerate the turbidity associated with a high-energy environment such as the near-shore. Authigenic chlorite that recrystallized from

detrital clay matrix is extensive in Britt sand-ridges but is much less abundant in delta-destructive bars. Removal of fines by winnowing takes place in the high-energy environment and thus, detrital clay matrix might be expected in sand bodies deposited in the relatively quiet shelf environment (Spearing, 1976).

In addition to the presence of certain sedimentary structures, the vertical variation of structures and grain size suggests changing energy conditions during vertical accretion of Britt shelf sand-ridges. Small-scale cross-bedding and parallel laminations are the dominant primary sedimentary structures in the lower portions of Britt sand-ridges (Figure 42). Bioturbated beds are rare. Parallel laminations, low-angle planar cross-beds, and evidence of bioturbation prevail in middle sections of these bedforms with features of bioturbation restricted to thin isolated zones. Disrupted and convoluted bedding, related to stress of overburden, is very common. Upper portions of sand-ridges are dominated by extensive bioturbated layers and disrupted bedding. Parallel laminations are common. Grain size increases upward abruptly from the base. Very fine-grained sand is typical of basal portions of Britt sand-ridges. Fine-grained sands dominate lower and middle sections with grain size becoming very fine-grained in upper sections. The upward decrease in grain size and extensive bioturbation in upper portions suggests decreasing water energy. Increased water depth would explain the decrease in

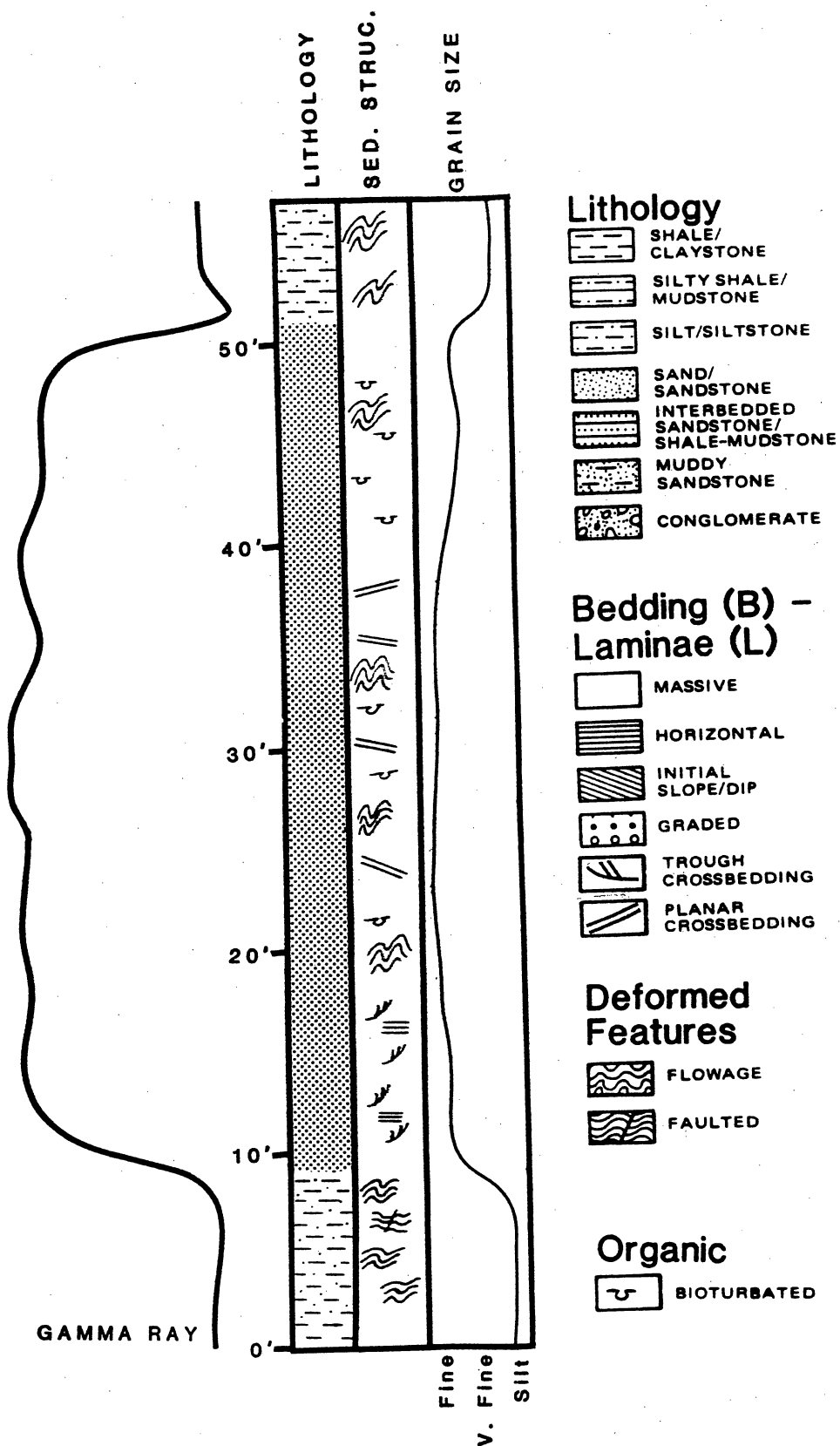


Figure 42. Idealized Vertical Sequence of Britt Shelf Sand-Ridge

energy. Increased water depth can be attributed to basinal subsidence related to the initiation of tectonic events described in Chapter III or to compaction of underlying sediments. An idealized vertical sequence of a Britt shelf sand-ridges is given in Figure 42.

Numerous similarities were noted during comparison of Britt sand-ridges to Jurassic and Cretaceous bedforms deposited in shelf areas of the Western Interior Seaway. Sand-ridges of the Britt and Jurassic/Cretaceous seaway parallel the paleoshoreline and appeared to have relatively flat bases and convex upper surfaces in dip-oriented cross-section view. Grain size increases upward from the base reaching its maximum in middle portions of Britt sand-ridges before decreasing in upper portions. Jurassic and Cretaceous sand bodies coarsen-upward throughout, becoming medium-grained at the top. This comparison in grain size suggests waning energy conditions affected the deposition of Britt sand-ridges. Sand-ridges are moderately well-sorted in both depositional systems. Detrital clay matrix is present throughout both types of sandstones suggesting relatively low energy conditions. Detrital clay matrix has been recrystallized since deposition. Large-scale planar cross-beds are abundant in middle and upper sections of Mesozoic sand-ridges but are sparse in Britt sand-ridges, and there are restricted to middle sections. This observation indicates that Britt sand-ridges were deposited in somewhat lower energy conditions. Planar cross-beds suggest that energy was

sufficient for migration of sand-ridges in the shelf environment (Brenner, 1980). Comparison of the internal structure of Britt sand-ridges to those deposited in western North America during the Mesozoic indicates that the former were deposited in conditions of lower energy. Whether Britt sand-ridges were deposited in deeper water or if energy within the shelf environment was less could not be ascertained. Investigation beyond the scope of this research is needed.

In summary, based primarily on internal features, Britt sand-ridges are interpreted to have been primary bedforms deposited in the low-energy shelf environment, and to have extended basically parallel to the coast. Well-studied Mesozoic shelf bedforms of the Western Interior Seaway provide means for direct comparison of ancient sand bodies deposited in the shelf environment to Britt sand-ridges. Whether Britt shelf sand-ridges were deposited in the inner- or outer-shelf regime could not be ascertained directly.

Storm Deposits

Within the last two decades, marine storms have been recognized as a mechanism for large-scale movement of near-shore sediments into the shelf environment. Thorough research of recent storms affecting coastal areas has been undertaken by numerous authors, including Hayes (1967) and Morton (1981). Study of the water movement and resultant bedforms produced during modern storms has resulted in

recognition of analogous deposits in ancient strata (Brenner and Davies, 1973; Hobday and Morton, 1984). Graded coquinoid sandstones in the Britt Member closely resemble modern and ancient storm deposits.

Three distinctly different types of storm deposits have been recognized by Brenner and Davies (1973) in the Lower Cretaceous Sundance Formation of Wyoming and Montana. Channel lags, storm lags, and swell lags each resulted from differing interactions between sediments and marine storms.

Channel lags are the thickest of the storm deposits. Channel lags are composed largely of coarse-grained bioclastic debris but some are quartz-dominant. Grain size decreases upward. These deposits collect in tidal channels which cut across bedforms in the marine environment. They possess an erosional base and a channel geometry in strike-oriented cross-section view.

Storm lags are thin, graded, sheet-like deposits that originate from the periodic flushing of tidal channels filled with bioclastic debris (channel lag) or from flushing of the near-shore environment. Individual sheets are restricted, covering no more than a few thousand square yards. They have an erosional base. Disarticulated tests of bivalved organisms lie roughly parallel to one another, preferentially with their convex sides up. Storm lags are interbedded with fine sands or muds, indicating a sudden short-term change from low to high energy.

In swell lags, elongated shells show preference to

parallel alignment with a majority of disarticulated bivalved shells positioned convex upward. Brenner and Davies (1973) noted such an occurrence in Cretaceous storm deposits of the Western Interior Seaway. This storm deposit differs from the others in that it lacks an erosional basal contact and sand-size material. Swell lags are generally composed of large shells, silt, and shale. Swell lags are deposited in a low-energy environment (below normal wave-base) conducive to deposition of silts and muds.

The movement of bioclastic and clastic sediment from the near-shore to shelf regime has been attributed to downward-flowing ocean currents (Walker, 1979). Storm-generated onshore winds that precede marine storms push the water against the landmass, forcing it downward along the bottom (Figure 43). These bottom-flowing currents flow obliquely away from the coast, carrying near-shore or tidal-channel sediments into the shelf environment (Morton, 1981). Brenner and Davies (1973) reported finding storm deposits in Cretaceous strata as far basinward as the outer-shelf environment.

The graded nature of storm deposits is a result of waning energy as seas quiet after a major storm pulse. Coarse-grained bioclastic debris, dominant in lower portions of storm deposits, graded into fine-grained quartz-dominated sands in upper portions. Each graded set represents a single storm surge.

A comparison of storm deposits in the Britt Member to

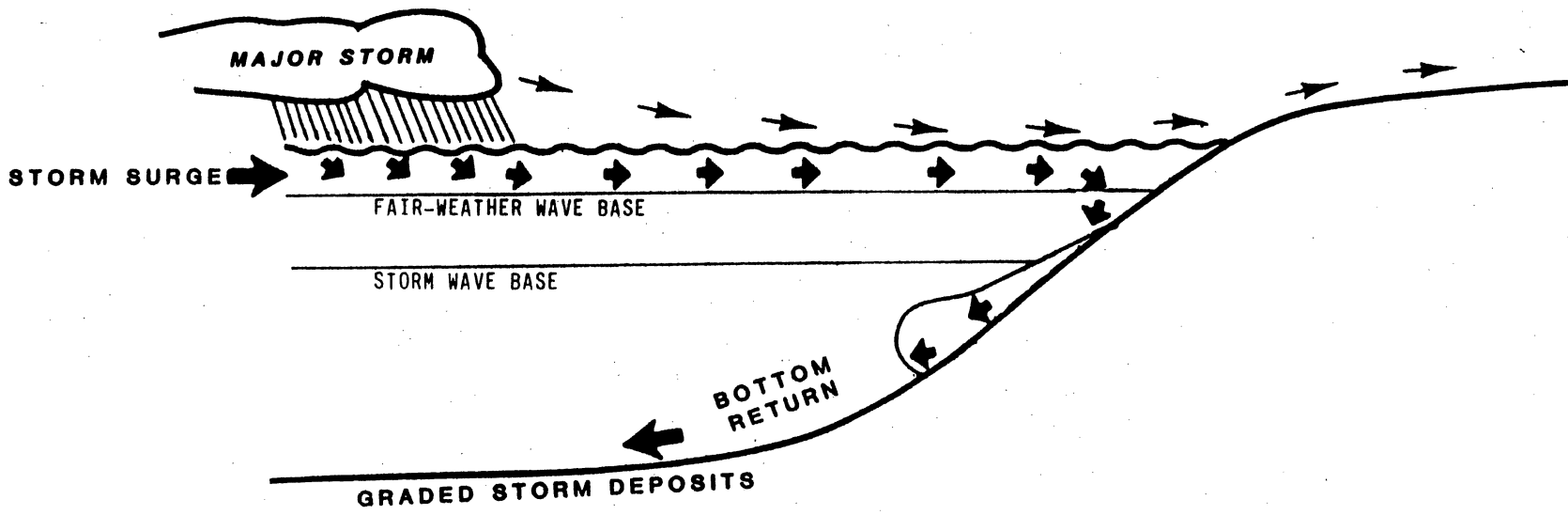


Figure 43. Origin of Graded Storm Deposits in the Shelf Regime (After Walker, 1979)

modern and ancient analogies indicates that storm lags are the only type represented. These units have a sharp erosional base and grade upward abruptly from coarse-grained coquinoid sandstone that contains less than 20% quartz to sparsely- to moderately-fossiliferous, fine-grained quartzitic sandstone. The upper contacts of Britt storm lags is abrupt. A return to normal marine shelf conditions is indicated by siltstone and shales overlying each of the Britt storm lags. The uppermost portions of some units are bioturbated. Britt storm deposits generally are devoid of structures, but faint small-scale planar cross-bedding was present in several storm lags. Individual units typically are less than one foot thick but some are as thick as 18 inches. Brachiopods and echinoids dominate the bioclastic debris with echinoid plates and disarticulated brachiopod shells aligned in a parallel fashion. In certain instances, a single fossil type composes the deposit (Figure 44). Such an occurrence may represent flushing of a habitat that was dominated by that organism. In general, storm lags of the Britt are cemented with acicular and sparry calcite that was precipitated in the shallow-marine and phreatic zones, respectively. Much of the cement has been altered to ferroan baroque dolomite.

Storm lags in the Lower Britt are found in marine shales both underlying and overlying shelf sand-ridges. Data from cores are sparse, as storm deposits were found only in two cores. Within the Apexco, Inc. Buell No. 1-A (Section

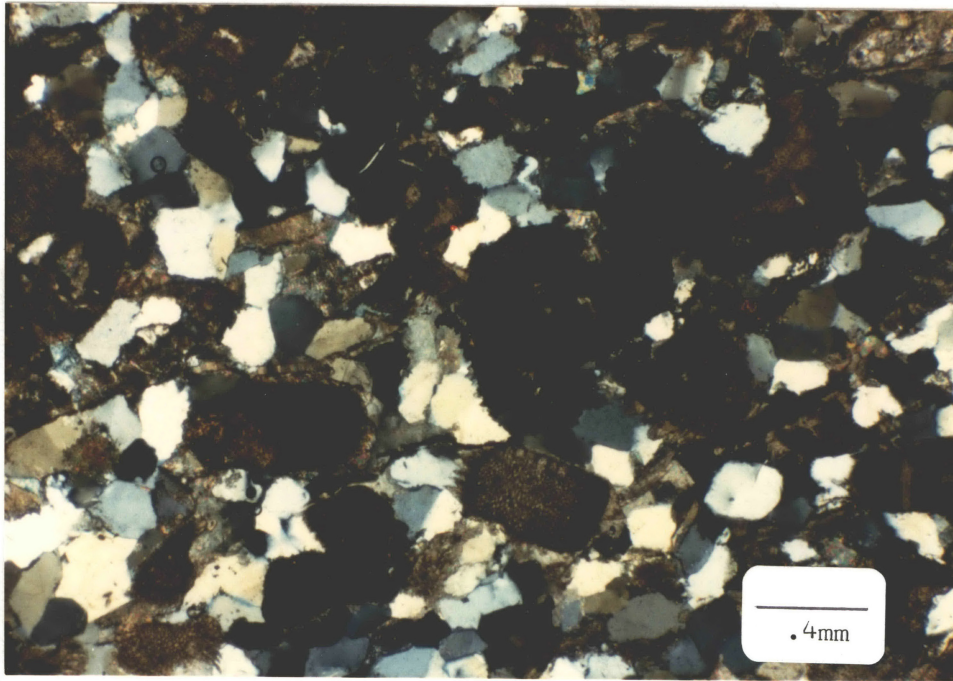


Figure 44. Photomicrograph of sediment from a storm deposit. Note that echinoderm plates (E) dominate the fossiliferous sediment, suggesting that a single habitat was affected by the storm surge.

10-T11N-R12W) three storm lags occur below a shelf sand-ridge. Three storm deposits are in the Amoco McClain No. 1 (Section 23-T10N-R12W), within marine shales immediately overlying a Lower Britt shelf sand-ridge. The sand-ridge in the McClain No. 1 was judged to be equivalent stratigraphically to the sand-ridge in the Buell No. 1-A. No storm lag deposits were found within shelf sand-ridges. However, they commonly were found within analogous units in Mesozoic strata of western North America (Brenner and Davies, 1973). This observation suggests that with continued coring, storm lags will be found within Britt shelf sand-ridges.

In summary, graded coquinoid sandstones in the Britt Member represent storm lags deposited during a single storm event as near-shore or tidal channel sediments were flushed into the shelf environment. Individual units commonly are less than a foot thick, with erosional bases and abrupt upper contacts. Analogous features have been recognized in both modern and ancient shelf regimes.

Phase III: Depositional Model for Strata of the Britt

Two distinct cycles of sedimentation were recorded by Britt sandstones in the study area. Within the early cycle, bar-finger sands, delta-destructive sand bars, and shelf sand-ridges are preserved. Only shelf sand-ridges record the late cycle. The purpose of this section is to construct a depositional model that accounts for the relationships

among facies.

Britt sandstones record four stages of evolution in the area of investigation. In ascending chronologic order, these are: 1) deltaic progradation, 2) abandonment of the delta, 3) subsidence of the delta, and 4) reoccupation. Multiple depositional environments coexisted in the thesis area.

Bar-finger sands record the initial phase of Britt deposition (Plate III). Bar-finger sands represent distributary channels in distal portions of the delta. These channels were conduits for clastic sediments deposited in the deltaic, near-shore, and shelf environments. The sediments were reworked into shelf sand-ridges and delta-destructural bars. Lower Britt distributary channels terminated within the thesis area.

The Lower Britt delta prograded into a marine environment, as made evident by deltaic shales that overlie marine sediments in the core from the Tenneco Willie Lefthand No. 1-23 (Section 23-T9N-R9W).

Sediments that composed bar-finger sands and associated interdistributary facies were derived from a parent fluvial system located immediately to the north (O'Donnell, 1986). The trend of this meandering river system was approximately north to south; it can be traced more than 40 miles to the area of truncation at the Mississippian-Pennsylvanian unconformity (Figure 33). The lack of appreciable amounts of metastable constituents (e.g., feldspars, micas) suggests a

distant source. Paleogeologic mapping (Figure 6) indicates that the Central Kansas Uplift shed sediments during the Late Mississippian; this is a likely source of sediments in the Britt. A more detailed petrologic analysis of detrital Britt sediments is needed.

Boatwright sandstones from cores of the Tenneco Willie Lefthand No. 1-23 and the Tenneco Grant Rumley No. 1-22 were poorly-sorted; they fine upward and contain large-scale trough cross-beds and erosional basal contacts. These features suggest a channel-form origin. If Boatwright sandstones from these cores are truly channels, strata from the Boatwright and Lower Britt may record stacked delta lobes in northeastern portions of the thesis area. Detailed analysis by O'Donnell (1986) of the Britt parent fluvial system showed that these sands appear to be equivalent partially to strata of the Boatwright. Based on this evidence, it is hypothesized that the aforementioned fluvial system served as the conduit for sediments of both the Britt and the Boatwright, in the area of investigation.

The second stage of deposition involved abandonment of the delta. Due to erosion of Britt strata immediately east of the thesis area, whether other delta lobes were active in the vicinity or whether the the Lower Britt delta was completely abandoned could not be ascertained directly. Due to this lack of information, whether sediments that were reworked into delta-destructive bars were relict sands or were derived from another delta lobe active to the east, is

not known. No deltaic sediments are known from regions west of the area of investigation.

The third stage of evolution involved subsidence-induced transgression of the abandoned delta. As shallow, wave-dominated seas inundated the Lower Britt delta in the thesis area, sands from several possible origins (discussed previously) were reworked, forming delta-destructive sand bars along the subsiding delta-front. These sand bodies parallel the paleoshoreline and generally are less than 15 feet thick. The relationship among bar-finger sands and delta-destructive bars was readily inferred from logs of wells in which destructive bars are presumed to overlie distributary channels (Figure 35). Presumed delta-destructive bars were also mapped immediately west and south of the Lower Britt delta (Figure 45).

Hypothetically, shelf sand-ridges were forming when the Lower Britt delta was active. A lack of consistent marker beds when correlating from bar-finger sands to shelf sand-ridges hampered judgement of the timing of deposition. Shelf sand-ridges and delta-destructive sand bars also may have formed contemporaneously in the Lower Britt sea. Again, a lack of consistent marker beds between near-shore and shelf sand bodies resulted in no compelling interpretation of the relative timing of deposition. Limited evidence of the relationship between delta-destructive bars and shelf sand-ridges was supplied in the core from the Apexco, Inc. Buell No. 1-A. The thick Lower Britt sand body located

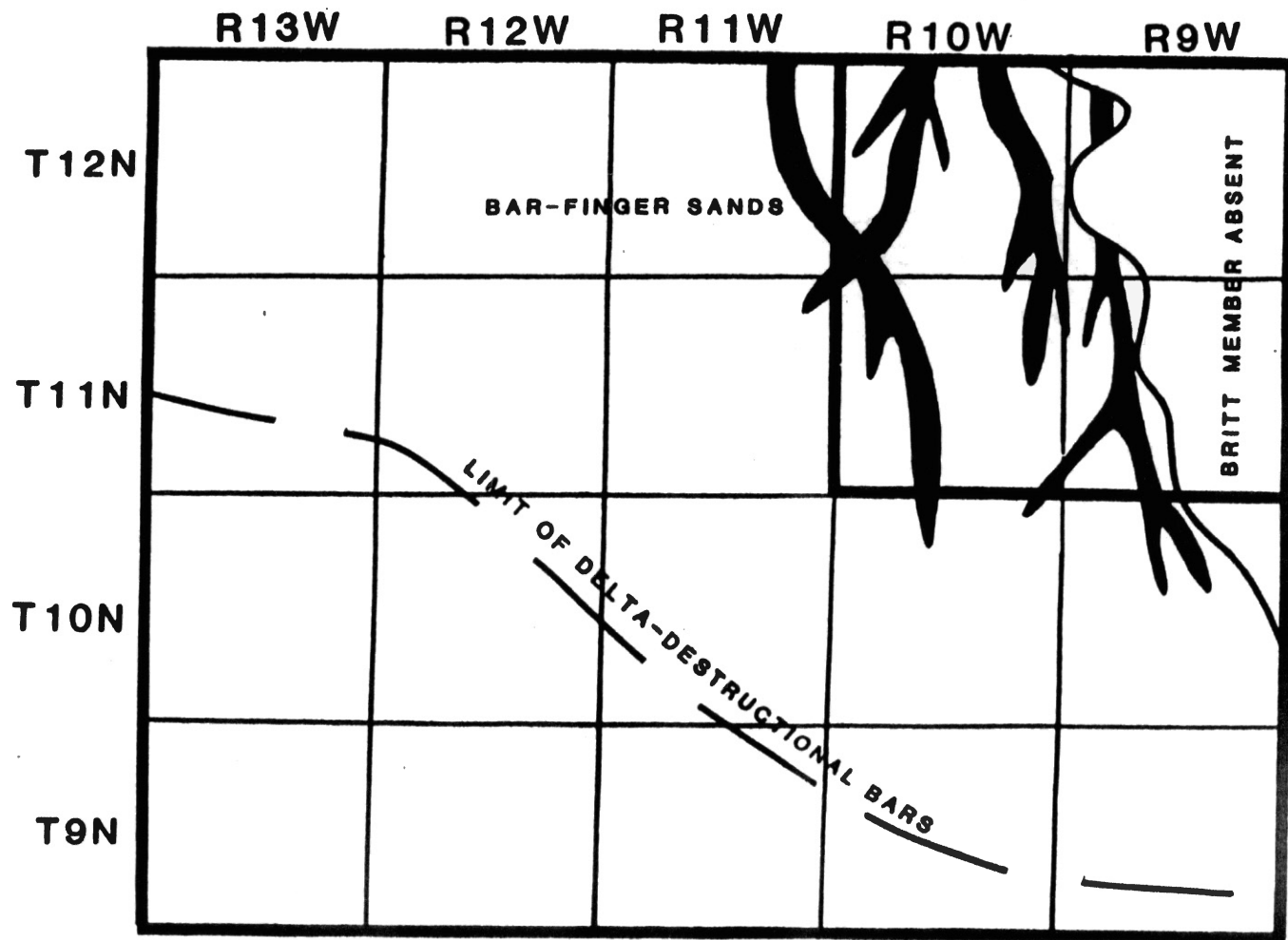


Figure 45. Approximate Basinward Limit of Britt Delta-Destructural Sand Bars

between 14,045 feet and 14,085 feet on well logs (Figure 7) was interpreted to be two stacked sandstones; the lower 13 feet a delta-destructive bar and the upper 27 feet a shelf sand-ridge. This relationship does not suggest that shelf sand-ridges formed only after delta-destructive bars, but does indicate that the near-shore regime was replaced by a quieter shelf environment as seas transgressed northward.

The final stage in the depositional evolution of the Britt in the thesis area involved deposition of the Upper Britt strata. These rocks record the second cycle of sedimentation. Unlike the Lower Britt, only shelf sand-ridges and associated shales record this late cycle. There was no evidence recorded of an Upper Britt delta within or around the thesis area. As discussed in Chapter II, a depositional hiatus occurred between deposition of the Upper Britt and Cunningham Member; thus, any record of a deltaic system in the Upper Britt may have been destroyed. Also as previously discussed, strata of the Britt have been removed by erosion in far northeastern and east-central portions of the area of investigation. If an Upper Britt deltaic system was present to the east, all evidence of such an environment has been destroyed. The exact point where Upper Britt sediments entered the basin may never be known.

Two independent Upper Britt shelf sand-ridge complexes were mapped in the thesis area (Plates IV, V). Ridges from these systems commonly are stacked, with the stratigraphically lower "A" sand-ridges thinner and less extensive than

the overlying "B" system (Figure 46). These sand-ridges are separated by a thin shale. The "B" system is an excellent natural gas reservoir in the study area.

Based on geometry and internal features, shelf sand-ridges of the Upper and Lower Britt were deposited in very similiar environments. These two sets of shelf bedforms are extensive regionally and parallel one another (Figure 33). Upper Britt sand-ridges were deposited basinward of sand-ridges of the Lower Britt. This relationship suggests a drop in sea level in response to the initiation of tectonism or an overall progradation of the Britt shelf, which resulted from deposition of large amounts of clastics in this environment. A judgment as to which of these hypotheses is truly correct cannot be made from available data. The relationship between these two shelf sand-ridge systems was brought to the reader's attention to demonstrate that tectonism and sedimentation may be related in deposition of the Goddard Formation, as suggested by Jacobsen (1959)

Summary of Britt Depositional System

Four stages in the depositional evolution of the Britt genetic interval have been recognized from the stratigraphic record. A cratonic river-dominated deltaic complex that prograded from the north delivered fine-grained sands, silts, and muds into the basin. With abandonment, delta-destructional bars formed along the subsiding delta-front from sands reworked by waves and storms. Lower Britt sand-

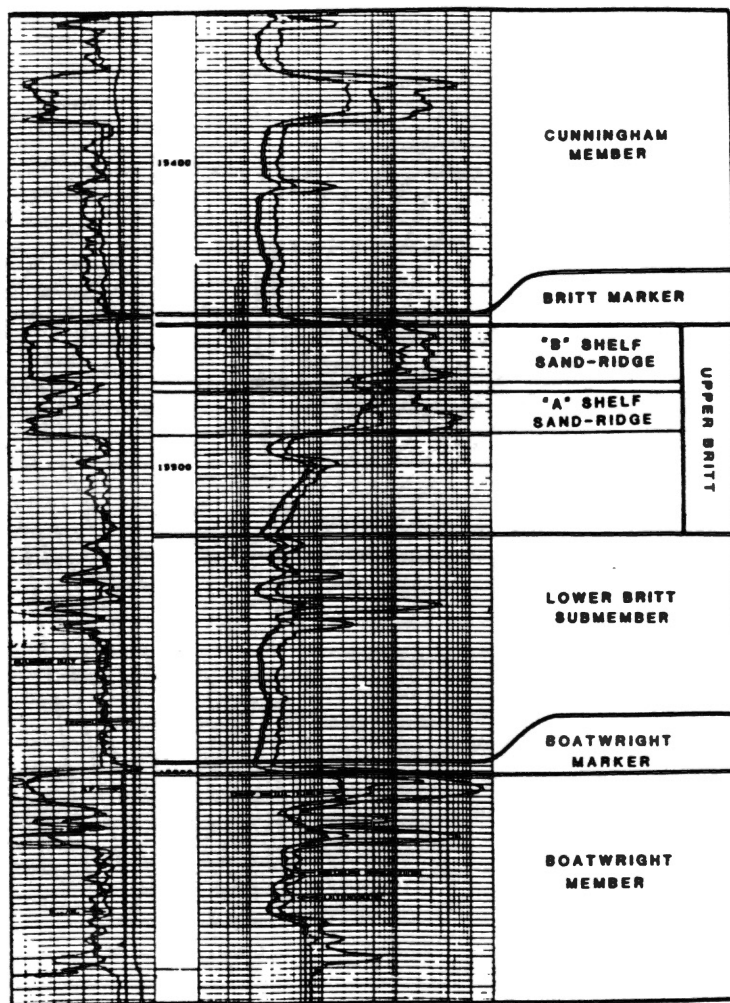


Figure 46. Type Log Illustrating Stratigraphic Position of Upper Britt "A" and "B" Shelf Sand-Ridges. Well Log from the Lear Petroleum Jones No. 1, Section 26-T11N-R13W, Caddo County, Oklahoma.

ridges deposited in the shelf regime may have coexisted with delta-destructive bars that formed in the high-energy near-shore environment. These shelf bedforms also may have been deposited contemporaneously with deltaic bar-finger sands. The final stage of evolution was recorded by Upper Britt shelf sand-ridges that record the second "pulse" of sedimentation in the thesis area. These bedforms were deposited basinward of the Lower Britt sand-ridge complex. The original extent of the Britt probably will never be known, due to pre-Pennsylvanian erosion and possibly to erosion that occurred between deposition of the Cunningham and Britt members.

CHAPTER VI

SUMMARY AND CONCLUSIONS

Major conclusions formulated during the study of the depositional, structural, stratigraphic, and petrologic aspects of Britt sandstones in southwestern Canadian and northern Caddo Counties of Oklahoma are given below. All conclusions listed pertain specifically to the Britt Member and unless noted, these inferences are applicable to areas surrounding the area of investigation.

Conclusions

1. The Britt is an ad hoc member of the Upper Mississippian Goddard Formation. The boundaries of this genetic interval are the underlying "Boatwright Marker" and the overlying "Britt Marker." Both of these delineating units are thin (generally less than 5 feet) and regionally extensive. The Britt is considered incorrectly to be a member of the Pennsylvanian Springer Formation by many petroleum geologists working this area.

2. Within the study area, the top of the Goddard Formation is delineated by an unconformity between Late Mississippian and Early Pennsylvanian clastic sediments. The unconformity is verifiable by dip-oriented stratigraphic

cross-sections (Plates IX - XI), which show pinching out of successively older units shelfward against the unconformity. The Britt Member is absent in northeastern portions of the study area (Plate III).

3. The stratigraphic position of the Mississippian-Pennsylvanian unconformity can be approximated closely from well logs. In this study, the first leftward deflection of the conductivity curve above 650 millimhos m but below correlatable Lower Pennsylvanian sandstones was chosen as the boundary. Correlation of the well log and core from the Apexco, Inc. Buell No. 1-A (Section 10-T11N-R12W) suggests that this technique is reliably accurate.

4. Structural deformation essentially was gentle basinal warping. Strike is approximately northwestward. Dip increases from approximately 2° in the northeast to approximately 4° in the southwest.

5. At least two faults are present in the study area. A major fault with 1,400 feet of throw is located in the southwestern portions of the study area, with a minor fault (250 feet of throw) present in northeastern portion. Both faults are oriented subparallel to structural strike and have nearly vertical fault planes. These faults were created during the Amarillo-Wichita Uplift.

6. Britt sandstones are predominantly quartzitic. Coquinoid sands and oolitic units also are present. Minor detrital constituents include volcanic and sedimentary rock fragments, potassic and plagioclase feldspars, glauconite,

siliceous matrix, and various heavy minerals. Detrital clay matrix is an important constituent in many instances.

7. Major authigenic constituents include carbonate and silica cements and chlorite. Minor authigenic constituents include kaolinite, illite, pyrite, collophane, and organic material.

8. Authigenic chlorite is a product of the recrystallization of detrital clay matrix. The presence of detrital grains "floating" in a clay matrix was the main criterion on which these clays were judged to be originally allogenic. Chlorite is well crystalline and possesses an edge-to-face relationship with detrital grains.

9. Silica cement types are dominated by syntaxial overgrowths and chert. Drusy megaquartz and chalcedony are rare. Silica cement is a product of the deep-burial diagenetic environment.

10. Carbonate cements are dominated by ferroan dolomite. Based on morphology and relationship with other diagenetic constituents, calcite was precipitated early in the diagenetic history of Britt sandstones. Much of these cements was converted to ferroan dolomite in the deep-burial environment. Carbonate cements are most common in skeletal sandstones.

11. Porosity is both primary and secondary. Primary porosity has been reduced greatly by compaction and by precipitation of authigenic minerals. Secondary porosity resulted from dissolution of both detrital and authigenic

constituents and from fracturing. Microporosity associated with authigenic chlorite, along with preserved primary porosity, is a major type of porosity. The amount of microporosity could not be ascertained with use of the standard petrographic microscope due to the small sizes of pores. Total porosity in sands with relatively high chlorite percentages may have been grossly underestimated for this reason.

12. Chlorite inhibited the formation of silica overgrowths, resulting in the preservation of primary porosity. The amount of chlorite is inversely proportional to that of authigenic silica. Chlorite percentages between 4% and 14% seem to be optimal for preservation of primary porosity. In samples where percentages are less than 4%, advanced silica cementation had occurred. Sandstones with chlorite percentages more than 14% did not originally possess reservoir-quality primary porosity.

13. The amount of silica and carbonate cements is inversely proportional. In skeletal sands and, rarely, quartzitic sands, early calcite cementation resulted in the total loss of porosity and permeability. Silica-saturated formation water, associated with the deep-burial diagenetic regime, could not pass through these rocks resulting in no precipitation of authigenic silica.

14. Britt sandstones in the thesis area record the transition from the deltaic to shelf regime. These sediments are only a portion of a regionally extensive

depositional system that covered thousands of square miles in west-central, southwestern, and south-central Oklahoma.

15. Four principle sandstone facies compose the depositional sequence: deltaic bar-finger sands, delta-destructive bars, shelf sand-ridges, and storm deposits. With the exception of storm deposits, these sands are quartzitic.

16. Two distinct cycles of sedimentation were recognized during this investigation, resulting in division of the Britt into upper and lower submembers. These submembers record four distinct stages in the depositional evolution of the Britt strata. Initially, a deltaic complex prograded into the area. The second stage involved abandonment of the delta. This was followed by subsidence of the abandoned lobes, resulting in formation of delta-destructive sand bars. Shelf sand-ridges may have been forming as the delta prograded into the thesis area. These longitudinal bedforms may have also been deposited as delta-destructive bars were being formed. Insufficient data hampered judgment about the relative timing of deposition of shelf sand-ridges. The final stage in the evolution of this system involved reoccupation of the area. Only shelf sand-ridges are present to record this stage. An unconformity or depositional hiatus overlies Britt strata in portions of the study area. The basinward extent of this hiatus could not be determined from available data.

17. Both delta-destructive sand bars and shelf-sand ridges trend parallel to the paleoshoreline. Shoreline-

normal orientation of marine sandstone units was not observed. The presence of storm deposits suggests that storms may have been a strong influence in movement of sediment in the marine environment and in the shaping of marine sandstone bodies.

18. Structural, sedimentologic, and stratigraphic evidence suggest that structural and sedimentologic strike coincide, except in northeastern portions of the thesis area.

19. The Central Kansas Uplift may have been the principle source of clastic sediments. Evidence supporting this statement includes paleogeologic mapping, which indicates that the Central Kansas Uplift was exposed during the Late Mississippian, maturity of the sands, and presence of a parent fluvial system which extends more than 40 miles northward from the thesis area but which is truncated at the Mississippian-Pennsylvanian unconformity.

20. Depositional environment and preservation of primary porosity are related. Preservation of primary porosity resulted from inhibition of silica overgrowths by authigenic chlorite. Chlorite originated from the recrystallization of detrital clay matrix, which was only in sands deposited in lower energy environments (such as shelf sand-ridges). In comparison, delta-destructive bars deposited in the high-energy nearshore regime lacked all but minor amounts of chlorite, due to winnowing of detrital clay. This resulted in advanced silica cementation and destruction of reservoir-

quality porosity. Shelf sand-ridges are excellent natural gas reservoirs in the area whereas delta-destructional bars are productive only in limited areas.

REFERENCES CITED

- Adams, W. L., 1964, Diagenetic Aspects of Lower Morrowan Pennsylvanian Sandstones, Northwestern Oklahoma: American Association of Petroleum Geologists Bulletin, Vol. 48, No. 9, pp. 1568-1580.
- Al-Shaieb, Z., 1986, Personal Communication, Oklahoma State University, Stillwater, Oklahoma.
- Al-Shaieb, Z., and Shelton, J. W., 1981, Migration of Hydrocarbons and Secondary Porosity in Sandstones: American Association of Petroleum Geologists Bulletin, Vol. 65, No. 11, pp. 2433-2436.
- Beckman, W. A., and Sloss, L. L., 1959, Possible Pre-Springeran Unconformity in Southern Oklahoma: American Association of Petroleum Geologists Bulletin, Vol. 50, No. 7, pp. 1342-1364.
- Berg, R. R., 1975, Depositional Environments of the Upper Cretaceous Sussex Sandstone, House Creek Field, Wyoming: American Association of Petroleum Geologists Bulletin, Vol. 59, pp. 2099-2110.
- Blatt, H., 1982, Sedimentary Petrology: W. H. Freeman and Company.
- Bloustone, D. A., 1975, Producing Characteristics of Lower Morrow Sandstone in Southern Ellis County, Oklahoma: American Association of Petroleum Geologists Mid-Continent Section Meeting, Wichita, Kansas. American Association of Geologists Bulletin, Vol. 59, No. 3, pp. 318-331.
- Brenner, R. L., 1980, Construction of Process-Response Models for Ancient Epicontinental Seaway Depositional Systems Using Partial Analogs: American Association of Petroleum Geologists Bulletin, Vol. 64, No. 8, pp. 1223-1244.
- _____, and Davies, D. K., 1973, Storm-Generated Coquinoid Sandstone: Genesis of High-Energy Marine Sediments from the Upper Jurassic of Wyoming and Montana: Geol. Soc. America Bull., Vol. 84, pp. 1685-1698.

- _____, 1974, Oxfordian Sedimentation in Western Interior United States: American Association of Petroleum Geologists Bulletin, Vol. 58, pp. 407-428.
- Brown, L. F. Jr., 1979, Deltaic Sandstone Facies of the Mid-Continent: in Pennsylvanian Sandstones of the Mid-Continent, Tulsa Geological Soc. Spec. Pub. No. 1, pp. 35-64.
- Caston, V. N. D., 1972, Linear Sand Banks in the Southern North Sea: Sedimentology, Vol. 16, pp. 63-78.
- Choquette, P. W., and Pray, L. C., 1970, Geologic Nomenclature and Classification of Porosity in Sedimentary Rocks: American Association of Petroleum Geologists Bulletin, Vol. 54, No. 2., pp. 207-250.
- Davis, H. G., 1974, High Pressure Morrow-Springer Gas Trends, Blaine and Canadian Counties, Oklahoma: Shale Shaker, Vol. 24, No. 6, pp. 104-118.
- Donovan, R. N., 1985, Personal Communication, Oklahoma State University, Stillwater, Oklahoma.
- Drake, D. D., 1976, Suspended Sediment Transport and Mud Deposition on Continental Shelves: in Marine Sediment Transport and Environmental Management, John Wiley and Sons, New York, pp. 127-158.
- Dunn, D. L., 1966, New Pennsylvanian Platform Conodonts from Southwestern United States: Journ. of Paleontology, Vol. 40, pp. 1294-1303.
- Elias, M. K., 1956, Upper Mississippian and Lower Pennsylvanian Formations of South Central Oklahoma in Petroleum Geology of Southern Oklahoma: American Association of Petroleum Geologists Bulletin, Vol. 1, pp. 56-134.
- Elliot, T., 1981, Deltas: in Sedimentary Environments and Facies, Blackwell Scientific Publications, New York.
- Evans, J. L., 1979, Major Structural and Stratigraphic Features of the Anadarko Basin: in Pennsylvanian Sandstones of the Mid-Continent: Tulsa Geological Soc. Spec. Pub. No. 1, pp. 97-113.
- Feinstein, S., 1981, Subsidence and Thermal History of the Southern Oklahoma Aulacogen: Implications for Petroleum Exploration: American Association of Petroleum Geologists Bulletin, Vol. 65, No. 12, pp. 2521-2533.

- Flugel, Erik, 1982, Microfacies Analysis of Limestones: Springer-Verlag Press, Berlin.
- Folk, R. L., 1962, Spectral Subdivision of Limestone Types: in Classification of Carbonate Rocks, American Association of Petroleum Geologists Spec. Pub. No. 1, pp. 62-84.
- _____, 1974, Petrology of Sedimentary Rocks: Hemphill's Book Store, Austin, Texas.
- Franks, S. G., and Forester, R. W., 1984, Relationships Among Secondary Porosity, Pore-Water Chemistry and Carbon Dioxide, Texas Gulf Coast: in Clastic Diagenesis, American Association of Petroleum Geologists Memoir 37, pp. 63-79.
- Garner, D. L., and Turcotte, D.L., 1984, The Thermal and Mechanical Evolution of the Anadarko Basin: Tectonophysics, Vol. 107 (1984), pp. 1-24.
- Geomap, 1981, Executive Reference Map No. 311.
- Gordon, M. Jr., and Mamet, B. L., 1978, The Mississippian-Pennsylvanian Boundary: in Contributions to the Geologic Time Scale, American Association of Petroleum Geologists, Tulsa, Oklahoma.
- Hayes, J. B., 1979, Sandstone Diagenesis-The Hole Truth: Society of Economic Paleontologists and Mineralogists Spec. Pub. 26, pp. 127-140.
- Hayes, M. O., 1967, Hurricanes as Geological Agents: Case Studies of Hurricane Carla, 1961, and Cindy, 1963: Univ. Texas. Bur. Econ. Geol. Rep. Invest. 61.
- Heald, M. T., and Larese, R.E., 1973, The Significance of Solution of Feldspar in Porosity Development: Journ. Sed. Pet., Vol. 43, pp. 458-460.
- Hobday, D. K., and Morton, R. A., 1984, Lower Cretaceous Shelf Storm Deposits, Northeast Texas: in Siliciclastic Shelf Sediments Society of Economic Paleontologists and Mineralogists Spec. Pub. No. 34, pp. 205-213.
- Jacobsen, L., 1959, Sedimentation of Some Springeran Sandstone (Mississippian-Pennsylvanian) Reservoirs, Southern Oklahoma: American Association of Petroleum Geologists Bulletin, Vol. 43, No. 11, pp. 2575-2591.

- Jordan, L., 1957, Subsurface Stratigraphic Names of Oklahoma, Oklahoma Geological Survey Guide Book VI.
- Khaiwa, M. H., 1968, Geometry and Depositional Environment of Morrow Reservoir Sandstones, Northwestern Oklahoma: Ph.d. Dissertation, University of Oklahoma, Norman, Oklahoma.
- Krynine, P. D., 1946, Microscopic Morphology of Quartz Types: 2nd Cong. Panam. Ing. Min. Geol. Anales, Vol. 3, pp. 35-39.
- Leder, F., and Park, W. C., 1986, Porosity Reduction in Sandstone by Quartz Overgrowth: American Association of Petroleum Geologists Bulletin, Vol. 70, No. 11, pp. 1713-1728.
- Lyons, G. M., 1971, Subsurface Stratigraphic Analysis, Lower "Cherokee" Group, Portions of Alfalfa, Major, and Woods Counties, Oklahoma: Shale Shaker, Vol. 22, No. 1, pp. 4-24.
- Moncure, G. K., Lahann, R. W., and Siebert, R. M., 1984, Origin of Secondary Porosity and Cement Distribution in a Sandstone/Shale Sequence from the Frio Formation (Oligocene): in Clastic Diagenesis, American Association of Petroleum Geologists Memoir 37, pp. 151-162.
- Mooers, C. N. K., 1976, Wind-Driven Currents on Continental Margins: in Sediment Transport and Environmental Management, John Wiley and Sons, New York, pp. 29-52.
- Moore, G. E., 1979, Pennsylvanian Paleogeography of the Southern Mid-Continent, in Pennsylvanian Sandstones of the Mid-Continent: Tulsa Geological Soc. Spec. Pub. No. 1, pp. 2-12.
- Morton, R. A., 1981, Formation of Storm Deposits by Wind-Forced Currents in the Gulf of Mexico and the North Sea: Internat. Association of Sedimentologists Spec. Pub. No. 5, pp. 385-396.
- O'Donnell, M., 1986, Personal Communication, Ward Petroleum Corporation, Enid, Oklahoma.
- Peace, H. W., 1965, The Springer Group of the Southeastern Anadarko Basin in Oklahoma: Shale Shaker, Vol. 15, No. 5, pp. 280-297.
- Pittman, E. D., 1979, Porosity, Diagenesis and Productive Capability of Sandstone Reservoirs: Society of Economic Paleontologists and Mineralogists Spec. Pub. No. 26., pp. 159-173.

- _____, and Larese, R. D., 1986, The Influence of Diagenesis on Porosity and Permeability Development with Reservoir Sandstones - An Overview: Unpublished Amoco Production Co. Report.
- Rascoe, B. Jr., and Adler, F. J., 1983, Permo-Carboniferous Hydrocarbon Accumulations, Mid-Continent, U.S.A.: American Association of Petroleum Geologists Bulletin, Vol. 67, No. 6, pp. 979-1001.
- Riley, L. R., 1966, The Challenge of Deep Exploration: The Chitwood Pool, Grady County, Oklahoma: Shale Shaker, Vol. 16, No. 12, pp. 298-305.
- Scholle, P., 1979, A Color Illustrated Guide to Constituents, Textures, Cements, and Porosities of Sandstones and Associated Rocks: American Association of Petroleum Geologists Memoir 28, American Association of Petroleum Geologists, Tulsa, Oklahoma.
- Schmidt, V., and McDonald, D. A., 1979, Texture and Recognition of Secondary Porosity in Sandstone: Society of Economic Paleontologists and Mineralogists Spec. Pub. No. 26, pp. 209-225.
- Shelby, J. W., 1980, Geologic and Economic Significance of the Upper Morrow Chert Conglomerate Reservoir of the Anadarko Basin: Journ. of Petroleum Technology, Vol. 32, No. 3, pp. 489-495.
- South, M. V., 1983, Stratigraphy, Depositional Environment, Petrology, and Diagenetic Character of the Morrow Reservoir Sands, Southwest Canton Field, Blaine and Dewey Counties, Oklahoma: M.S. Thesis, Oklahoma State University, Stillwater, Oklahoma, 169 p.
- Spearing, D. R., 1976, Upper Cretaceous Shannon Sandstone: An Offshore, Shallow-Marine Sand Body: Wyoming Geological Association 28th Annual Guidebook, p. 65-72.
- Straka, J. J., 1972, Conodont Evidence of Goddard and Springer Formations, Ardmore Basin, Oklahoma: American Association of Petroleum Geologists Bulletin, Vol. 56, No. 7, pp. 1087-1099.
- Surdam, R. C., Boese, S. W., and Crossey, L. J., 1984, The Chemistry of Secondary Porosity: in Clastic Diagenesis, American Association of Petroleum Geologists Memoir 37, pp. 127-149.
- Swanson, D. C., 1967, Some Major Factors Controlling the Accumulation of Hydrocarbons in the Anadarko Basin: World Oil, Vol. 184, No. 1.

- Swift, D. J. P., 1976, Coastal Sedimentation: in Marine Sediment Transport and Environmental Management, John Wiley and Sons, New York, pp. 255-310.
- Tillman, R. W., and Martinson, R. S., 1984, The Shannon Shelf Sand-Ridge Complex, Salt Creek Anticline Area, Powder River Basin, Wyoming: in Siliciclastic Shelf Sediments, Society of Economic Paleontologists and Mineralogists Spec. Pub. 34, pp. 85-142.
- Tomlinson, C. W., and McBee W. Jr., 1959, Pennsylvanian Sediments and Orogenies of the Ardmore District, Oklahoma: in Petroleum Geology of Southern Oklahoma, American Association of Petroleum Geologists, Vol. 2, pp. 2-52.
- Waddel, W. E., 1966, Pennsylvanian Fusilinids in the Ardmore Basin, Love and Carter Counties, Oklahoma: Oklahoma Geological Survey Bulletin, Vol. 113, 128 p.
- Walker, R. G., 1979, Shallow Marine Sandstones: in Facies Models, Geoscience Canada Reprint Series No.1, pp. 75-89.
- Westheimer, J. M., 1956, The Goddard Formation: in Petroleum Geology of Southern Oklahoma: American Association of Petroleum Geologists, Vol. 1, pp. 392-396.
- Wroblowski, E. F., 1966, Exploration Problems in the "Deep" Anadarko Basin: Shale Shaker, Vol. 17, No. 7, p. 131.

APPENDIX A

METHODS USED FOR CONSTRUCTION OF GROSS-SAND
ISOPACH AND STRUCTURAL MAPS

Construction of Gross-Sand Isopach Maps

Data used in the construction of gross-sand isopach maps of Britt sandstones were derived from the gamma-ray or SP (spontaneous potential) curves of well logs. The majority of the data was determined from gamma-ray curves. In the absence of this curve, the SP curve was used. SP was used to determine sand thickness in less than ten wells.

The first step was to determine the shale base line. This line was chosen by observing the gamma-ray intensity of shales associated with sandstones of the Britt. The shale base-line was drawn at the average API intensity of the shales. The second step involved drawing a sand cut-off line on the gamma-ray curve. The sand cut-off line was chosen 30 API units to the left of the shale base-line. Any sand that recorded gamma-ray intensity left of this line was counted as part of the gross sand.

The method used for determining gross sand from the SP curve was very similiar to the gamma-ray technique. Again a shale base-line was drawn which represented the average shale in association with Britt sandstones. The sand cut-off line was chosen 20 millivolts to the left of the shale base-line. Sands that recorded millivolt intensity left of the sand cut-off line were counted as gross sand.


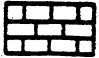
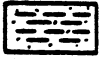
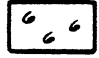
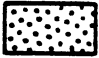
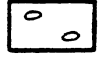


Construction of Structural Contour Maps

Structural elevations of datums used to construct structural contour maps were determined using the standard method. Well logs were used exclusively.


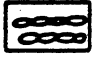





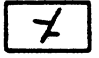



The first step involved location of the datum from well logs. After this depth was determined it was subtracted from the kelly bushing elevation giving the structural elevation of the datum in relation to sea level. The kelly bushing elevation is the standard from which borehole depths are measured when running well logs. In the absence of an available kelly bushing elevation, the ground elevation was used. Eighteen feet was added to the ground elevation to approximate elevation of the kelly bushing. The amount of adjustment was determined from averaging the difference between ground and kelly bushing elevations in the thesis area. Less than fifteen structural elevations were determined using this adjustment.

APPENDIX B**DESCRIPTIONS OF CORES**

COMPOSITION

	SHALE		LIMESTONE
	SILTSTONE		FOSSILS
	SANDSTONE		SIDERITE NODULES
	CONGLOMERATE		SEDIMENTARY ROCK FRAGMENTS

SEDIMENTARY STRUCTURES

	LAMINATED BEDDING		LENTICULAR BEDDING
	IRREGULAR, WAVY BEDDING		STYLOLITES
	CONVOLUTED BEDDING		FLAME STRUCTURE
	LARGE-SCALE CROSS-BEDDING		MICRO-FAULT
	SMALL-SCALE CROSS-BEDDING		LOAD CAST
	BIOTURBATION		

WELL: Apexco, Inc. Buell No. 1-A

LOCATION: C NE/4 SW/4 Section 10-T11N-R12W

CORED INTERVAL: 13,736-14,103 on core; 13,723-14,090 on well logs

STRATIGRAPHIC POSITION: Morrow, Cunningham, Lower Britt

CUMULATIVE PRODUCTION: 75,892 bo
(Time Interval) 8/75-6/86)

PRODUCING INTERVAL: Marchand

A series of continuous cores was taken from the Apexco Buell No. 1-A, from 13,736 to 14,102 feet. Strata from the Morrow, Cunningham, and Lower Britt intervals are included. Only the lower 296 feet (13,806-14,102) were logged for this research. Included in this interval are the Lower Britt, Cunningham, and lower portions of the Morrow Formation. The Mississippian-Pennsylvanian unconformity was recognized in the core.

The Lower Britt strata (14,033-102) are entirely marine in origin. Basal portions (14,075-102) consist of sparsely fossiliferous, laminated to lenticular-bedded, dark gray siltstone, sandstone, and shale. Microfaulting and disrupted bedding are rare to common. This sequence is interrupted by three thin coquinoid sandstones (14,083-84; 14,086; 14,095-96). These units have erosional lower contacts and abrupt upper contacts. They are coarse-grained and highly-fossiliferous at the base, grading to fine to very fine near the top. Quartzitic sand is the primary constituent in upper portions. Coquinoid sandstones of the Britt are interpreted as storm deposits.

A thick sandstone (14,033-74) grades upward from the laminated marine rocks. Detailed analysis of this unit indicates it is actually two stacked sandstones deposited in different environments. The lower 13 feet (14,062-75) were deposited in a high-energy marine environment as suggested by the presence of ooids in lower portions. It is silty at the base and highly fossiliferous in lower sections, grading to moderately-fossiliferous in upper sections. Common varieties of fossils are echinoderms and brachiopods. The sandstone is fine-grained throughout. Disrupted bedding was the only sedimentary structure observed.

The transition from fine- to very fine-grained sandstone at 14,062 delineates the boundary between the stacked sandstones. A decrease in the gamma-ray intensity also occurs at this point. The upper sandstone (14,033-61) is sparsely fossiliferous throughout. Small clay clasts are scattered throughout the lower 8 feet of the sand and are rare in the remainder. The lower 3 feet are very fine-

grained with the remainder of the unit fine-grained. The sand is massive with stylolites and inclined bedding rare. Based on the trend of the sand (Plate III), the presence of fossils, and the abundance of clay matrix, this sand is interpreted as shelf sand-ridge.

Cunningham strata occur between 13,828 and 14,032 in the Buell No. 1-A. The interval between 13,861 and 14,032 is composed of sparsely-fossiliferous, black, laminated shale of marine origin. These strata were deposited in very quiet water, probably in the outer shelf regime. Intervals containing very thin sand lenses (less than 1 mm) are common throughout the sequence. A sandy sub-interval occurs between 13,962 and 13,983 in the shale. Three, thin, fossiliferous sandstones are within this sub-interval (13,962-66; 13,973-76; 13,979-83). Fossils, predominantly brachiopods and echinoderms, and intraclasts are abundant immediately overlying the erosional base. This unit grades from coarse-grained coquinoid sand at the base to fine-grained, quartzitic sand at the top. Cross-bedding and disrupted bedding are the dominant sedimentary structures. This unit is interpreted as a storm deposit. The upper sand units have gradational upper and lower contacts. They are fine- to very fine-grained and sparsely-fossiliferous. Laminated and lenticular bedding are the primary sedimentary structures. These sands are thought to have been deposited as small sand-ridges in the shelf environment. Laminated to lenticular-bedded siltstones separate these three Cunningham sandstones.

A Cunningham sand is present between 13,840 and 13,860. It is very fine-grained in lower portions, grading to fine in upper portions. It is fossiliferous throughout, containing occasional clay clasts. The dominant sedimentary structures are lenticular bedding and stylolites. A thin shale break (13,843.5) separates the main body of the sand from the uppermost three feet, which are very fine-grained and moderately bioturbated. Black, laminated, marine shale overlies this unit (13,830-40).

A moderately-sorted, fine-grained, quartzitic sand (13,827-28) composes the uppermost Cunningham. The Mississippian-Pennsylvanian unconformity overlies this two-foot unit. A very fine-grained, argillaceous Morrow sand (13,816-36) overlies the unconformity. The contact was recognized by an increase in the amount of argillaceous material and decrease in grain size from the Cunningham sandstone to the Morrow sandstone. Load features immediately overlie the unconformity. Sedimentary structures in the Morrow sand include lenticular and disrupted bedding. No fossils were found.

The remainder of the Morrow section that was logged consists of black, lenticular-bedded shale (13,809-15) with thin sand lenses abundant. The shale is overlain by a massive, fine-grained sandstone (13,806-08) with mud rip-ups common in basal portions. The lower contact was missing.

PETROLOGIC LOG OSU

Well APEXCO, INC. BUELL NO. 1-A

Location C NE/4 SW/4 Sec. 10 T. 11 N., R. 12 W

CADDO Co., OKLAHOMA

AGE/STRATIGRAPHIC UNIT	ENVIRONMENT	DEPTH/THICKNESS	S. P./GAMMA RAY	LITHOLOGY	SEDIMENTARY STRUCTURES	COLOR	GRAIN SIZE		SORTING	POROSITY		CONSTITUENTS		ROCK CLASSIFICATION	REMARKS
							CLAY	SAND		Thin-section	Log	DET. TRAIL	PERM		
PENNSYLVANIAN/MORROW FM.	Marine Shelf	13,810													
		13,815													
MISSISSIPPIAN/CUNNINGHAM	Insufficient Information	13,820													
		13,825													
MISSISSIPPIAN/CUNNINGHAM	II	13,830													
		13,835													
MISSISSIPPIAN/CUNNINGHAM	Marine Shelf	13,840													
		13,845													
	SR														

ENVIRONMENT ABBREVIATIONS
 II - Insufficient Information
 SR - Shelf Sand Ridge
 DDB - Delta Distributional Sand Bar
 MS - Marine Shelf
 SD - Storm Deposit

AGE/STRATIGRAPHIC UNIT		ENVIRONMENT		DEPTH/THICKNESS	S.P./GAMMA RAY	LITHOLOGY	SEDIMENTARY STRUCTURES	COLOR	GRAIN SIZE and / or %	SORTING	POROSITY	CONSTITUENTS	ROCK CLASSIFICATION	REMARKS
MISSISSIPPIAN / CUNNINGHAM		MARINE SHELF		13,850 - 13,900	S.P./GAMMA RAY	[Lithology patterns: coarse sand, fine sand, silt, clay]	[Sedimentary structures: ripple marks, cross-bedding]	[Color: tan, yellow, brown]	[Grain size: 1/2, 1, 2, 4, 8, 16, 32, 64, 128, 256, 512, 1024, 2048, 4096, 8192, 16384, 32768, 65536, 131072, 262144, 524288, 1048576, 2097152, 4194304, 8388608, 16777216, 33554432, 67108864, 134217728, 268435456, 536870912, 1073741824, 2147483648, 4294967296, 8589934592, 17179869184, 34359738368, 68719476736, 137438953472, 274877906944, 549755813888, 1099511627776, 2199023255552, 4398046511104, 8796093022208, 17592186044416, 35184372088832, 70368744177664, 140737488355328, 281474976710656, 562949953421312, 1125899906842624, 2251799813685248, 4503599627370496, 9007199254740992, 18014398509481984, 36028797018963968, 72057594037927936, 144115188075855872, 288230376151711744, 576460752303423488, 1152921504606846976, 2305843009213693952, 4611686018427387904, 9223372036854775808, 18446744073709551616, 36893488147419103232, 73786976294838206464, 147573952589676412928, 295147905179352825856, 590295810358705651712, 1180591620717411303424, 2361183241434822606848, 4722366482869645213696, 9444732965739290427392, 18889465931478580854784, 37778931862957161709568, 75557863725914323419136, 151115727451828646838272, 302231454903657293676544, 604462909807314587353088, 1208925819614629174706176, 2417851639229258349412352, 4835703278458516698824704, 9671406556917033397649408, 19342813113834066795298816, 38685626227668133590597632, 77371252455336267181195264, 154742504910672534362390528, 309485009821345068724781056, 618970019642690137449562112, 1237940039285380274899124224, 2475880078570760549798248448, 4951760157141521099596496896, 9903520314283042199192993792, 19807040628566084398385987584, 39614081257132168796771975168, 79228162514264337593543950336, 158456325028528675187087900672, 316912650057057350374175801344, 633825300114114700748351602688, 1267650600228229401496703205376, 2535301200456458802993406410752, 5070602400912917605986812821504, 10141204801825835211973625643008, 20282409603651670423947251286016, 40564819207303340847894502572032, 81129638414606681695789005144064, 162259276833213363391578010288128, 324518553666426726783156020576256, 649037107332853453566312041152512, 1298074214665706907132624082305024, 2596148429331413814265248164610048, 5192296858662827628530496329220096, 10384593717325655257060992658440192, 20769187434651310514121985316880384, 41538374869302621028243970633760768, 83076749738605242056487941267521536, 166153499477210484112975882535043072, 332306998954420968225951765070086144, 664613997908841936451903530140172288, 1329227995817683872903807060280344576, 2658455991635367745807614120560689152, 5316911983270735491615228241121378304, 10633823966541470983230456482242756608, 21267647933082941966460912964485513216, 42535295866165883932921825928971026432, 85070591732331767865843651857942052864, 170141183464663535731687303715884105728, 340282366929327071463374607431768211456, 680564733858654142926749214863536422912, 1361129467717308285853498429727072845824, 2722258935434616571706996859454153691648, 5444517870869233143413993718908307383296, 10889035741738466286827987437816614766592, 21778071483476932573655974875633229533184, 43556142966953865147311949751266459066368, 87112285933907730294623899502532918132736, 174224571867815460589247799005061762665472, 348449143735630921178495598010123525330944, 696898287471261842356991196020247050661888, 1393796574942523684713982392040494101323776, 2787593149885047369427964784080988202647552, 5575186299770094738855929568161976405295104, 11150372599540189477711859136323952810590208, 22300745199080378955423718272647905621180416, 44601490398160757910847436545298011242360832, 89202980796321515821694873090596022484721664, 1784059615926430316433897461811920449694432, 3568119231852860632867794923623840899388864, 7136238463705721265735589847247681798777728, 14272476927411442531471179694495363597555456, 28544953854822885062942359388990727195111104, 5708990770964577012588471877798145439022208, 11417981541929154025176943755596288798044416, 22835963083858308050353887511192577596088832, 4567192616771661610070777502238515519217664, 9134385233543323220141555004477031038435328, 1826877046708664644028311000895406207687056, 3653754093417329288056622001790812415374112, 7307508186834658576113244003581624830748224, 1461501637366931715222648800716324966149648, 2923003274733863430445297601432649932299296, 5846006549467726860890595202865299864598592, 11692013098935453721781190405730599729197184, 23384026197870907443562380811461199458394368, 46768052395741814887124761622922398916788736, 93536104791483629774249523245844797833577472, 187072209582967259548499046491689595667154848, 374144419165934519096998092983379191334309696, 748288838331869038193996185966758382668619392, 149657767666373807638799237193351676533723776, 299315535332747615277598474386703353067447552, 598631070665495230555196948773406706134895104, 1197262141330990461110393897546813412297902208, 2394524282661980922220787795093626824595804416, 4789048565323961844441575590187253649191608832, 9578097130647923688883151180374507298383217664, 1915619426129584737776630236074901459676643528, 38312388522591694755532604721498029193532871056, 76624777045183389511065209442996058387065742112, 153249554090366779022130418885992116774131484224, 306499108180733558044260837771984233548262968448, 612998216361467116088521675543968467096525936896, 1225996432722934232177043351087936934193051877792, 2451992865445868464354086702175873868386103755584, 4903985730891736928708173404351747736772207511168, 9807971461783473857416346808703495473544415022336, 19615942923566947714832693617406990947088830044672, 39231885847133895429665387234813981894177660089344, 7846377169426779085933077446962796378835532017888, 15692754338853558171866154893925592757671064035776, 31385508677707116343732309787851185515342128071552, 62771017355414232687464619575702371030684256143104, 125542034710828465374929239151404742061368512862208, 251084069421656930749858478302809484122737025724416, 50216813884331386149971695660561896824547405144832, 100433627768662772299943391321123793649094810289664, 200867255537325544599886782642247587298189620579328, 401734511074651089199773565284495175996379241158656, 803469022149302178399547130568990351992758482317312, 160693804429860435679909426113798070398551696464624, 321387608859720871359818852227596140797103392929248, 642775217719441742719637704455192281594206785858496, 1285550435438883485439275408910384563188413571716992, 2571100870877766970878550817820769126376827443433984, 5142201741755533941757101635641538252753654886867968, 10284403483511067883514203271283076505507309773735936, 20568806967022135767028406542566153011014619547471872, 41137613934044271534056813085132306022029239094943744, 82275227868088543068113626170264612044058478189887488, 164550455736177086136227252340529224088116956379774976, 329100911472354172272454504681058448176233912759549952, 658201822944708344544909009362116834232467825519099904, 1316403645889416689089818018724236684644935651038199808, 2632807291778833378179636037448469369288871302076399616, 5265614583557666756359272074896938738577742604152799232, 1053122916711533351271854414979387747715544520830559664, 21062458334230667025437088299587754954310910416611136, 42124916668461334050874176599175509908621820833222272, 84249833336922668101748353198351019817243641666444544, 168499666673845336203496706396702039634487283332888888, 33699933334769067240699341279340407926897456666577776, 67399866669538134481398682558680918533795133333155552, 134799733339076268962797365117361837067590266666311104, 269599466678152537925594730234723674135180533332622208, 539198933356305075851189460469447348270361066665244448, 1078397866712610151702378920938894696540722133330488896, 2156795733425220303404757841877789393081444266660977792, 4313591466850440606809515683755578786162888533321555584, 8627182933700881213619031367511157572325777066643111168, 17254365867401762427238062735022314544651554133282222336, 34508731734803524854476125470044629089303108666564444672, 69017463469607049708952250940089258178606217333128889344, 138034926939214099417904501880178516357212434666257778688, 27606985387842819883580900376035703271442486933255557376, 55213970775685639767161800752071406542884973866511111552, 11042794155137127953432360150414281308576994773302222304, 22085588310274255906864720300828562617153989546604444608, 44171176620548511813729440601657125234307979093208889216, 88342353241097023627458881203314250468615958186417778432, 176684706482194047254917762406628509337231916372835556864, 353369412964388094509835524813257018674463832745671113728, 706738825928776189019671049626514037348927665491342227456, 1413477651857552378039342099253028074697853310982684454912, 28269553037151047560786841985060561493957066219653689088, 56539106074302095121573683970121122987914132439307378176, 113078212148604190243147367940242245975828264878614756352, 226156424297208380486294735880484491951655327557229517104, 452312848594416760972589471760968983903310655114458234208, 904625697188833521945178943521937967806621310228916458416, 1809251394377667043890357887043875935613242604457832816832, 3618502788755334087780715774087751871226485208915665637664, 7237005577510668175561431548175503742452970417831331375328, 1447401115502133635112286289635100748490594083566266270656, 2894802231004267270224572579270201496981188167132532541312, 5789604462008534540449145158540402993962376334265065082624, 1157920892401706908089829031708080598792475266853013014528, 2315841784803413816179658063416161197584950533706026029056, 4631683569606827632359316126832322395169901067412052058112, 9263367139213655264718632253664644790339802134824104116224, 1852673427842731052943726500732929580677960426964820822448, 3705346855685462105887453001465859161355920853929641644896, 7410693711370924211774906002931718322711841707859283289792, 14821387422741848423549812005863436645423683415718576579584, 29642774845483696847099624011726873290847366831437155115968, 59285549690967393694199248023453746581694733662874310313936, 118571099381934787388398496046907493163389467325748626627872, 237142198763869574776796992093814986326778934651497352455744, 474284397527739149553593984187629972653557869302994710911488, 948568795055478299107187968375259945307115738605989421822976, 1897137590110956598214375376750519890614234772111978843645952, 3794275180221913196428750753501039781228469544223957687111904, 7588550360443826392857501507002079562456939088447915374223808, 15177100720887652785715003014004159124913878176895830748447616, 30354201441775305571430006028008318249827756353791661496895232, 60708402883550611142860012056016636499655512707583322993710464, 121416805767101222285720024112033272999311025415166649887421128, 24283361153420244457144004822406654599862205083033329764484256, 48566722306840488914288009644813309199724410166066658888968512, 97133444613680977828576019289626618399448820332133317777937024, 194266889227361955657152038579253236798897640664266635558874048, 388533778454723911314304077158506473597795281328533371117748096, 777067556909447822628608154317012947195590562657066642235496192, 1554135113818895645257216308634025943911181125314133324470992384, 310827022763779129051443261726805188782236225062826664794198576, 621654045527558258102886523453610377564472450125653329583997152, 124330809105511651620577304690722075528894490025130665816798304, 248661618211023303241154609381444151057789800050261331633596608, 497323236422046606482309218762888302115579600100522663267193216, 994646472844093212964618437525776604231159200201045325334386432, 1989292945688186425929236875051553208462318400402090650668772864, 3978585891376372851858473750103106416924636800804181301337545728, 7957171782752745703716947500206212833849273601608362602675091456, 15914343565505491407433895000412425667698547203216725205350182912, 31828687131010982814867790000824851335397094406433450410700365824, 63657374262021965629735580001649702670794188812866900821400731648, 127314748524043931259471160003299405341588377625733801642801463296, 254629497048087862					

AGE/STRATIGRAPHIC UNIT	ENVIRONMENT	DEPTH/THICKNESS	S.P./GAMMA RAY	LITHOLOGY	SEDIMENTARY STRUCTURES	COLOR	GRAIN SIZE		SORTING	POROSITY		CONSTITUENTS		ROCK CLASSIFICATION	REMARKS
							mm	mm		Thin-section	Log	DETRITAL ALLOGENIC	PENE CONTEMPORANEOUS/AUTHIGENIC		
MISSISSIPPIAN / LOWER BRITT															
Marine Shelf															
DOB		14,070												AB-14066	
		14,075												AB-14070	
		14,080												AB-14072	
		14,085												AB-14074	
		14,090												AB-14083	
		14,095												AB-14086	
		14,100												AB-14095	
		14,105													

WELL: Tenneco Willie Lefthand No. 1-23

LOCATION: C NE/4 Section 23-T9N-R9W, Caddo County

CORE INTERVAL: 13,339-13,396 on core; 13,332-13,389 on well logs

STRATIGRAPHIC POSITION: Lower Britt, Boatwright

CUMULATIVE PRODUCTION: 242 mmcfg + 2,049 bo
(Time Interval) (3/76-6/86)

PRODUCING INTERVALS: Morrow, Lower Britt

The cored interval consists of a massive, fine- to very fine-grained quartzitic Boatwright sandstone (13,372-86) encased in a laminated, black shales, interbedded with a few thin sand lenses. A thin sandstone (1339-42) of marine origin is present in uppermost portions of the core.

The lowermost portion of the core (13,387-96) consists of black, laminated shales with abundant siderite nodules. No fossils were observed. This Boatwright sequence has been interpreted as prodeltaic or distal delta-front in origin. Overlying these shales is a massive, quartzitic Boatwright sandstone (13,373-86) with faint, large-scale cross-beds near the base. This sandstone is interpreted as a small deltaic channel-fill sand, based on the erosional nature of the basal contact, lack of fossils and glauconite, and fining upward of the grain size. A thin shale unit (13,380) is in middle portions of the sand.

Four feet of fossiliferous, brown to black, laminated shale (13,369-72) caps the Boatwright sandstone which, in turn, is overlain by two feet of fossiliferous, fine-grained sand (13,367-68). This six feet of fossiliferous strata represent a marine transgression of the Boatwright delta. The base of the fossiliferous strata was designated the base of the Lower Britt Submember.

Black, laminated shales (13,342-46) with abundant siderite nodules and thin sand lenses overlie the lowermost Britt. These strata are interpreted as prodeltaic, distal delta-front, or interdistributary in origin, recording the encroachment of the Lower Britt delta into the area.

A silt to very-fine grained, fossiliferous sand (13,339-42) caps the Britt deltaic shales. This unit records transgression of the marine environment after abandonment of the Lower Britt delta.

PETROLOGIC LOG OSU

Well TENNECO WILLIE LEFTHAND NO. 1-23

Location C NE/4 Sec. 23 T. 9 N., R. 9 W

CADDO Co., OKLAHOMA

AGE/STRATIGRAPHIC UNIT	ENVIRONMENT	DEPTH/THICKNESS	S.P./GAMMA RAY	LITHOLOGY	SEDIMENTARY STRUCTURES	COLOR	GRAIN SIZE				POROSITY		CONSTITUENTS										ROCK CLASSIFICATION	REMARKS
							CLAY	SILT	SAND	GRAVEL	Thin-section	Log	QUARTZ	LABILE	NON-LABILE	GLAUCOPHANE & OLIVINE	PLAGIOCLASE	FOSSILS	PERM	POROSITY	PRE-CAMBRIAN/ANTHROPOGENIC	PERM-CAMBRIAN/AUTOGENIC		
MISSISSIPPIAN/LOWER BRITT	DDB	13,340	[Hand-drawn curve]	[Lithology symbols]	[Structures symbols]	[Color/Grain symbols]	GRAN. PERCENTAGE				PERM		CONSTITUENTS										THIN SECTION LOCATIONS	
		13,345					PERCENTAGE				PERM		CONSTITUENTS											
		13,350					PERCENTAGE				PERM		CONSTITUENTS											
		13,355					PERCENTAGE				PERM		CONSTITUENTS											
		13,360					PERCENTAGE				PERM		CONSTITUENTS											
	13,365	PERCENTAGE				PERM		CONSTITUENTS																
MISS./BOATWRIGHT Distributory Channel-Fill	IS	13,370	[Hand-drawn curve]	[Lithology symbols]	[Structures symbols]	[Color/Grain symbols]	GRAN. PERCENTAGE				PERM		CONSTITUENTS										TWL-13367	
		13,375					PERCENTAGE				PERM		CONSTITUENTS											

AGE/STRATIGRAPHIC UNIT	ENVIRONMENT	DEPTH/THICKNESS	S.P./GAMMA RAY	LITHOLOGY	SEDIMENTARY STRUCTURES	COLOR	GRAIN SIZE	SORTING	POROSITY	CONSTITUENTS	ROCK CLASSIFICATION	REMARKS
MISSISSIPPIAN/BOATWRIGHT	Distributary Channel-fill	13.380										TML-13380
		13.385										TML-13386
		13.390										
		13.395										
		13.400										
	Deltaic											ENVIRONMENT ABBREVIATIONS DDB - Delta-Destructional Sand Bar IS - Inner-Shelf

WELL: Tenneco Grant Rumley No. 1-22

LOCATION: C NW/4 Section 22-T9N-R9W, Caddo County

CORE INTERVAL: 13,771-13,834 on core; 13,762-13,825 on well logs

STRATIGRAPHIC POSITION : Lower Britt, Boatwright

CUMULATIVE PRODUCTION: 3.02 bcfg + 39,936 bo
(Time Interval) (9/75-6/86)

PRODUCING INTERVAL: Cunningham, Lower Britt

The cored interval consists of strata belonging to the Britt and Boatwright genetic intervals. Deltaic and marine depositional settings are inferred for this strata.

The Boatwright interval (13,822-34) is represented by a one-foot thick, laminated to lenticular-bedded siltstone at the base. It is overlain by a cross-bedded, moderately-sorted, fine-grained sandstone (13,831-33) that is bioturbated in uppermost portions. A thin shale break separates this sand from a cross-bedded, poorly-sorted, medium-grained, quartzitic sand (13,822-29). Four distinct fining-upward sequences are present in this unit. Based on sedimentary structures and the lack of fossils and glauconite, this sand is interpreted as a small deltaic channel-fill or bar-finger sandstone. The contact with underlying strata is sharp, but due to the poor condition of the core, whether the contact was erosive could not be ascertained.

The boundary between the Boatwright and Britt intervals was chosen as the top of the Boatwright sand (13,822). This sand is overlain by black, laminated shales (13,398-822) containing abundant siderite nodules and some thin sand lenses. The lowermost three feet of the shale contain abundant brachiopods and silt. Lenticular-bedding is rare in lower portions of the shale, becoming more abundant in upper portions. These shales are interpreted as prodelta, distal delta-front, or interdistributary-bay in origin.

The Lower Britt sand between 13,782 and 13,797 is interpreted as a delta-destructive sand bar. This unit records the change from a deltaic to marine environment. Oolitic sandy limestone at the base, it contains abundant small-scale trough cross-beds and fossils, predominantly echinoderms and brachiopods, in association with the ooids. Bioturbated layers are not present in lower portions of the unit. Content of fossils decreases upward. Fine-grained sand is the dominant constituent in upper sections of this unit. Bioturbated beds and disrupted bedding are the more common sedimentary structures.

Lenticularly-interbedded sandstones, siltstones, and shales (13,775-81) overlie the destructive bar. These

strata are moderately to highly fossiliferous. The uppermost portion of the core (13,771-74) consists of a silty, lenticular-bedded sand with abundant fossils. This unit possibly represents the lowermost portions of a delta-destructural sand bar.

PETROLOGIC LOG OSU

Well TENNECO GRANT RUMLEY NO. 1-22

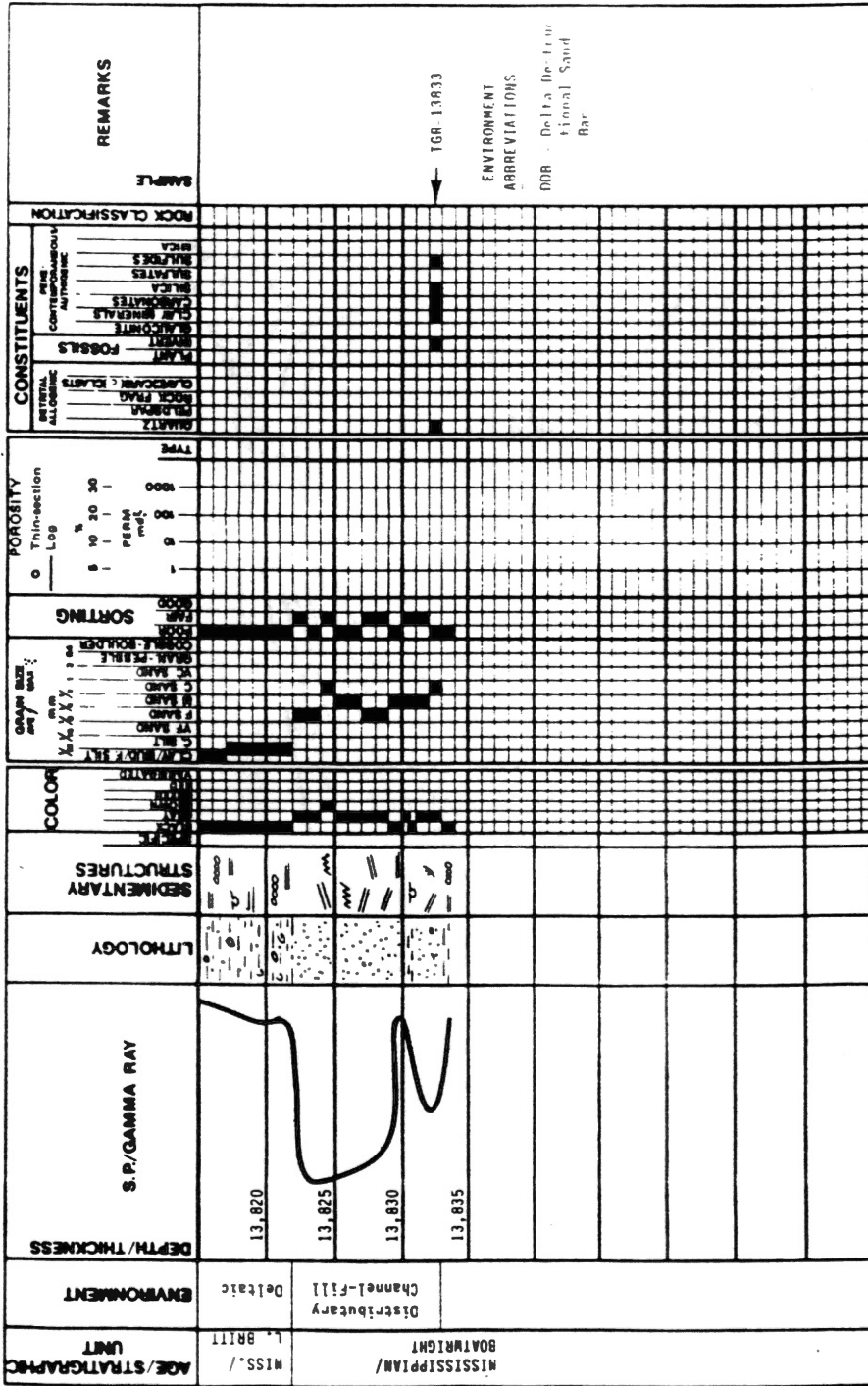
Location C NW/4 Sec. 22 T. 9 N., R. 9 W.

CADDO

Co.,

OKLAHOMA

AGE/STRATIGRAPHIC UNIT	ENVIRONMENT	DEPTH/THICKNESS	S.P./GAMMA RAY	LITHOLOGY	SEDIMENTARY STRUCTURES	COLOR FRESH WET DRIED HEATED	GRAIN SIZE mm X.X XXX X	SORTING FAIR GOOD POOR	POROSITY Thin-section Log PERM % 100 1000	CONSTITUENTS		ROCK CLASSIFICATION	REMARKS
										DETITAL ALLOGENIC CLASTIC CLASTIC CLASTIC	PERE CONTEMPORANEOUS AUTOGENIC		
MISSISSIPPIAN / LOWER BRITT D e l t a i c	DOB	13,775										THIN SECTION LOCATIONS TGR 13774	
	Marine Shelf	13,780										TGR 13783	
	Delta-Destructional Sand Bar	13,785										TGR 13789	
		13,790										TGR 13792	
		13,795										TGR 13796	
		13,800											
		13,805											
		13,810											
		13,815											



WELL: Tenneco Parton No. 1-3

LOCATION: C SE/4 Section 3-T9N-R9W, Caddo County

CORED INTERVAL: 12,987-13,018 on core; not correlatable to well logs

STRATIGRAPHIC POSITION: Boatwright/Lower Britt?

CUMULATIVE PRODUCTION: 1.74 bcfg + 7,641 bo
(Time Interval) (11/75-6/86)

PRODUCING INTERVAL: Morrow

The cored interval consists of siltstones, shales, and fine- to very fine-grained sandstones. The core could not be correlated to the well logs because numerous thin sandstone beds were not detected by the logging tools. Whether this core was taken from the Boatwright or Lower Britt genetic interval could not be ascertained.

The basal six feet consist of laminated to wavy-bedded siltstone (13,013-18). A fossiliferous siltstone unit is at 13,012. This silt is overlain by a moderately-sorted, very fine-grained sand (13,008-11) with large-scale cross-bedding throughout. Fossils throughout the core are dominated by echinoderms and brachiopods. Pelecypods were common in some intervals. The sandstone is argillaceous and seems to contain no fossils. It is overlain by a thin, black, laminated shale (13,007) that underlies highly-fossiliferous, poorly-sorted sandstone (13,006) which may represent a storm deposit.

A black, laminated shale is located between 13,001 to 13,005. Sparse fossils and siderite nodules were noted. A coarsening upward sequence extends from 12,996 to 13,000. Siltstones and sandstones in this interval are argillaceous. Wavy bedding and microfaulting are the dominant sedimentary structures. The remainder of the core (12,987-12,995) consists of gray to black, laminated to wavy-bedded shales, siltstones, and sandstones. Disrupted bedding is common. Siderite nodules are rare.

Strata in this core are interpreted as interdistributary-bay in origin. Laminated and wavy bedding suggest low flow energy. The cross-bedded sand between 13,008 and 13,011 may represent a crevasse splay.

WELL: Amoco McClain No. 1

LOCATION: NE/4 SW/4 Section 23-T10N-R12W, Caddo County

CORE INTERVAL: 15,460-15,488 on core; Same on well logs

STRATIGRAPHIC POSITION: Lower Britt

CUMULATIVE PRODUCTION: 1.12 bcfg
(Time Interval) (9/82-6/86)

PRODUCING INTERVAL: Cunningham

This core was taken from the Lower Britt genetic interval and consists of a very fine-grained, quartzitic sandstone (15,478-84), and three thin coquinoid sandstones (15,471; 15,472.5-73; 15,475.5 -77.5), encased in interbedded silts and shales.

The basal 3.5 feet of the core consists of black to dark gray, lenticularly-interbedded, fossiliferous sandstones, siltstones, and shales. These strata grade abruptly into a sandstone unit (15,478-84). The sand is very fine-grained and is fossiliferous throughout. Echinoderms and brachiopods are the dominant fossil varieties. Small-scale trough cross-beds and laminated bedding are the dominant structures in basal portions whereas lenticular and laminated bedding are associated with upper portions of the sand. Bioturbated layers are also common in upper portions. Disrupted bedding is found throughout. Based on the sequence of sedimentary structures and the abundance of fossils and detrital clay matrix, this sand is interpreted as a small shelf sand-ridge.

A poorly-sorted, graded, coquinoid sandstone caps the shelf sand-ridge (15,475.5-77.5). Two other thin coquinoid units are within eight feet of the upper contact of the sand-ridge (15,471; 15,472.5-73). These sandstones have erosional basal contacts and abrupt upper contacts. They are separated by lenticularly-interbedded to laminated siltstones, sandstones, and shales. Coquinoid sandstones of the Lower Britt are interpreted as storm deposits; each unit represents a single storm surge.

The upper ten feet are composed of lenticularly-interbedded, bioturbated, fossiliferous, siltstones and shales with thin sand lenses. Disrupted bedding is common in this portion of the core.

PETROLOGIC LOG OSU

Well AMOCO McCLAIN NO. 1

Location NE/4 SW/4 Sec. 23 T. 10 N., R. 12 W.

CADDO Co., OKLAHOMA

AGE/STRATIGRAPHIC UNIT	ENVIRONMENT	DEPTH/THICKNESS	S.P./GAMMA RAY	LITHOLOGY	SEDIMENTARY STRUCTURES	COLOR	GRAIN SIZE		POROSITY	CONSTITUENTS		REMARKS
							mm	µm		Thin-section	Log	
MISSISSIPPIAN - UPPER BRITT	Marine Shelf	15,460					X	X	-	-		THIN SECTION LOCATIONS ← AN-15,473 → AN-15,476 → AN-15,477 → AN-15,479 → AN-15,481 → AN-15,483 → AN-15,484 ENVIRONMENT ABBREVIATIONS SD - Storm Deposit SR - Shelf Sand-Ridge MS - Marine Shelf
		15,465										
	SD	15,470										
	SD	15,475										
	MS	15,480										
	SD	15,485										
	SR	15,490										
	MS											

WELL: Amoco Haas "A" No. 3

LOCATION: NE/4 Section 35-T10N-R12W, Caddo County

CORED INTERVAL: 15,595-15,601 and 15,625-15,651 on core;
Same on well logs

STRATIGRAPHIC INTERVAL: Upper Britt

CUMULATIVE PRODUCTION: Unknown

PRODUCTION STATUS: Natural Gas Well

The core from the Amoco Haas "A" No. 3 consists of two parts. Portions of the core between the two intervals were lost in the borehole.

The lower core (15,625-51) is typified by dark gray, laminated siltstone and shale from 15,646 to 15,651. Disrupted bedding and microfaulting are common. These strata grade into fossiliferous, quartzitic sandstone (15,625-45). Varieties of fossils include echinoderms, brachiopods, and pelecypods. The lowermost six feet of the sand (15,640-45) are fine-grained with bioturbated layers, stylolites, and disrupted bedding as the dominant sedimentary structures. Middle portions of the sand (15,632-39) are very fine-grained and contain structures similar to those in the lower portions. The amount of bioturbated beds increases upward. The sand is fine-grained in upper portions of the core. The upper fourteen feet of the sandstone unit was lost during coring (as inferred from the gamma-ray curve). The rare stylolites and load casts are the only sedimentary structures.

Isopach mapping (Plate V), and the abundance of fossils and clay matrix suggest that the sand is a shelf sand-ridge. The change from very fine-grained sediments in the middle portion, to fine-grained sediments in upper portions indicates that two sand-ridges are stacked. Core of the upper section of the youngest sand-ridge was lost.

The upper core (15,595-601) is an argillaceous, fossiliferous sandstone (15,595-98) underlain by laminated, fossiliferous siltstone, sandstone, and shale. The contact is gradational. The sand is massive except for rare bioturbated layers at the base. Disrupted bedding is common in the siltstone. The thin sand may represent a small shelf sand-ridge.

WELL: Amoco Leonard No. 3

LOCATION: NE/4 Section 30-T12N-R14W, Washita County

CORED INTERVAL: 15,470-15,512 on core; 15,455-15,497 on well logs

STRATIGRAPHIC POSITION: Upper Britt

PRODUCTION STATUS: Dry and Abandoned

The cored interval consists of a very fine- to fine-grained, fossiliferous, quartzitic sandstone (15,484-507) underlain by interbedded siltstones, sandstones, and shale and overlain by black, laminated marine shale. A thin, fossiliferous, oolitic unit (15,471) occurs in upper portions of the core.

The basal portion of the core (15,508-12) is wavy, lenticularly-interbedded siltstone, sandstone, and shale. Fossils, predominantly echinoderms and brachiopods, are common. These strata grade abruptly into fossiliferous, quartzitic sandstone (15,484-15,507) that grades from fine-grained in lower and middle portions, to very fine-grained in upper portions. The content of fossils is almost consistent. Small shale clasts (less than 5 cm) are scattered throughout lower portions of the sand. Sedimentary structures include stylolites, bioturbated layers, disrupted bedding, and microfaulting. Stylolites and disrupted bedding are common in middle and upper portions. Bioturbation was most common in upper sections with microfaulting rare. The lower portion of the sandstone is massive. The sand is interpreted as a shelf sand-ridge based on the abundance of fossils, the clay matrix, and on the results of isopach mapping.

The sand is overlain by slightly fossiliferous, black, laminated shale (15,472-83). Siderite nodules are rare to common. A poorly-sorted, oolitic unit occurs at 15,471; it may be a storm deposit, or it may be related to the depositional hiatus between the Cunningham and Britt members (See Chapter II). Black, laminated shale overlies the oolitic unit.

PETROLOGIC LOG OSU

Well AMOCO LEONARD NO. 3

Location NE/4 Sec. 30 T. 12 N., R. 14 W.

WASHITA

Co.,

OKLAHOMA

AGE/STRATIGRAPHIC UNIT	ENVIRONMENT	DEPTH/THICKNESS	S.P./GAMMA RAY	LITHOLOGY	SEDIMENTARY STRUCTURES	COLOR	GRAIN SIZE		POROSITY	CONSTITUENTS		ROCK CLASSIFICATION	REMARKS		
							mm	mic		Thin-section	Log			DETITAL ALLOGENIC	PERE CONTEMPORANEOUS AUTOGENIC
							CLAY	GRAIN	PERCENT	PERCENT					
							mm	mic	%	%	QUARTZ	GLAUCOPHANE	PLANT	FOSSILS	
							mm	mic	5	10	20	30	CLAY MINERALS	CLAY MINERALS	
							mm	mic	PERME	PERME	PERME	PERME	SILICA	SULFATES	
							mm	mic	100	1000	TYPE		SULFIDES	SILICA	
							mm	mic							
MISSISSIPPIAN / UPPER BRITT	Marine Shelf	15,470												THIN SECTION LOCATIONS	
		15,475												← AL-15471	
		15,480													
		15,485												← AL-15485	
	Shelf Sand - Ridge	15,490												← AL-15487	
		15,495												← AL-15490	
		15,500												← AL-15493	
		15,505												← AL-15494	
													← AL-15498		
													← AL-15501		

AGE/STRATIGRAPHIC UNIT	ENVIRONMENT	DEPTH/THICKNESS	LITHOLOGY	SEDIMENTARY STRUCTURES	COLOR	GRAIN SIZE	SORTING	POROSITY	CONSTITUENTS		REMARKS
MISSISSIPPIAN - UPPER BRITT	SR Marine Shelf	15,510								AL-15507	
		15,515								ENVIRONMENT ABBREVIATIONS SR - Shelf Sand-Ridge	

WELL: Amoco Sylvester No. 1

LOCATION: SW/4 Section 21-T11N-R13W, Caddo County

CORED INTERVAL: 15,518-15,545 on core; same on well logs

STRATIGRAPHIC POSITION: Upper Britt

CUMULATIVE PRODUCTION: 6.23 bcfg
(Time Interval) (4/82-6/86)

PRODUCING INTERVAL: Upper Britt

The Amoco Sylvester No. 1 core consists of massive, quartzitic sandstone (15,525-44) underlain by interbedded sandstone, siltstone, and shale and overlain by siltstones, shales, and a thin, fine-grained sandstone (15,520-22). Echinoderms and brachiopods are the dominant fossil types in this core. Pelecypod and coral fragments were observed also.

A single foot of strata underlying the massive sandstone unit was cored (15,545). This bed consists of sparsely fossiliferous, interbedded sandstone, siltstone, and shales. Stylolites and disrupted bedding are the only sedimentary structures. This stratum grades into massive, fine-grained, fossiliferous sandstone (15,525-44). Stylolites are common throughout the sand and are the only sedimentary structures detectable by ordinary means. Grain size is always consistent. The sand is capped by two feet of fossiliferous, gray siltstone and shale (15,523-24). The boundary is gradational. Wavy, disrupted bedding is common.

A thin, fine-grained, fossiliferous sand is present from 15,520 to 15,522. Small (less than 5 cm) clay clasts are common in this unit. Both contacts are gradational.

The uppermost two feet of the Sylvester core (15,518-19) are composed of disrupted to laminated siltstones and shales with rare fossils.

Based on the abundance of fossils and abundant clay matrix, and isopach mapping (Plate IV), the massive sandstone (15,525-44) is interpreted as a shelf sand-ridge. The thin sandstone (15,520-22) is believed to be near the edge of another shelf sand-ridge. A marine origin is inferred for all strata in this core.

PETROLOGIC LOG OSU

Well AMOCO SYLVESTER NO. 1

Location SW/4 Sec. 21 T. 11 N., R. 13 W

CADDO Co., OKLAHOMA

AGE/STRATIGRAPHIC UNIT	ENVIRONMENT	DEPTH/THICKNESS	S.P./GAMMA RAY	LITHOLOGY	SEDIMENTARY STRUCTURES	COLOR	GRAIN SIZE	POROSITY	CONSTITUENTS	REMARKS
							GRAIN SIZE mm % X X X X X 1 2 4 8 16 32 64	POROSITY Thin-section Log % 5 10 20 30 PERM md 100 1000	CONSTITUENTS DETRITAL ALLOTHENE QUARTZ FELDSPAR ROCK FRAG CLASTIC CLASTS PLANT FOSSILS PRESENT PERE CONTEMPORANEOUS AUTOGENIC CALZ MINERALS CHLORITIDES SILICA SULFATES SULFIDES SILICA	
MISSISSIPPIAN/UPPER BRITT	Shelf Sand - Ridge	SR	15,520							THIN SECTION LOCATIONS
		MS	15,525							← AS-15521
			15,530							← AS-15526
			15,535							← AS-15529
			15,540							← AS-15536
			15,545							← AS-15540
		MS								← AS-15543 ← AS-15545

APPENDIX C
CONSTITUENT TYPES AND PERCENTAGES
IN THIN SECTIONS

Detrital constituents include trace amounts of heavy minerals, sedimentary rock fragments, and volcanic rock fragments.

Authigenic constituents include trace amounts of kaolinite, illite, megaquartz, and chalcedony.

TABLE I
 CONSTITUENT TYPES AND PERCENTAGES - APEXCO, INC. BUELL NO. 1 -- A

DEPTH/ SAMPLE #	Detrital Constituents (%)									Authigenic Constituents (%)								Porosity
	MONOAXIAL QUARTZ	POLYAXIAL QUARTZ	PLAGIOCLASE FELDSPAR	POTASSIUM FELDSPAR	SILICEOUS MATRIX	GLAUC- ONITE	FOSSILS	COIDS	SILICA OYERGROWTHS	CHERT CEMENT	CALCITE	DOLOMITE	CHLORITE	PYRITE	COLLOPHANE	ORGANIC MATERIAL		
									SHALF	SAND-RIDGE								
AB-14034	57	T	T	T	0	0	T	0	T	T	T	41.5	T	1	0	0	T	
AB-14040	62	T	T	0	0	0	1	0	T	T	T	25.5	3	3	0	0	3	
AB-14045	73	T	T	0	0	0	1	0	7	T	T	12.5	3	1	0	0	3.5	
AB-14052	82	T	T	0	0	0	T	0	7	T	T	8.5	5	T	0	0	2	
AB-14061	79	T	T	T	0	0	1	0	12	T	T	1	2	1	0	T	1	
	(57-82)	(T)	(T)	(0-T)	(0)	(0)	(T-1)	(0)	(T-12)	(T)	(T)	(1-41.5)	(T-3)	(T-3)	(0)	(0-T)	(T-3.5)	
									DELTA-DESTRUCTIONAL	SAND BAR								
AB-14062	79	T	T	T	T	0	T	0	6.5	T	T	2.5	11	2	0	T	2	
AB-14066	77	T	T	0	T	0	1	0	7	T	T	T	9	T	0	3	3.5	
AB-14070	56	T	0	0	T	0	13	9	T	T	T	21	T	T	0	T	0	
AB-14072	62	T	0	0	6	0	5.5	T	1	T	1	1	19	1	0	2.5	0	
AB-14074	15	T	0	0	75	0	T	0	0	T	3	T	0	0	0	4	0	
RANGE	(15-79)	(T)	(0-T)	(0-T)	(T-75)	(0)	(T-13)	(0-9)	(0-7)	(T)	(T-3)	(T-21)	(0-19)	(0-3)	(0)	(T-4)	(0-3.5)	
									STORM	DEPOSITS								
AB-14083	14	T	0	0	0	0	60	T	1	0	13	8	0	T	0	0	0	
AB-14086	18	T	0	0	.5	0	13	T	T	T	47	20	0	1	0	0	0	
AB-14093	58	T	0	0	0	0	T	0	T	T	T	31	7	3	0	0	0	
RANGE	(14-58)	(T)	(0)	(0)	(0-.5)	(0)	(T-60)	(0-T)	(T-1)	(0-T)	(T-47)	(0-31)	(0-7)	(T-3)	(0)	(0)	(0)	

TABLE II
 CONSTITUENT TYPES AND PERCENTAGES - TENNECO GRANT RUMLEY NO. 1 - 22

DEPTH/ SAMPLE #	Detrital Constituents (%)								Authigenic Constituents (%)								Porosity
	MONOCRYSTALLINE QUARTZ	POLYCRYSTALLINE QUARTZ	PLAGIOCLASE FELDSPAR	POTASSIUM FELDSPAR	SILICEOUS MATRIX	GLAUCO- ONITE	FOSSILS	ODDS	SILICA OVERGROWTH	CHERT CEMENT	CALCITE	DOLomite	CLORITE	PYRITE	COLLOPHANE	ORGANIC MATERIAL	
TGR-13774	T	0	0	0	5	0	74	T	STORM 0	DEPOSIT 0	T	14	2	1	0	0	0
DELTA - DESTRUCTURAL SAND BAR																	
TGR-13783		Calcite	Coated	Fossiliferous	Siltstone												
TGR-13789	45	T	T	0	0	11	1	7	T	T	3	28	T	T	0	3	1
TGR-13792	3	0	0	0	0	0	6	86	0	T	T	3	0	T	0	0	T
TGR-13796	7	0	0	0	0	0	5	73	0	0	T	13	0	1	0	0	0
RANGE	(3-45)	(0-T)	(0-T)	(0)	(0)	(0-11)	(1-6)	(7-86)	(0-T)	(0-T)	(T-3)	(3-28)	(0-T)	(T-1)	(0)	(0-3)	(0-1)
DAYRIGHT SAND																	
TGR-13833	74	T	0	0	0	0	T	0	7	T	0	2	10	2	0	0	5

TABLE III

CONSTITUENT TYPES AND PERCENTAGES - TENNECO WILLIE LEFTHAND NO. 1 - 23

DEPTH/ SAMPLE #	<u>Detrital Constituents (2)</u>								<u>Authigenic Constituents (2)</u>							<u>Porosity</u>	
	MONOAXIALINE QUARTZ	POLYAXIALINE QUARTZ	PLAGIOCLASE FELDSPAR	POTASSIUM FELDSPAR	SILICEOUS MATRIX	GLAUC- ONITE	FOSSILS	OOIDS	SILICA OVERGROWTHS	CHERT CEMENT	CALCITE	DOLomite	CHLORITE	PYRITE	COLLOPHANE	ORGANIC MATERIAL	POROSITY
									BOATHRIGHT	SAND							
TML-13367	59	T	T	0	0	T	T	0	7	T	T	37	T	1	0	T	0
TML-13380	78	T	0	T	0	0	0	0	5	T	0	T	6	T	0	0	7
TML-13386	75	1	T	T	0	0	T	0	13	T	T	2	6	T	0	2	T
RANGE	(59-76)	(T-1)	(0-T)	(0-T)	(0)	(0-T)	(0-T)	(0)	(7-13)	(T)	(0-T)	(T-37)	(T-6)	(T-1)	(0)	(0-2)	(0-7)

TABLE IV

CONSTITUENT TYPES AND PERCENTAGES - TENNECO PARTON NO. 1 - 3

DEPTH/ SAMPLE #	<u>Detrital Constituents (2)</u>								<u>Authigenic Constituents (2)</u>							<u>Porosity</u>	
	MONOAXIALINE QUARTZ	POLYAXIALINE QUARTZ	PLAGIOCLASE FELDSPAR	POTASSIUM FELDSPAR	SILICEOUS MATRIX	GLAUC- ONITE	FOSSILS	ORIBS	SILICA OVERGROWTHS	QUERT CEMENT	CALCITE	DOLOMITE	CHLORITE	PYRITE	COLLOPHANE	ORGANIC MATERIAL	POROSITY
								DISTAL	DELTA-FRONT								
TP-12999		Sparsely	Fossiliferous	Siltstone													
TP-13010	29	T	0	0	0	T	2	0	T	0	46	22	T	T	0	0	0
TP-13015		Sparsely	Fossiliferous	Siltstone													

TABLE V

CONSTITUENT TYPES AND PERCENTAGES -- AMOCO McCLAIN NO. 1

DEPTH/ SAMPLE #	Detrital Constituents (2)								Authigenic Constituents (2)								Porosity
	MONOAXIALINE QUARTZ	POLYAXIALINE QUARTZ	PLAGIOCLASE FELDSPAR	POTASSIUM FELDSPAR	SILICEOUS MATRIX	GLAUC- ONITE	FOSSILS	ODDS	SILICA OVERGROWTHS	CHERT CEMENT	CALCITE	DOLOMITE	CHLORITE	PYRITE	COLLOPHANE	ORGANIC MATERIAL	
									STORM DEPOSITS								
AM-15473	12	T	T	0	0	0	76	0	T	0	6	4	0	1	0	0	0
AM-15476	7	T	0	0	0	0	86	0	T	0	4	1	0	1	0	0	0
AM-15477	10	T	0	0	0	0	73	T	T	0	6	T	0	T	0	0	0
RANGE	(7-10)	(T)	(0-T)	(0)	(0)	(0)	(75-86)	(0-T)	(T)	(0)	(4-6)	(T-4)	(0)	(T-1)	(0)	(0)	(0)
									SHELF SAND-RIDGE								
AM-15479	71	T	0	0	0	0	T	0	1	0	T	3	24	T	0	0	0
AM-15481	72	T	T	T	0	0	10	0	7	0	T	T	4	1	0	0	5
AM-15483	86	T	T	T	0	0	T	0	4	0	T	T	5	1	0	0	3
AM-15484	80	T	0	0	0	0	T	0	3	0	T	2	14	T	0	0	T
RANGE	(71-86)	(T)	(0-T)	(0-T)	(0)	(0)	(T-10)	(0)	(1-7)	(0)	(T)	(T-3)	(4-24)	(T-1)	(0)	(0)	(0-5)

TABLE VI
 CONSTITUENT TYPES AND PERCENTAGES - AMOCO HAAS "A" NO. 3

DEPTH/ SAMPLE #	Detrital Constituents (%)								Authigenic Constituents (%)								Porosity
	MONOCRYSTALLINE QUARTZ	POLYCRYSTALLINE QUARTZ	PLAGIOCLASE FELDSPAR	POTASSIUM FELDSPAR	SILICEOUS MATRIX	GLAUCO- ONITE	FOSSILS	OOIDS	SILICA OVERGROWTHS	CHERT CEMENT	CALCITE	DOLOMITE	CHLORITE	PYRITE	COLLOPHANE	ORGANIC MATERIAL	
									SHELF	SAND-RIDGE							
AM-15595	42	T	0	T	0	0	T	0	T	20	2	0	27	1	0	T	0
AM-15598	44	T	T	T	0	0	0	0	1	19	1	7	25	3	0	T	0
RANGE	(42-44)	(T)	(0-T)	(T)	(0)	(0)	(0-T)	(0)	(T-1)	(19-20)	(1-2)	(7-8)	(25-27)	(1-3)	(0)	(T)	(0)
									B* SHELF	SAND-RIDGE							
AM-15625	73	T	0	T	0	0	0	0	5	T	7	5	0	T	0	0	1
AM-15629	63	T	0	T	0	0	T	0	1	1	3	29	2	T	0	0	T
AM-15632	73	T	0	T	0	0	T	0	5	4	T	T	17	T	0	0	T
AM-15635	75	T	0	T	1	0	0	0	10	1	T	T	12	T	0	0	T
AM-15639	82	T	T	T	0	0	T	0	0	2	T	T	7	T	0	0	T
AM-15643	76	T	0	T	0	0	0	0	3	17	T	T	1	2	0	0	T
RANGE	(63-82)	(T)	(0-T)	(T)	(0-1)	(0)	(0-T)	(0)	(1-10)	(T-17)	(T-7)	(T-29)	(1-17)	(T-2)	(0)	(0)	(0-T)

TABLE VII
 CONSTITUENT TYPES AND PERCENTAGES - AMOCO LEONARD NO. 3

DEPTH/ SAMPLE #	Detrital Constituents (2)								Authigenic Constituents (2)							Porosity	
	MONOAXIALINE QUARTZ	POLYAXIALINE QUARTZ	PLAGIOCLASE FELDSPAR	POTASSIUM FELDSPAR	SILICEOUS MATRIX	GLAUC- ONITE	FOSSILS	OOIDE	SILICA OVERGROWTHS	CHERT CEMENT	CALCITE	DOLomite	CHLORITE	PYRITE	COLLOPHANE	ORGANIC MATERIAL	POROSITY
									B* SHELF SAND-RIDGE								
AL-15471	34	T	0	0	0	0	4	20	1	0	1	2	0	2	22	0	0
									B SHELF SAND-RIDGE								
AL-15483	73	T	0	0	0	0	2	0	2	0	11	9	5	1	0	0	0
AL-15487	75	T	0	0	0	0	1	1	1	T	T	5	12	1	0	2	T
AL-15499	75	T	0	0	0	0	T	0	5	T	0	2	16	1	0	T	T
AL-15493	79	T	T	T	0	0	1	0	8	T	T	2	6	1	0	2	1
AL-15494	70	T	0	0	0	0	2	0	2	T	2	4	16	2	0	0	T
AL-15498	74	T	0	T	0	0	1	0	2	T	2	T	10	1	0	1	T
AL-15501	72	T	0	0	0	0	2	0	5	0	0	2	6	1	0	2	4
AL-15507	79	T	T	0	T	T	T	0	12	2	1	T	4	T	0	0	T
RANGE	(10-79)	(T)	(0-T)	(0-T)	(0-T)	(0-T)	(T-2)	(0-1)	(1-12)	(0-2)	(0-11)	(T-9)	(4-16)	(T-2)	(0)	(0-2)	(0-4)

TABLE VIII

CONSTITUENT TYPES AND PERCENTAGES - AMOCO SYLVESTER NO. 1

DEPTH/ SAMPLE #	Detrital Constituents (%)									Authigenic Constituents (%)							Porosity
	MONOTALLINE QUARTZ	POLYIALLINE QUARTZ	PLAGIOCLASE FELDSPAR	POTASSIUM FELDSPAR	SILICEOUS MATRIX	GLAUC- ONITE	FOSSILS	OOLDS	SILICA OVERGROWTHS	CHERT CEMENT	CALCITE	DOLONITE	CHLORITE	PYRITE	COLLOPHANE	ORGANIC MATERIAL	POROSITY
									"A" SHELF	SAND-RIDGE							
AS-15521	35	T	T	T	T	0	T	0	1	T	1	5	16	1	0	1	T
AS-15526	70	T	T	0	T	0	1	0	3	T	1	1.5	11	1	0	0	0
AS-15529	83	T	T	T	0	0	T	0	4	0	T	T	5	1.5	0	T	2
AS-15536	83	T	T	T	0	0	T	0	9	0	T	T	5	1	0	0	T
AS-15540	81	T	T	T	0	0	T	0	4	T	T	2	9	T	0	0	4
AS-15543	81	T	T	T	0	0	T	0	4	0	T	2	5	T	0	0	7
AS-15545	84	T	T	T	0	0	T	0	4	0	T	1	7	2	0	0	1
RANGE	(75-85)	(T)	(T)	(0-T)	(0-T)	(0)	(T-1)	(0)	(1-9)	(0-T)	(T-1)	(T-5)	(5-16)	(T-2)	(0)	(0-1)	(0-7)

VITA

John Paul Haiduk

Candidate for the Degree of
Master of Science

Thesis: FACIES ANALYSIS, PALEOENVIRONMENTAL INTERPRETATION, AND DIAGNETIC HISTORY OF BRITT SANDSTONE (UPPER MISSISSIPPIAN), IN PORTIONS OF CADDO AND CANADIAN COUNTIES, OKLAHOMA

Major Field: Geology

Biographical:

Personal: Born in Enid, Oklahoma, on September 10, 1961, the son of Mr. and Mrs. R. P. Haiduk.

Education: Received Bachelor of Science degree in Geology, December, 1983, from Oklahoma State University, Stillwater, Oklahoma; completed requirements for the Master of Science degree at Oklahoma State University in May, 1987.

Professional Experience: Assistant Geologist for Geologic Consultants, Enid, Oklahoma, May, 1983 to June, 1984; Geologist for Epoch Resources, Enid, Oklahoma, June, 1984 to October, 1984; Graduate Teaching Assistant, Department of Geology, Oklahoma State University, Stillwater, Oklahoma, August, 1985 to May, 1986; Exploration/Development Geologist, Henry Gungoll Operating, Inc., Enid, Oklahoma, October, 1984 to Present.

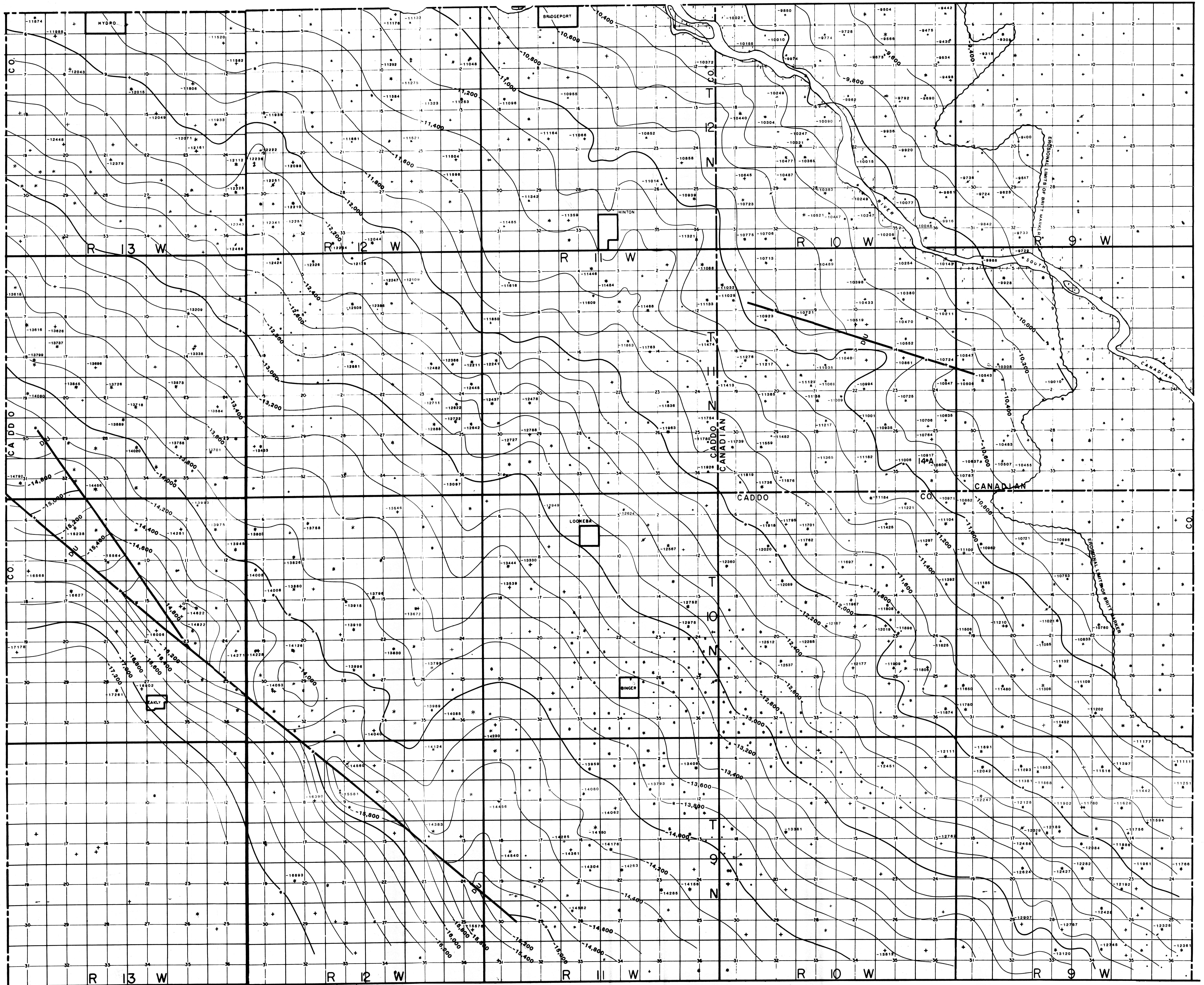


PLATE I
STRUCTURAL CONTOUR MAP

DATUM: TOP OF BRITT MARKER
CONTOUR INTERVAL: 200 FEET
JOHN HAIKUK, 1987

Thesis
1987
H149C
cop 2

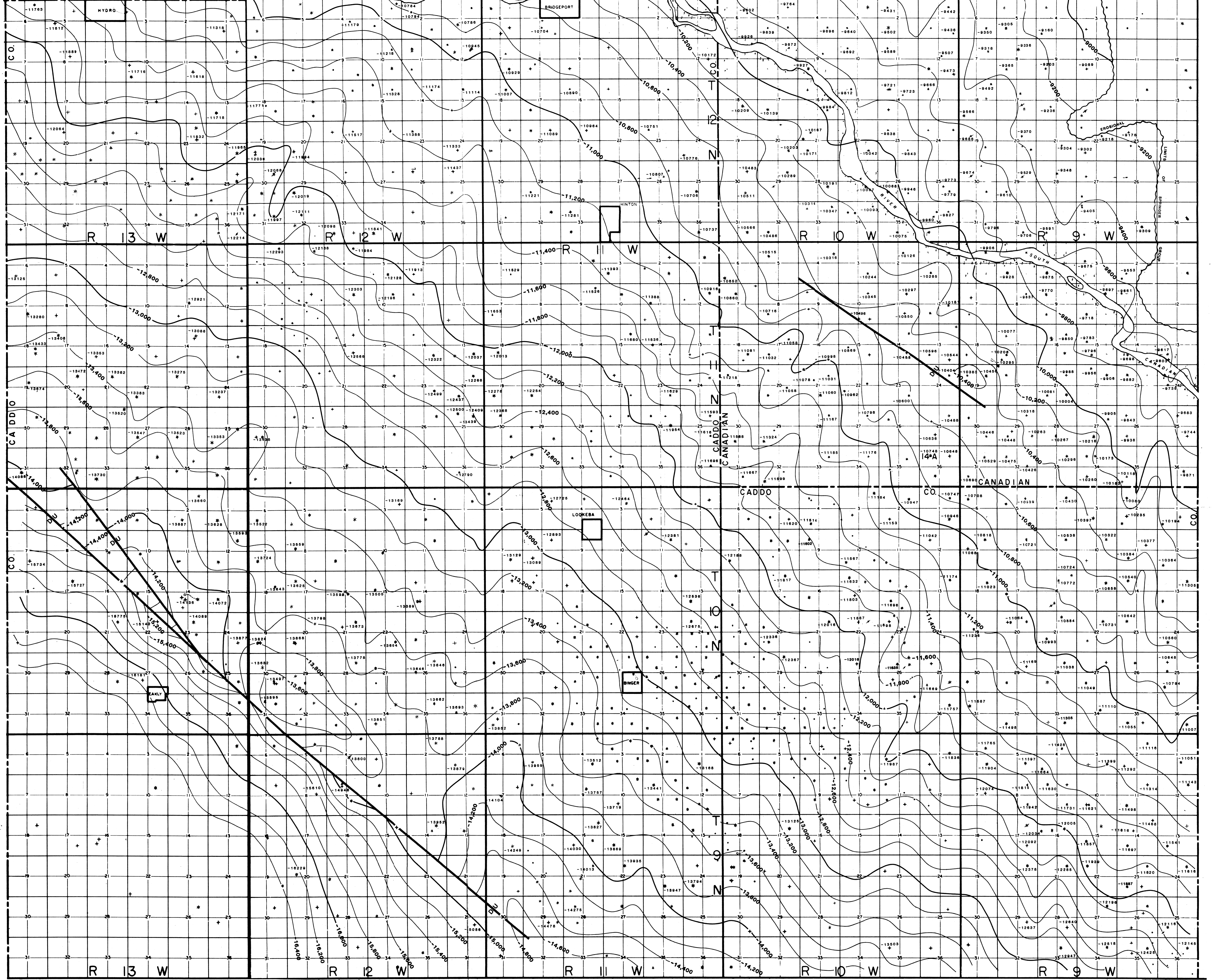


PLATE II
 STRUCTURAL CONTOUR MAP

DATUM: TOP OF SPRINGER GROUP (BASE OF PENNSYLVANIAN)

CONTOUR INTERVAL: 200 Feet

JOHN HAIDUK, 1987

Thesis
 1987
 H149f
 1p.2

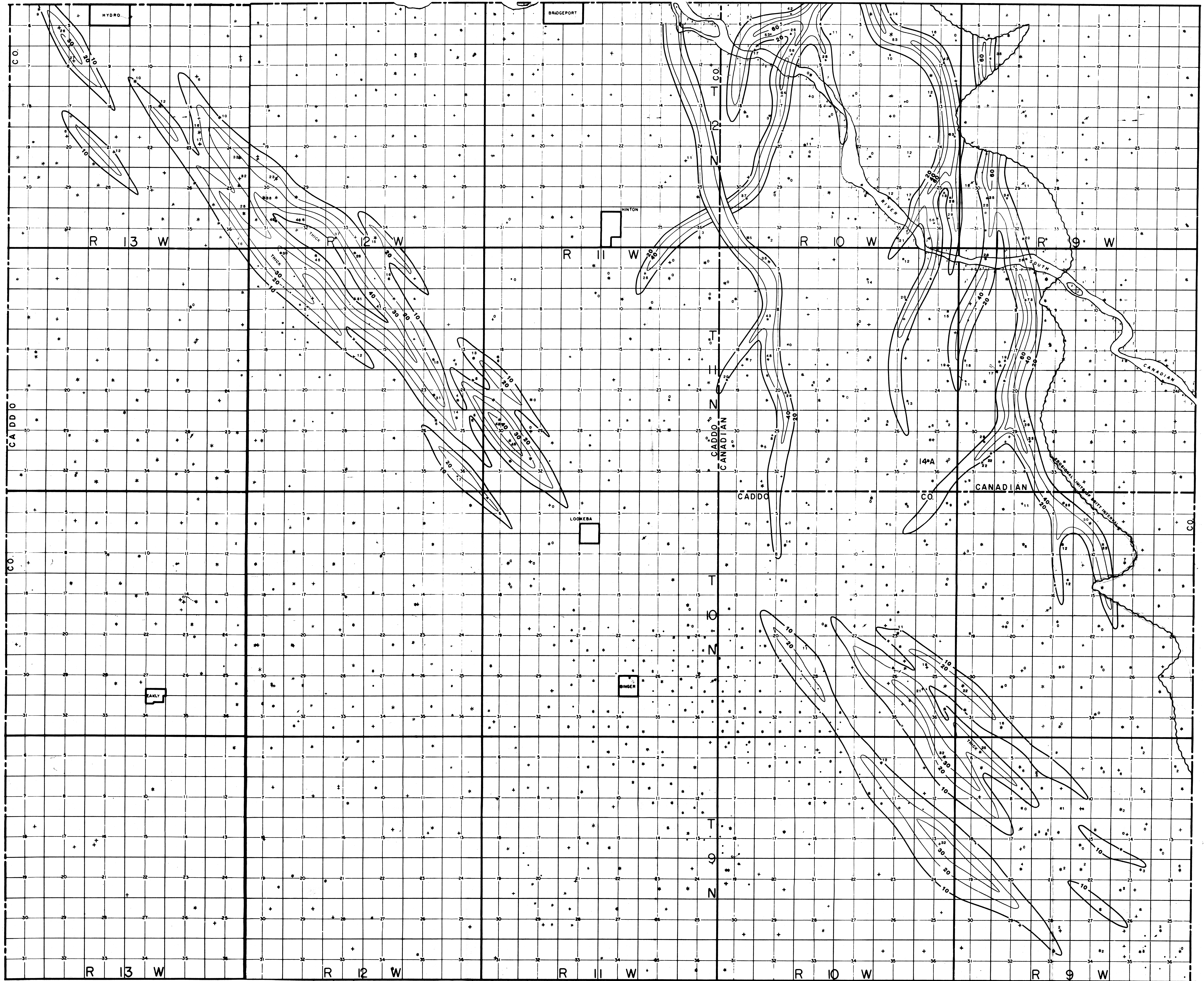


PLATE III

**LOWER BRITT
GROSS SAND ISOPACH MAP**
(EXCLUDING DELTA-DESTRUCTURAL BAR SANDS)

CONTOUR INTERVAL:
SHELF SAND RIDGES: 10 FEET
DELTAIC SYSTEM: 20 FEET

JOHN HAIDUK, 1987

Thesis
1987
H149F
Cap. 2

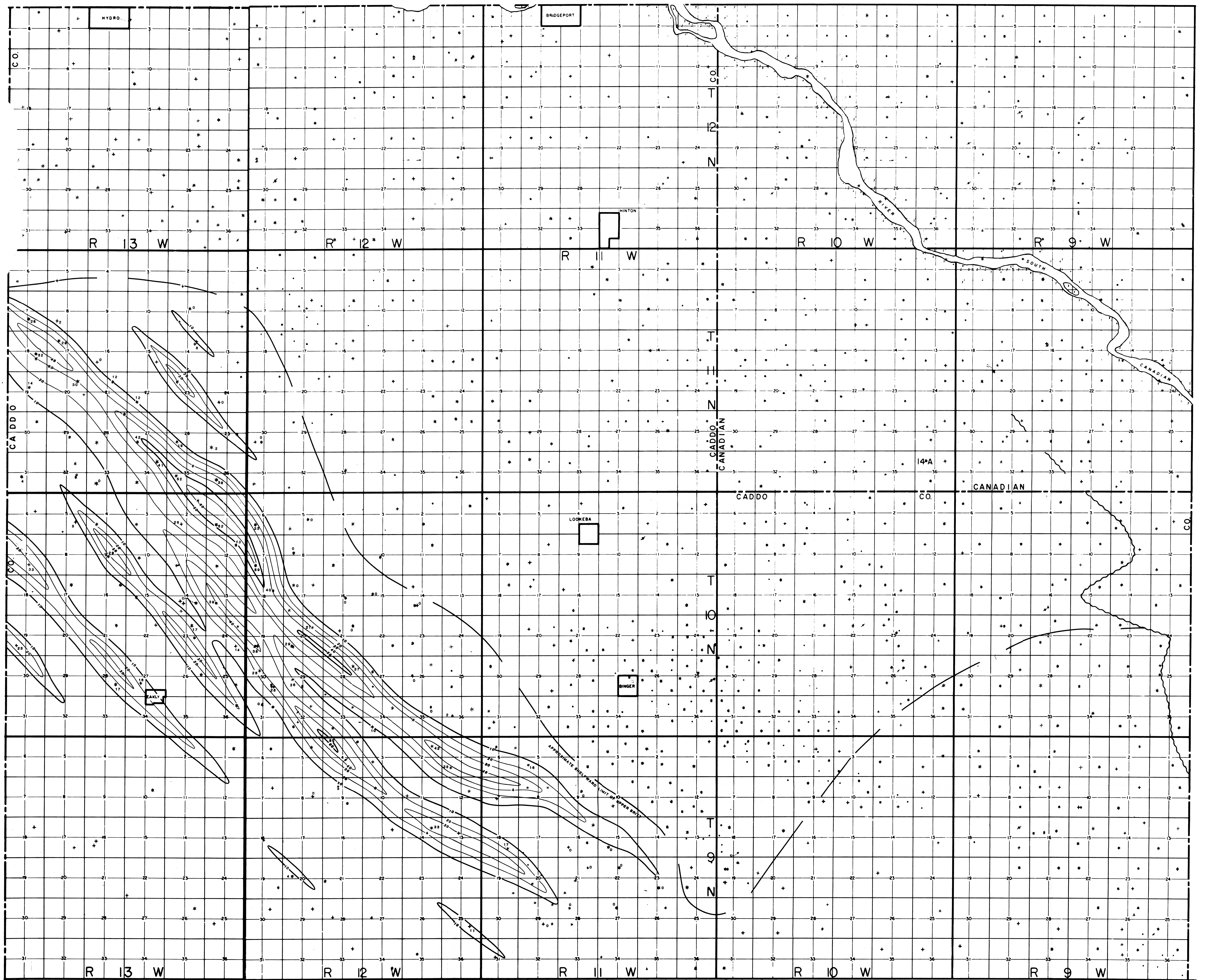


PLATE IV
 UPPER BRITT "B" SAND
 GROSS SAND ISOPACH MAP

CONTOUR INTERVAL: 10 FEET

JOHN HAIDUK, 1987

Thesis
 1987
 H-49f
 cop. 2

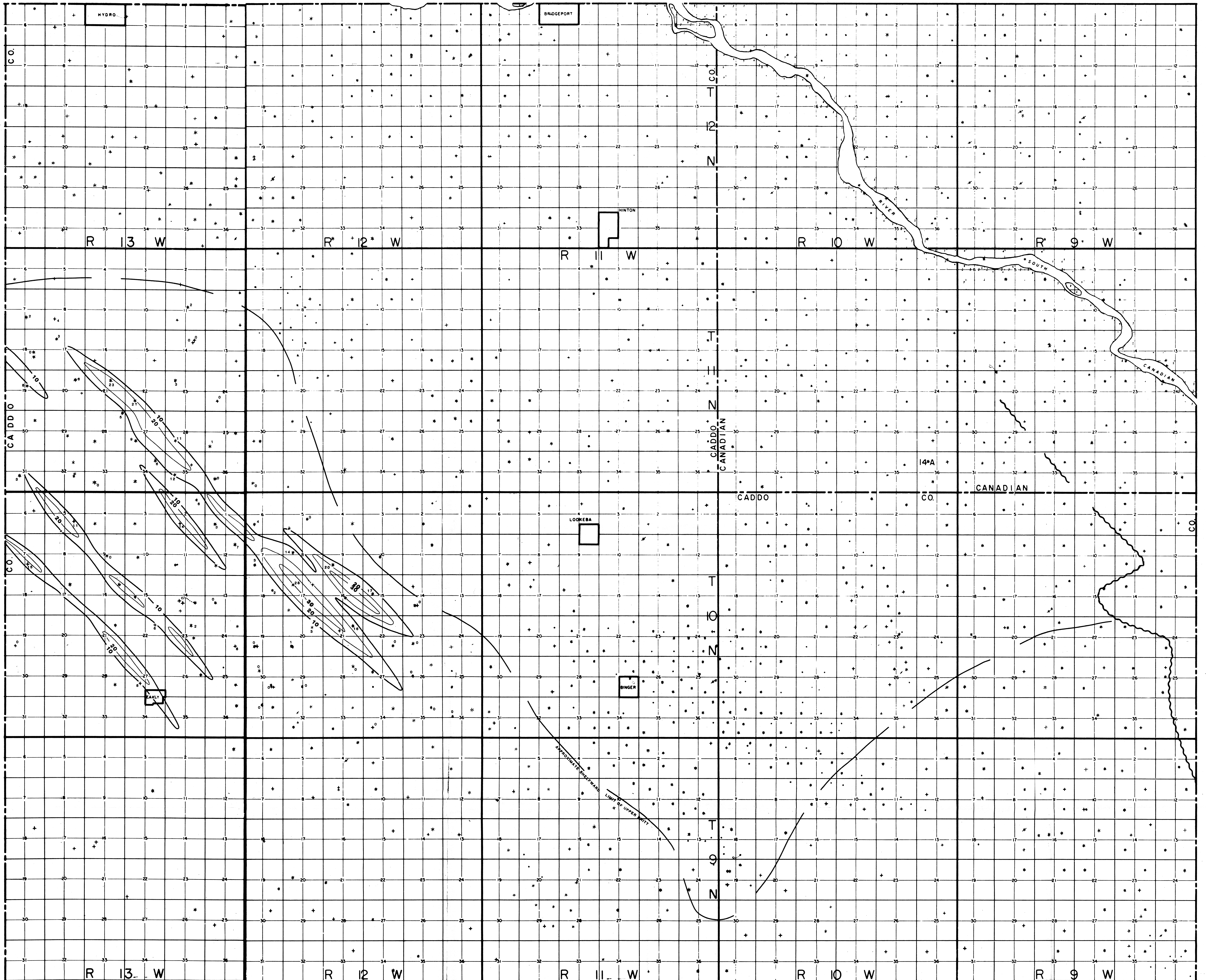


PLATE V
 UPPER BRITT "A" SAND
 GROSS SAND ISOPACH MAP

CONTOUR INTERVAL: 10 FEET

JOHN HAIDUK, 1987

Thesis
 1987
 H194F
 cap 2

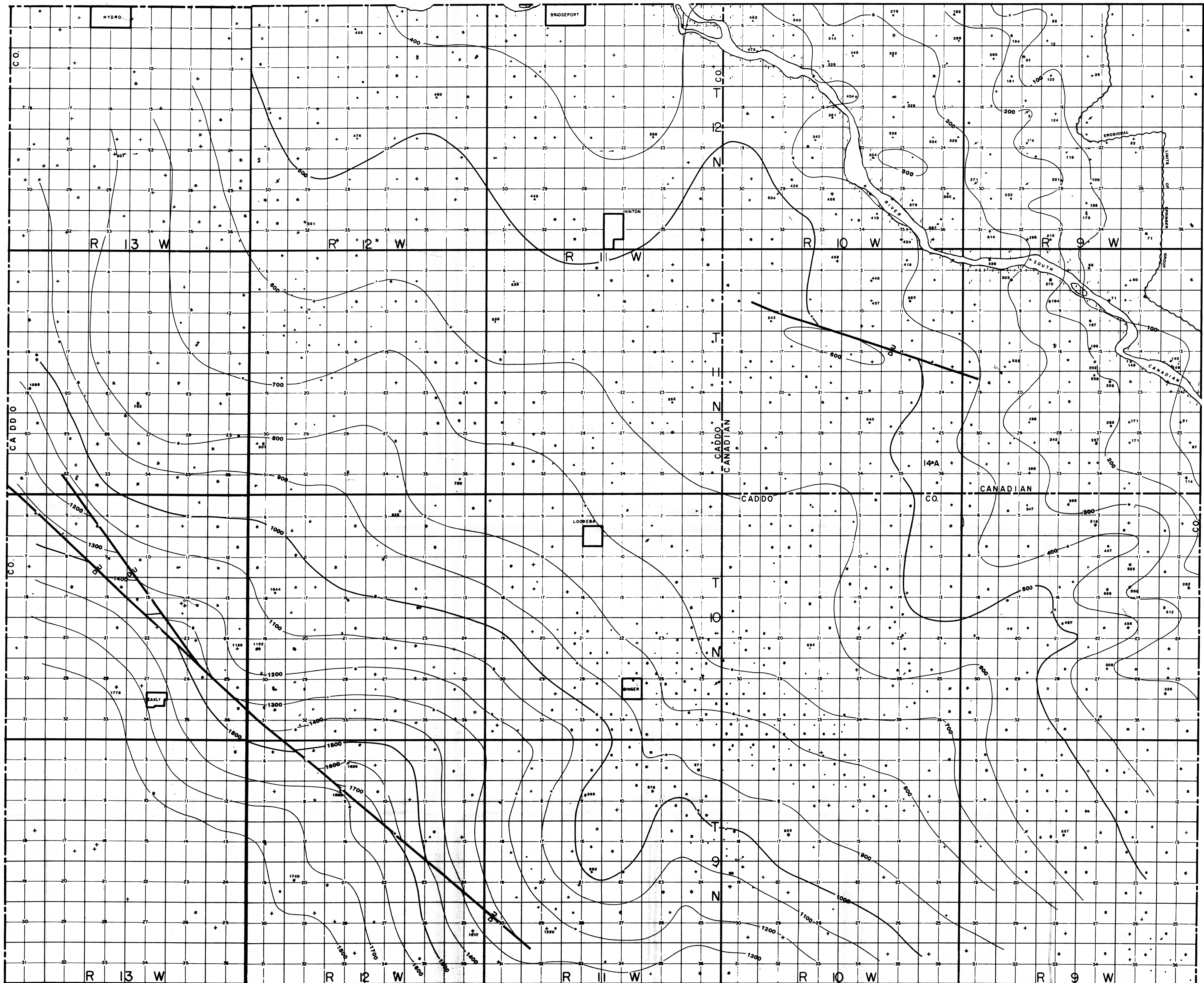


PLATE VI
ISOPACH MAP - SPRINGER GROUP

CONTOUR INTERVAL: 100 Feet

JOHN HAIDUK, 1987

Thesis
1987
H149f
cap. 2

B

B'

AMOCO PRODUCTION
SYLVESTER UNIT #1
SEC. 21-T11N-R13W
CADDO COUNTY, OK

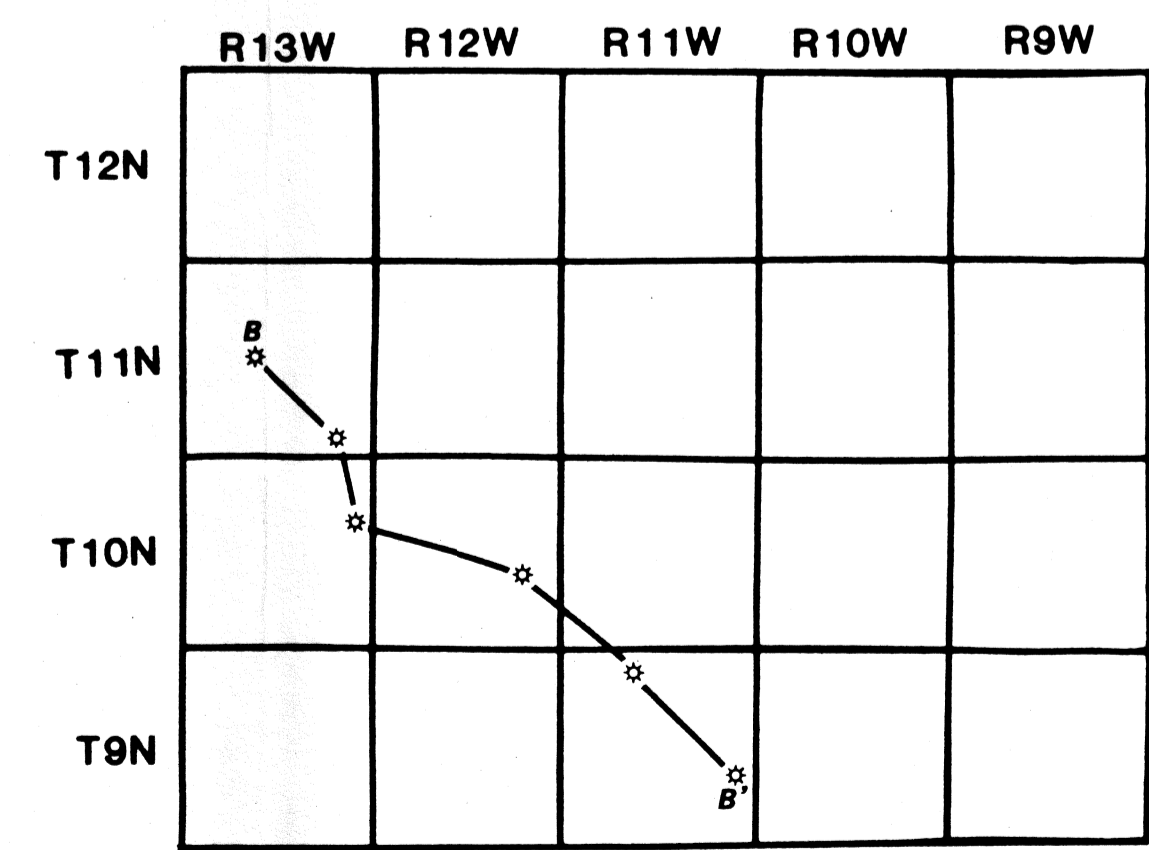
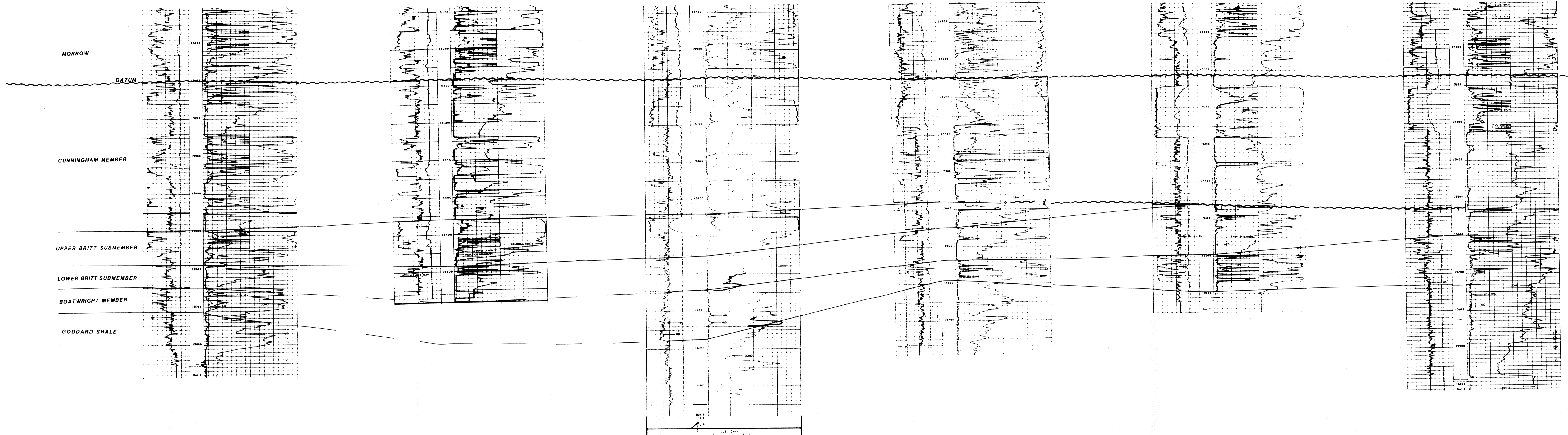
LEAR PETROLEUM
MCLONE #1-35
SW/4 SEC. 35-T11N-R13W
CADDO COUNTY, OK

ANR PRODUCTION
OKLAHOMA STATE #1-13
SW/4 SEC. 13-T10N-R13W
CADDO COUNTY, OK

AMOCO PRODUCTION
MCLAIN UNIT #1
SEC. 23-T10N-R12W
CADDO COUNTY, OK

SANGUINE, LTD.
BROWN #1
SE 1/4 SEC. 4-T9N-R11W
NTY, OK

SANGUINE, LTD.
GOODFELLOW #1
SW/4 SEC. 24-T9N-R11W
CADDO COUNTY, OK



CROSS-SECTION LOCATION MAP

PLATE VIII
CROSS-SECTION B - B'

JOHN HAIKUK, 1987

DATUM: MISSISSIPPIAN - PENNSYLVANIAN
UNCONFORMITY

Thesis
1987
H149f
Cap 2

C

CONTINENTAL OIL
MOORE #1
NE/4 SEC. 28-T10N-R13W
CADDO COUNTY, OK

ANR PRODUCTION
OKLAHOMA STATE #1-13
SW/4 SEC. 13-T10N-R13W
CADDO COUNTY, OK

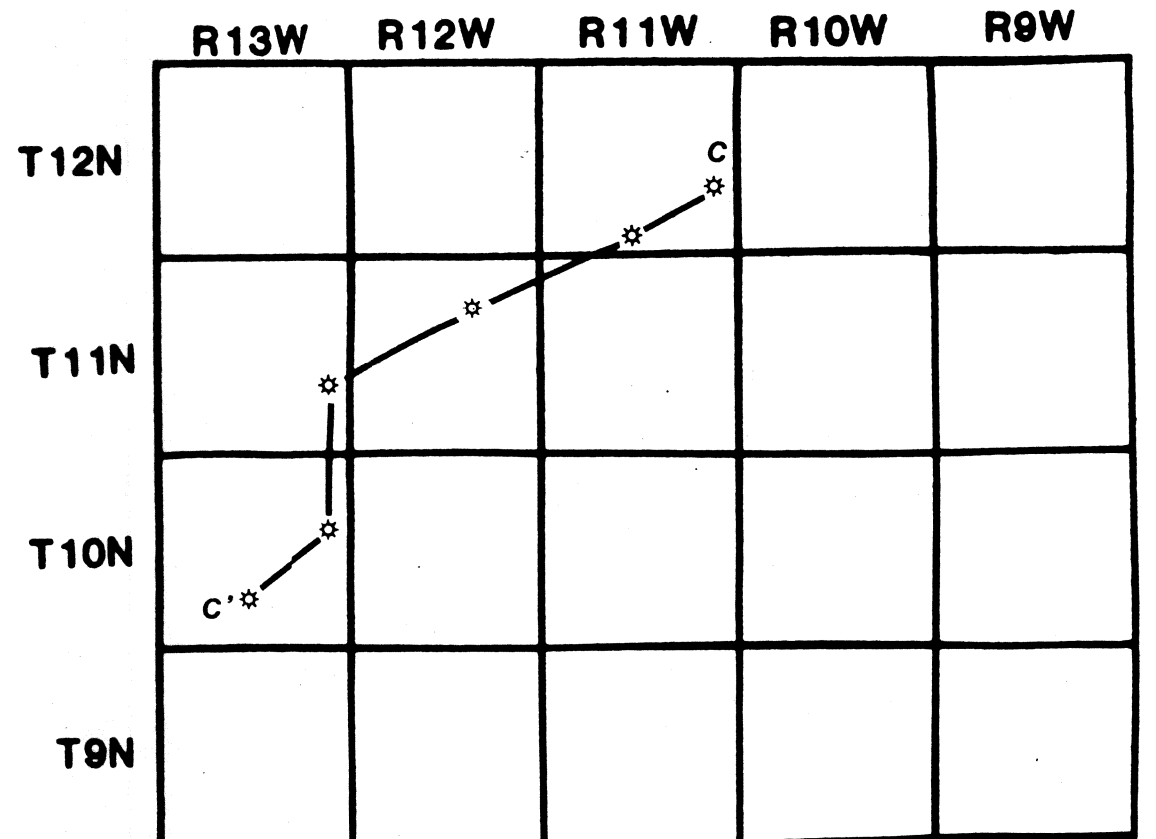
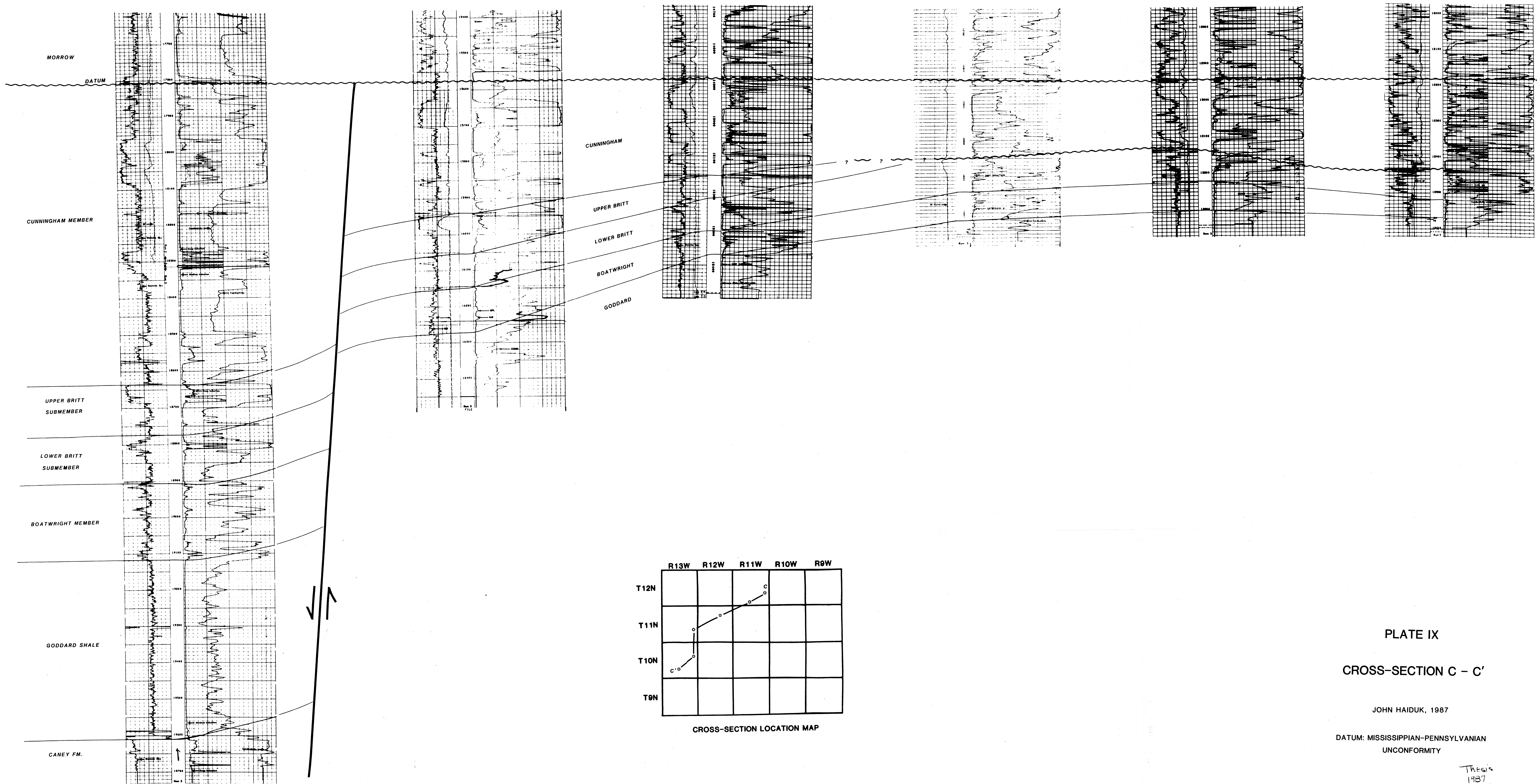
LEAR PETROLEUM
MCCLAIN #1
SEC. 24-T11N - R13W
CADDO COUNTY, OK

APEXCO, INC.
BULL # 1 - A
SW/4 SEC. 10-T11N-R12W
CADDO COUNTY, OK

SANGUINE, LTD.
MAJORS #1-33
SW/4 SEC. 33-T12N-R11W
CADDO COUNTY, OK

SANGUINE, LTD.
GRAY #1-24
SW SEC. 24-T12N-R11W
CADDO COUNTY, OK

C



CROSS-SECTION LOCATION MAP

PLATE IX
CROSS-SECTION C - C'

JOHN HAIDUK, 1987

DATUM: MISSISSIPPIAN-PENNSYLVANIAN
UNCONFORMITY

Thesis
1987
H149F
Cop. 2

D'

CONTINENTAL OIL COMPANY
MOORE #1
SE/4 SEC. 28-T10N-R13W
CADDO COUNTY, OK

HUNT ENERGY
GRIFFIN #1
NE/4 SEC. 20-T9N-R12W
CADDO COUNTY, OK

ROBINSON BROTHERS
STEVENS #18-1
NE/4 SEC. 18-T0N-R12W
CADDO COUNTY, OK

KING RESOURCES
FERGUSON #1-36
SW/4 SEC. 36-T11N-R10W
CADDO COUNTY, OK

JONES & PELLOW
SCOTT #1
SW/4 SEC. 20-T10N-R10W
CADDO COUNTY, OK

DONALD SLAWSON
MAJORS UNIT #1
NE/4 SEC. 10-T11N-R10W
CANADIAN COUNTY, OK

L.O. WARD
ANKEY #1
SW/4 SEC. 27-T12N-R9W
CANADIAN COUNTY, OK

D

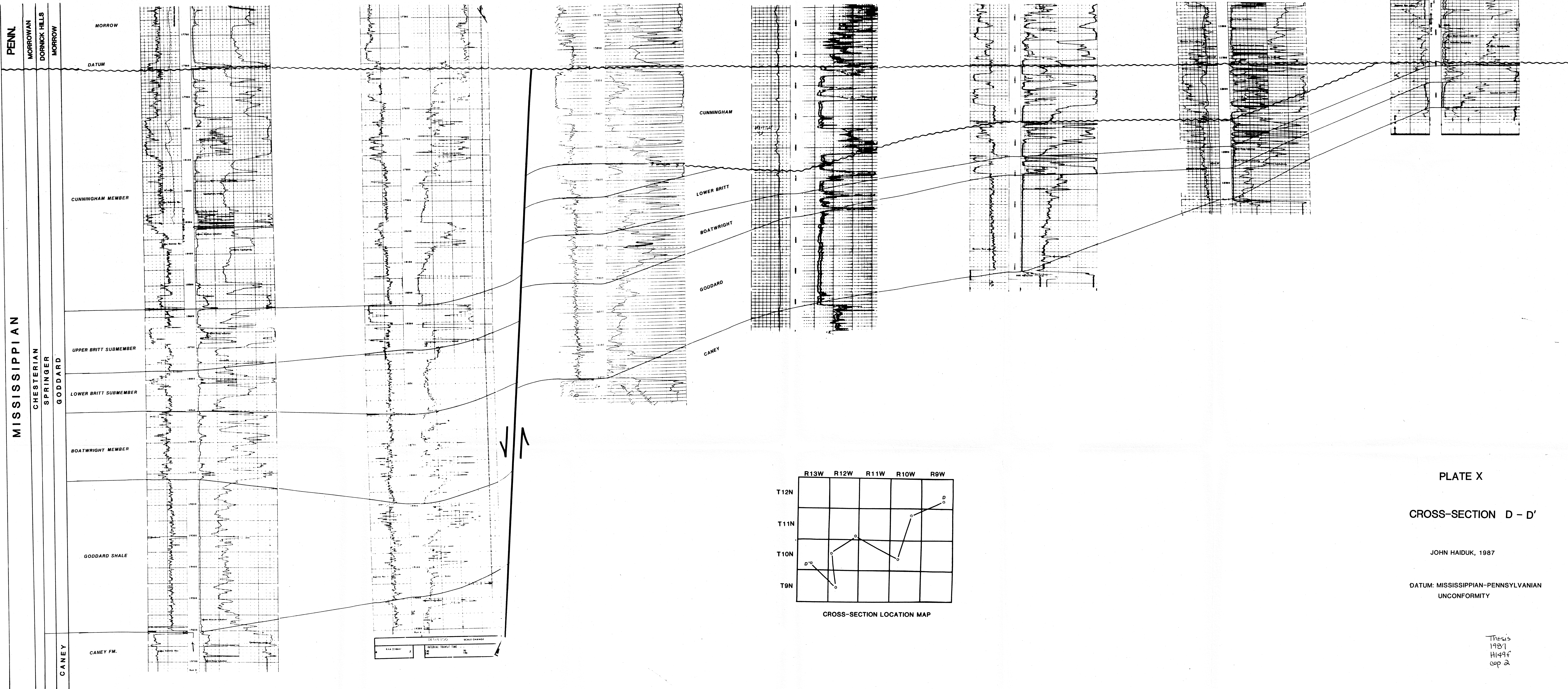


PLATE X

CROSS-SECTION D - D'

JOHN HAIK, 1987

DATUM: MISSISSIPPIAN-PENNSYLVANIAN
UNCONFORMITY

Thesis
1987
H149f
cop 2

E'

E

HARPER OIL
 MOBIL #1
 NE/4 SEC. 17-T9N-R10W
 CADDO COUNTY, OK

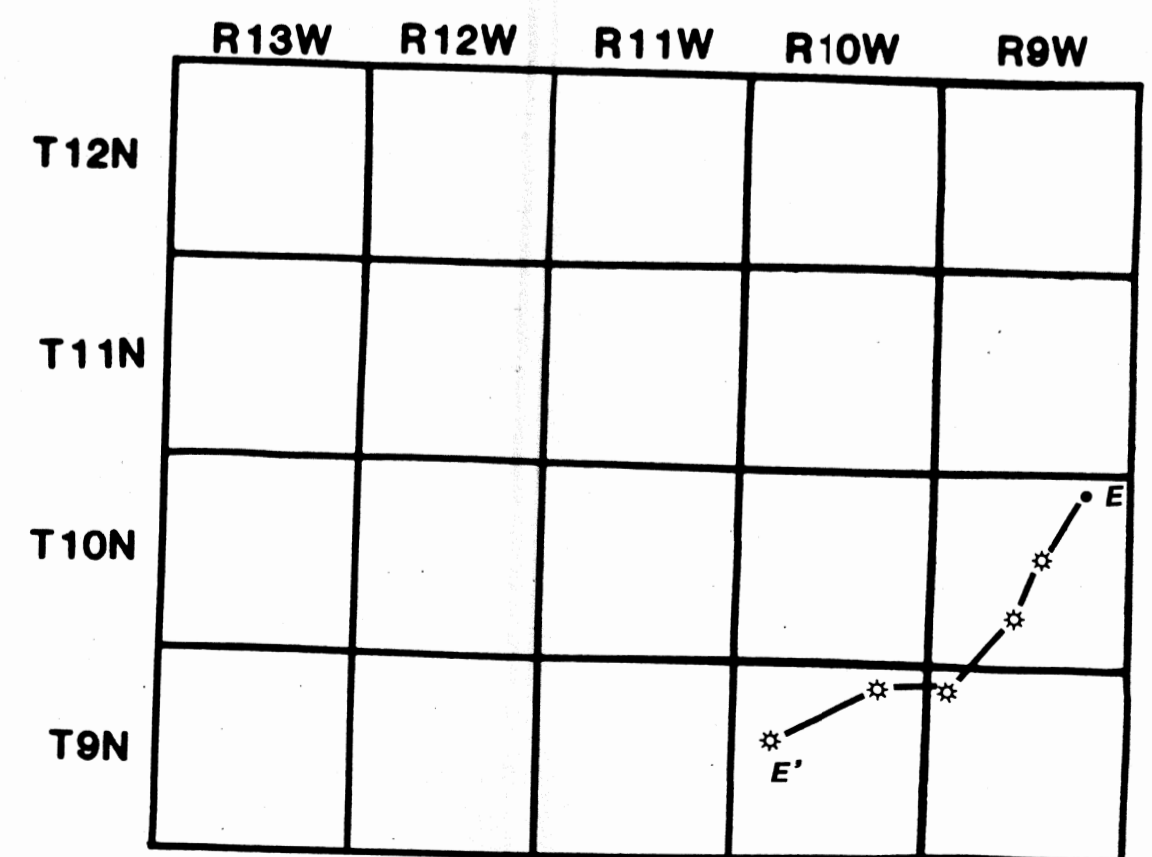
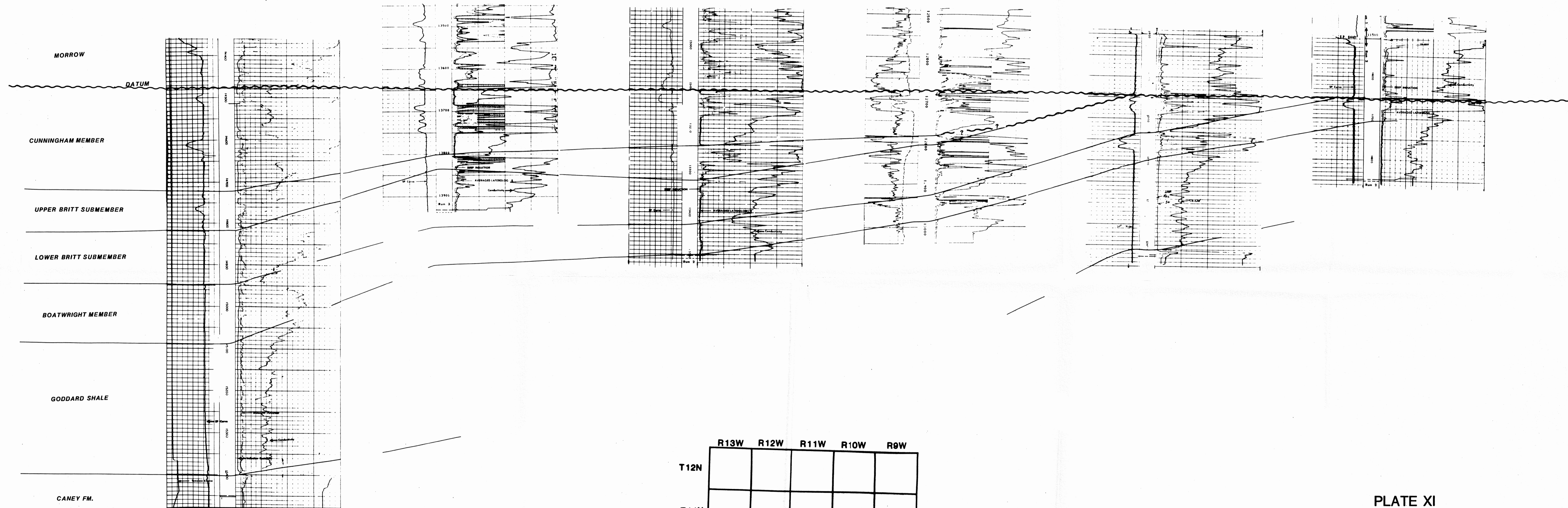
STOLTZ, WAGNER, & BROWN
 MILLS #1
 SW/4 SEC. 2-T9N-R10W
 CADDO COUNTY, OK

HELMERICH & PAYNE
 SHOOK #1
 SEC. 6-T9N-R9W
 CADDO COUNTY, OK

AMOCO PRODUCTION
 KELLEY # B-2
 SEC. 28-T10N-R9W
 CADDO COUNTY, OK

AMOCO PRODUCTION
 DARNELL GAS UNIT #1
 NE/4 SEC. 15 - T10N - R9W
 CADDO COUNTY, OK

KAISER OIL
 GILBERT #1
 NW/4 SEC. 2-T10N-R9W
 CADDO COUNTY, OK



CROSS-SECTION LOCATION MAP

PLATE XI
 CROSS-SECTION E - E'

JOHN HAIDUK, 1987

Thesis
 1987
 H149f
 cop 2

DATUM: MISSISSIPPIAN-PENNSYLVANIAN
 UNCONFORMITY

A

A'

AN-SON CORPORATION
JOYCE #A-1
NE/4 SEC. 8-T12N-R13W
CADDO COUNTY, OK

DAVIS OIL COMPANY
OTTINGER # 1
NE/4 SEC. 36-T12N-R13W
CADDO COUNTY, OK

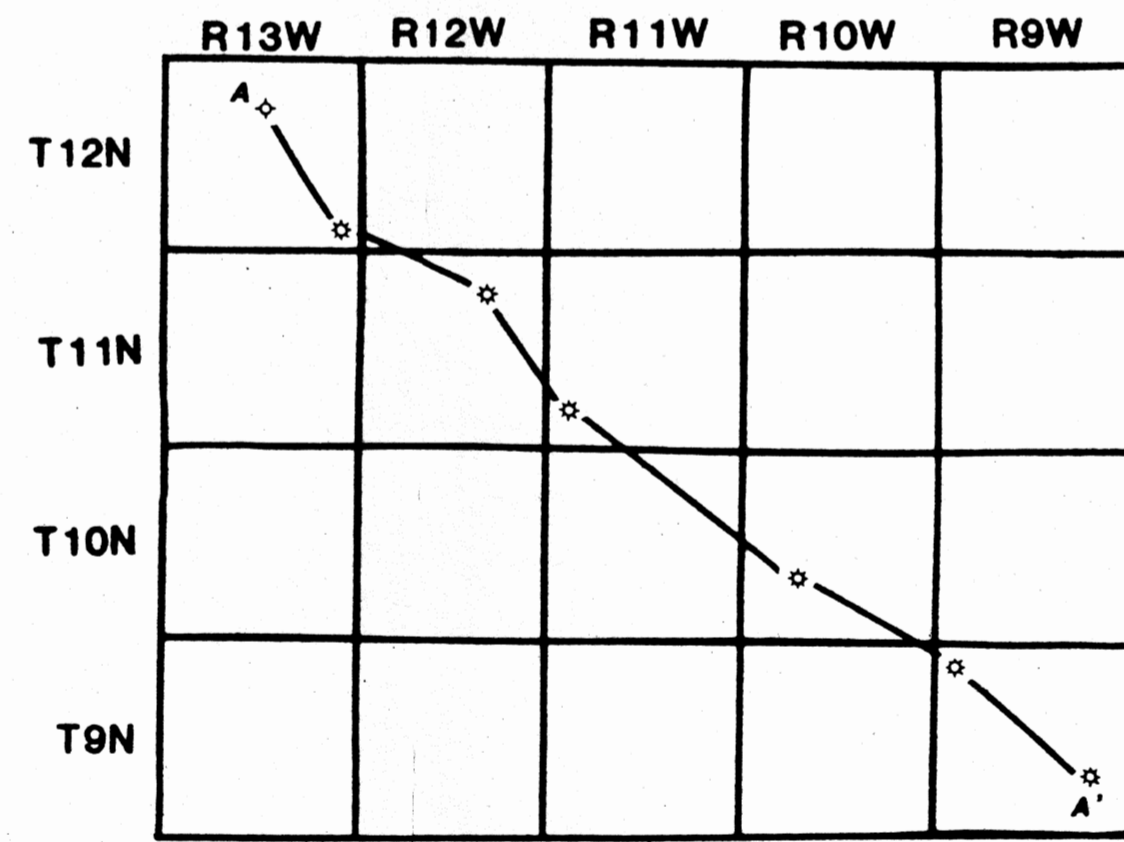
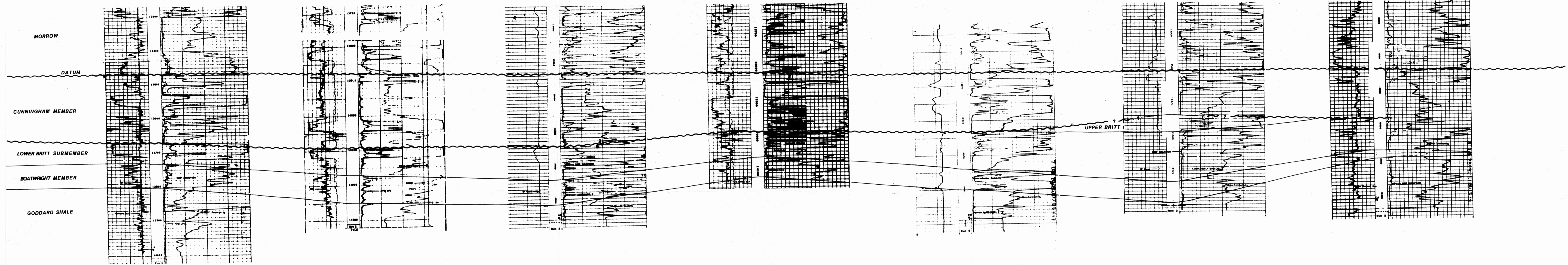
APEXCO, INC.
BUELL #1-A
NW/4 SEC. 10-T11N-R12W
CADDO COUNTY, OK

GETTY OIL COMPANY
BENNIE LINDLEY #A - 2
NE/4 SEC. 30-T11N-R11W
CADDO COUNTY, OK

JONES & PELLOW
SCOTT #1
SW/4 SEC. 20-T10N-R10W
CADDO COUNTY, OK

HELMERICH & PAYNE
SHOOK #1
Sec. 6-T9N - R9W
CADDO COUNTY, OK

TENNECO OIL
WILLIE LEFTHAND #1-23
NE/4 SEC. 23-T9N-R9W
CADDO COUNTY, OK



CROSS-SECTION LOCATION MAP

Thesis
1987
H149f
cop. 2

PLATE XII
CROSS-SECTION A-A'

JOHN HAIDUK, 1987

DATUM: MISSISSIPPIAN - PENNSYLVANIAN
UNCONFORMITY